2018

Mechanical Bar Splices for Accelerated Construction of Bridge Columns

Puskar Kumar Dahal
South Dakota State University

MECHANICAL BAR SPLICES FOR ACCELERATED CONSTRUCTION OF BRIDGE COLUMNS

BY

PUSKAR KUMAR DAHAL

A thesis submitted in partial fulfillment of the requirements for the

Master of Science

Major in Civil Engineering

South Dakota State University

2018

MECHANICAL BAR SPLICES FOR ACCELERATED CONSTRUCTION OF BRIDGE COLUMNS

PUSKAR KUMAR DAHAL

This thesis is approved as a creditable and independent investigation by a candidate for the Master of Science degree and is acceptable for meeting the thesis requirements for this degree. Acceptance of this thesis does not imply that the conclusions reached by the candidate are necessarily the conclusions of the major department.

Mostafa Tazarv, Ph.D., P.E.
Thesis Advisor — Date
Civil and Environmental Engineering

Nadim Wehbe, Ph.D., P.E.
Department Head — Date
Civil and Environmental Engineering

Kinchel C. Doerner, Ph.D.
Dean, Graduate School — Date

ACKNOWLEDGEMENTS

A debt of gratitude is owed to my academic advisor Dr. Mostafa Tazarv for my master's degree program. He provided me a research opportunity and continuous guidance throughout this study. His suggestions and innovative ideas will always be a source of inspiration for my future career.

I would like to express my special thanks of gratitude to Prof. Nadim Wehbe for his valuable suggestions and support during my master's degree.

I am grateful to Mountain- Plains Consortium (MPC)-University Transportation Center (UTC) for their sponsorship on this research project. I would like to acknowledge Bar splice company, Dayton Superior Corp., Dextra America, Erico International Corp., Epsilon Technology, Headed Reinforcement Corp. and Splice Sleeve North America for collaborating on our research by providing their products without any cost.

I would like to acknowledge my research colleagues Sandip Rimal, Abdullah Boudaqa, Heath Pederson, Abdullah Al Hashib, Lucas Bohn, and Zachary Carnahan. They all are wonderful people, and I will never forget their help and effort for my study. I want to give special thanks to Zach Gutzmer for his help on my test set up and instrumentation.

Finally, I will always be indebted to my father, mother, wife and friends for their encouragement and support during my study.

TABLE OF CONTENTS

LIST OF ABBREVIATIONS

Abbreviation	**Definition**
AASHTO	American Association of State Highway and Transportation Officials
ASTM	American Society of Testing and Materials
ABC	Accelerated Bridge Construction
ACI	American Concrete Institute
DOT	Department of Transportation
ft	Feet
GS	Grouted Sleeve Coupler
HPC	High Performance Concrete
HRC	Headed Reinforcement Coupler
HY	Hybrid Coupler
in.	Inch
kip	1000 pounds
ksi	kip per square inch
SDSU	South Dakota State University
SH	Shear screw Coupler
SW	Swaged Coupler
TH	Threaded Coupler

LIST OF FIGURES

LIST OF TABLES

ABSTRACT

MECHANICAL BAR SPLICES FOR ACCELERATED CONSTRUCTION OF BRIDGE COLUMNS

PUSKAR KUMAR DAHAL

2018

Mechanical bar splicing is an alternative method of connecting reinforcing bars in concrete structures compared to conventional lap splicing mainly to reduce bar congestion in joints. Recently, mechanical bar splices, which are also referred to as bar couplers, have been used to connect precast members to accelerate construction of concrete bridges and buildings. Current codes prohibit the use of couplers in the plastic hinge regions of bridge columns in high seismic zones. This may be because of a lack of systematic test data on the coupler performance, limited experimental studies on mechanically spliced bridge columns, and an engineering precaution. The present experimental and analytical study was performed to (1) generate the first-of-it-kind database of the bar coupler performance, (2) quantify the coupler stress-strain relationship, and (3) quantify the seismic performance of mechanically spliced bridge columns. All manufacturers of mechanical bar splices in the Unites States were contacted to collect test samples, nine different coupler products were selected, and more than 160 mechanical bar splices were tested under uniaxial monotonic and cyclic loading to failure. Properties of the couplers were established, and a coupler material model adopted from the literature was verified. Furthermore, a parametric study was carried out

to investigate the seismic performance of mechanically spliced bridge columns utilizing the verified coupler models. More than 240 pushover analyses were performed. It was found that columns with couplers have up to 40% lower displacement ductility capacity compared to conventional RC columns and the force capacity of these columns is slightly higher than the RC columns. Columns with more rigid and longer couplers will show the lowest displacement capacities.

Chapter 1. Introduction

1.1 Introduction

In reinforced concrete structures, splicing of reinforcing steel bars is inevitable due to bar length limitations. The conventional method of splicing, lap splicing, is done by placing a sufficient length of connecting bars side-by-side and tying them with steel wires. An alternative method is the use of mechanical devices, which are commonly referred to as "mechanical bar splices" or "bar couplers". Lap splicing has historically been the most common splice type. Nevertheless, the use of bar couplers is increasing since they reduce bar congestion and may result in more cost-effective construction.

Accelerated bridge construction (ABC) is a new paradigm in the USA with an ultimate goal of faster bridge construction. ABC heavily relies on prefabricated bridge elements. However, the main challenge of ABC especially in seismic regions is how to connect precast elements with sufficient strength and deformability.

Even though a few ABC column connections have been developed and proof tested in laboratories, the use of precast bridge columns incorporating mechanical bar splices are rare in actual bridges. This is because (1) current codes prohibit the use of bar couplers in plastic hinge regions of bridge columns, (2) there is a lack of unified standard testing methods, acceptance criteria, and material models for couplers, (3) there is no systematic experimental work in which the behavior of different coupler types and sizes was

established and compared, and (4) there is a few studies on the seismic performance of mechanically spliced bridge bridges.

1.2 Objectives and Scope

The main objectives of the present study were to establish the behavior of mechanical bars splices suited for bridge columns, to generate an experimental database for such couplers, and to quantify the effect of such couplers on the seismic performance of bridge columns.

Experimental and analytical programs were completed to achieve these objectives: (1) all the US mechanical bar coupler manufacturers were contacted to collect test samples, (2) test matrix, setup, and loading protocols were prepared, (3) more than 160 bar couplers were tested under unified monotonic and cyclic loading to failure, (4) a comprehensive database of coupler behavior was established, and (5) more than 240 pushover analyses were carried out to quantify the effect of bar couplers on the seismic performance of bridge columns.

1.3 Document Outline

Chapter 1 presents an introduction of the study and the scope of the work done. A literature review on mechanical bar splices was conducted and a summary is presented in Chapter 2. Chapter 3 discusses the experimental program (including test setup, loading protocols, and instrumentation plans) undertaking in this study on three sizes of nine different mechanical bar splices. Chapter 4 presents the results of the bar coupler experimental study including monotonic and cyclic tests. Furthermore, coupler properties were established, and a coupler material model adopted from the literature was verified in this chapter. The results of an analytical study on the seismic performance of

mechanically spliced bridge columns are presented in Chapter 5. The summary and conclusions of the study are presented in Chapter 6.

Chapter 2. Literature Review

2.1 Introduction

The process of transferring the load from one reinforcing bar to other in concrete structures may be done through lap splicing or using mechanical devices. The main advantages of utilizing mechanical bar splices, which are commonly referred to as bar couplers, are to reduce bar congestion and to minimize the splice length. Furthermore, mechanical bar splicing is a better alternative to lap splicing, which is more susceptible to splitting failure in flexural members (Hurd, 1998).

Mechanical bar splices are the focus of this chapter, which includes a review of different coupler types, couplers in the US codes, and past studies on couplers.

2.2 Mechanical Bar Splices (Couplers)

Figure 2-1 shows nine different product of tension-compression mechanical bar splices. Other products such as shear-screw couplers are also available but not shown in the figure. Based on the anchoring mechanism, couplers can be categorized in six general types: threaded, headed, swaged, grouted, shear-screw, and hybrid (combination of two types). Note different manufacturers produce these couplers types with different commercial names and usually with minor differences in size and detailing. However, the load-transfer mechanism of any tension-compression coupler is through one of these six types.

Figure 2-1. Different mechanical bar splice products

In threaded couplers, bar ends are threaded and are connected through a long nut. Bar ends are headed in headed couplers and then are connected using a male-female threaded connection lucking the heads in-place. Steel bars and a steel sleeve are pressed together using a hydraulic jack to anchor bars in a swaged coupler. In grouted couplers, bars are inserted in a steel sleeve then a high-strength grout is poured to complete the connection through bond. Bars are connected to a steel sleeve using screws in a shear screw coupler. Finally, a hybrid coupler connects bars through two of the abovementioned mechanism, one at each end. More discussions are provided in Sec. 2.4.2.

2.3 Mechanical versus Lap Splicing

The performance of a mechanical bar splice mostly depends on the configuration and performance of the splice itself while a lap splice entirely depends on the bond strength

between concrete and steel to transfer load. The advantages of mechanical splicing compared to lap splicing can be summarized as:

- **Strength:** Mechanical splices can fully develop bars to their fracture.
- **Time aspect:** Mechanical splices may reduce engineering design time since development length calculations may not be needed.
- **Congestion:** Mechanical splices reduce bar congestion especially at the joints.
- **Economic:** Mechanical splices may reduce the cost since lower steel is used.

2.4 Mechanical Bar Splices in Codes

Mechanical bar splices are usually classified in different codes based on their performance. The definition and requirements of couplers in ACI 318-14 (2014), AASTHO LRFD (2014), and Caltrans SDC (2010) are summarized herein.

2.4.1 Mechanical Bar Splices in Codes

Table 2-1 presents a summary of the US code requirements for mechanical bar splices. ACI classifies bar couplers as either Type 1 or Type 2. This classification is based on the strength that the coupler can develop. For example, a coupler that can withstand more than 1.25 times the yield strength is Type 1. Caltrans SDC (2013) allows "service" and "ultimate" couplers, which are calcified based on their strain capacity. AASHTO LRFD (2014) only allows couplers that can developed a minimum of 1.25 times the yield strength of the bar. Furthermore, couplers are allowed to be used in different locations of ductile members depends on their classification.

Table 1 Table 2-1. Mechanical bar splices in the US codes

Code	Splice Type	Stress Limit	Strain Limit	Max Slip	Location Restriction
ACI 318 (2014)	Type 1	≥ 1.25f_y	None	None	Shall not be used in the plastic hinge of ductile members of special moment frames neither in longitudinal nor in transvers bars (Article 18.2.7)
	Type 2	≥ 1.0f_u	None	None	Shall not be used within one-half of the beam depth in special moment frames but are allowed in any other members at any location (Articles 18.2.7 & 25.5.7)
Caltrans SDC (2013)	Service	None	> 2%	None	No splicing is allowed in "No-Splice Zone" of ductile members, which is the plastic hinge region. Ultimate splices are permitted outside of the "No-Splice Zone" for ductile members. Service splices are allowed in capacity protected members (Ch. 8)
	Ultimate	None	> 9% for No. 10 (32 *mm*) and smaller[a] > 6% for No. 11 (36 *mm*) and larger[a]	None	
AASHTO (2013 & 2014)	Full Mechanical Connection[b]	≥ 1.25f_y	None	No. 3-14: 0.01 *in*. No. 18: 0.03 *in*.	Shall not be used in plastic hinge of columns in SDC C and D (AASHTO Guide Spec 2014, Article 8.8.3)
Eurocode 8 (2004)	N.A.	N.A.	N.A.	N.A.	Cannot be used if couplers are not covered by appropriate testing under conditions compatible with the selected ductility class
NZS 3101 (1995)		≥ breaking strength of spliced reinforcing bar	< elongation occurrence of equal length of unspliced reinforcing bar under 0.7*fy*	N.A.	N.A.

Note: [a] For ASTM A706 Reinforcing Steel Bars. There is also a maximum strain demand limit (e.g. 2% for ultimate splices and 0.2% (the bar yield strain) for service splices) [Caltrans Memo to Designers 20-9].
[b]AASHTO LRFD (2013) Article 5.11.5.2.2.

2.4.2 Coupler Load Transfer Mechanism

Couplers are categorized based on their anchoring mechanism and also their performance in the previous sections. In addition to these variations, some couplers resist only compressive loads (Fig. 2-2a), some resists only tensile loads (Fig. 2-2b), and some can withstand both compressive and tensile loads (all couplers in Fig. 2-1). Since couplers suitable for bridge columns are the focus of this study, the load transfer mechanism of tension-compression couplers is discussed in this section.

.

a) Compression coupler (source www.theconstructor.org)

b) Tension coupler (source www.theconstructor.org)

Figure 2-2. Compression-only and tension-only mechanical bar splices

2.4.2.1 Threaded Couplers

Figure 2-3 shows one sample of threaded couplers in which bar ends are threaded and are engaged with the coupler internal threads to complete the splice. Threads can have different orientations and lengths. For example, regular threaded couplers have straight threads (running parallel). However, tapered threaded couplers have non-parallel threads in which bar diameter is reduced from the coupler ends toward the middle of the coupler. In some products, bar ends may be forged to be bigger in diameter thus after threading the ends won't be the weak link. Threaded couplers can be used in new construction or the repair of reinforced concrete structures.

Figure 2-3. One sample of threaded coupler

2.4.2.2 Headed Reinforcement Couplers

Figure 2-4 shows one sample of a headed coupler, which consists of male and female components with threads on the male component to be fit in internal threads of the female component. Bar ends are headed using a hydraulic jack. Headed reinforcement couplers can be used in new construction or the repair of reinforced concrete structures.

Figure 2-4. One sample of headed reinforcement coupler

2.4.2.2 Shear-Screw Couplers

Figure 2-5 shows one example of shear-screw couplers in which bars are connected to the steel sleeve utilizing screws. Since these couplers do no need bar end preparation, they can be installed quickly using simple tools. These couplers are usually used in new construction due to their large sizes. However, Yang et al. (2014) used these couplers in an experimental study to replace column fractured longitudinal bars with new ones.

Figure 2-5. One sample of shear screw coupler (www.bar-us.com)

2.4.2.3 Swaged Couplers

Figure 2-6 shows one example of swaged couplers. A swaged coupler consists of a seamless steel sleeve that is pressed to bars to provide mechanical interlock. Similar to

shear-screw couplers, these couplers are usually used in new construction due to their large sizes. However, Yang et al. (2014) used these couplers in an experimental study to replace column fractured longitudinal bars with new ones.

Figure 2-6. One sample of swaged coupler

2.4.2.4 Grouted Sleeve Couplers

Grouted sleeve couplers are made of grouted filled steel sleeves to connect bars through bond (Fig. 2-7). Grouted sleeve couplers are usually used in precast structures to connected precast elements.

a) Grouted sleeve coupler by Dayton Superior

b) Grouted sleeve coupler by NMB

Figure 2-7. Samples of grouted sleeve couplers

2.4.2.5 Hybrid Couplers

Couplers that use two of the abovementioned anchoring mechanisms are categorized as hybrid couplers. Figure 2-8 shows two samples of hybrid couplers: threaded-grouted (thread on one end of the coupler, grouted sleeve on another end), and threaded-swaged (two swaged pieces were connected at the middle using a threaded mechanism).

a) Threaded-grouted hybrid coupler

b) Threaded-swaged hybrid coupler

Figure 2-8. Samples of hybrid couplers

2.5 Testing Methods and Results from Previous Studies

A summary of standard testing methods, coupler acceptance criteria for ductile members, and a review of past experimental studies are presented in this section.

2.5.1 Testing Methods for Mechanical Bar Splices

Three testing standards are currently available for mechanical bar splices: ASTM A1034 (2016), Caltrans 670 (2004), and ISO (2009). The following section discusses the key testing methods specified in these standards.

2.5.1.1 ASTM A1034 (2016)

ASTM A1034 (2016) includes testing procedures for monotonic, full cyclic, high-cycle fatigue, slip, differential elongation, and low temperature tests. Nevertheless, this ASTM standard does not offer any acceptance criteria for couplers. A summary of monotonic and cyclic testing of couplers is presented herein.

2.5.1.1.1 Monotonic Tensile Testing

This test measures the performance of mechanical bar splices under increasing tensile loads. A specimen is placed in a testing machine and pulled to failure.

2.5.1.1.2 Full-Cycle Testing

This test is used to investigate how mechanical bar splices perform under alternating tensile and compressive loads. A specimen is placed in a testing machine and is loaded in tension, then in compression, and loading again in tension until a specified number of cycles is reached. Each cycle may exceed the yield strain of the bar and is intended to simulate the demands of earthquake loading on the specimen.

2.5.1.2 Caltrans 670 (2004)

Caltrans 670 (2004) includes testing procedure for slip test, tensile test, cyclic test and fatigue test. Nevertheless, this Caltrans 670 standard does not offer any acceptance criteria for couplers. A summary of tensile and monotonic testing of couplers is presented herein.

2.5.1.2.1 Monotonic Tensile Testing

Tensile testing must be done in general accordance with ASTM A 370 Sections 13 and A9.

a) Apply an axial tensile load to the sample sufficient to cause failure.

b) Document the maximum load obtained.

c) Calculate the ultimate tensile strength by dividing the maximum load by the sample's nominal cross-sectional area. ASTM A706, Table 1, provides the nominal cross-sectional areas for A 706 reinforcing steel. Record the ultimate tensile strength on the Test Form.

d) Check for necking.

2.5.1.2.2 Cyclic Testing

a) Cyclically load the sample from 5% to 90% of the specified yield strength (σy) of the sample for 100 cycles. Use a haversine waveform at 0.5 cps for No. 10, No. 11, No. 14, and No. 18 bars, and a haversine waveform at 0.7 cps for smaller bars. Record whether or not the sample fractures.

b) If sample does not fracture during the cyclical test, increase the axial tensile load until the sample fractures.

c) On the Test Form, record whether the sample passed the cyclical testing and, if applicable, the ultimate tensile strength, location of failure, and any necking.

2.5.1.3 International Organization for Standardization (ISO, 2009)

International Organization for standardization (ISO, 2009) includes testing procedure for tensile test, slip test, high cycle fatigue test and low cycle reverse loading test Nevertheless, and this standard does not offer any acceptance criteria for couplers. A summary of tensile and high cycle fatigue testing of couplers is presented herein.

2.5.1.3.1 Tensile Testing

The testing equipment shall conform to ISO 15630-1. The test shall be carried out according to ISO 15630-1. The A_{gt} in the spliced bar shall be tested and measured

according to ISO 15630-1 outside the length of the mechanical splice (as defined in ISO 15835-1) on both sides of the connection. Both values shall be recorded and the largest shall be used to assess conformity. However, if the length of the test piece has been reduced to accommodate the stroke of the testing machine, the A_{gt} may be measured on only one side of the connection. Where a transitional coupler is tested, A_{gt} is only measured on the smaller bar.

2.5.1.3.2 High Cycle Fatigue Testing

ISO has provided testing procedure for coupler under high cycle fatigue test as given below: This test measures the performance of mechanical bar splices under high cycle fatigue test. The test piece shall be gripped in the testing equipment in such a way that the force is transmitted axially and as much as possible free of any bending moment on the whole test piece. The frequency of load cycles shall be constant during the test and also during the test series. The frequency shall be between 1 Hz and 200 Hz. If the frequency is higher than 60 Hz, it shall be checked that the temperature of the test sample shall not exceed 40°C during the test. The test is terminated upon fracture of the test piece or upon reaching the specified number of cycles without fracture.

2.5.2 Acceptance Criteria for Couplers

It was disused that the standard testing methods currently do not provide acceptance criteria for mechanical bars splices. Furthermore, the requirements of current codes for couplers were reviewed in Section 2.4. These codes do not specify how and when a coupler can be allowed for incorporation in ductile members especially in the plastic hinge regions. This can be the reason why code requirements on couplers are mainly

force based not displacement based. New acceptance criteria are needed for successful incorporation of couplers in ductile members.

2.5.3 Past Studies

Tazarv and Saiidi (2016) performed a state-of-the-art review of mechanical bar splices and mechanically spliced columns. They also proposed acceptance criteria, material model, and design methods for couplers and columns with couplers. A summary of their findings is presented first. Then new coupler studies became available after Tazarv and Saiidi (2016) were reviewed.

2.5.3.1 Study by Tazarv and Saiidi (2016)

This study proposed minimum requirements for mechanical bar splices to be incorporated in plastic hinge regions of bridge columns as:

1) The total length of a mechanical bar splice (L_{sp}) should not exceed $15d_b$ (d_b is the diameter of the smaller of the two spliced bars).
2) A spliced bar should fracture outside coupler region regardless of the loading type (e.g. monolithic, cyclic, or dynamic). Only ASTM A706 reinforcement should be used in mechanically spliced bridge columns.

2.5.3.1.1 Coupler Stress-Strain Material Model

Figure 2-9(a) shows a mechanical bar splice and regions defined in Tazarv and Saiidi (2016). When a spliced bar is in tension, it can be assumed that only a portion of the coupler contributes to the overall elongation and the remaining portion of the coupler (βL_{sp}) is rigid due to its anchoring mechanism. The rigid portion of the coupler does not contribute to the total elongation of the splice and can be estimated using coupler rigid

length factor (β). This factor should be determined through experiments and might be different for different coupler sizes and types.

The coupler and bar regions can be identified for each mechanical bar splice as shown in Fig.2-9(a). The coupler region (L_{cr}) includes the coupler length (L_{sp}) plus α times the bar diameter ($\alpha.d_b$) from each end of the coupler. For the same tensile force, the coupler region axial deformation will be lower resulting in a lower strain in the coupler region (ε_{sp}) compared to the strain of the connecting reinforcing bar (ε_s) due to the coupler rigidity (Fig. 2-9(b)). Eq. 2-1 or 2-2 relates the coupler strains to a reference unspliced bar strains as:

$$\frac{\varepsilon_{sp}}{\varepsilon_s} = \frac{L_{cr} - \beta L_{sp}}{L_{cr}} \qquad \text{(Eq. 2-1)}$$

Or:

$$\frac{\varepsilon_{sp}}{\varepsilon_s} = \frac{(1-\beta)L_{sp} + 2\alpha d_b}{L_{sp} + 2\alpha d_b} \qquad \text{(Eq. 2-2)}$$

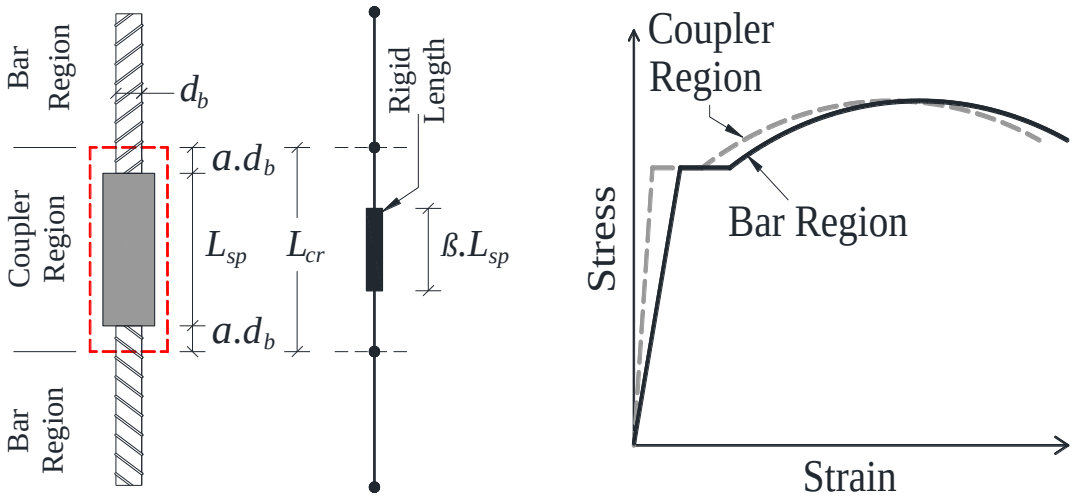

a) Coupler Region b) Stress-Strain Model for Couplers

Figure 2-9. Stress-strain model for mechanical bar splices (Tazarv and Saiidi (2016)

It can be assumed that the bar stress is independent of the presence of the coupler or its size, stiffness, and anchoring mechanism as long as the couplers are stronger than the connecting bars. It should be noted that couplers that are not at least as strong as the connecting bars are unacceptable.

Overall, the stress-strain relationship of any type of mechanical bar splices can be determined by knowing only the coupler rigid length factor (β). The condition in which $\beta = 0$ is similar to an unspliced connection in which the stress-strain of the coupler region is the same as the anchoring bar. Higher beta indicates that the coupler region strains are lower than those for unspliced bars at any given stress.

2.5.3.2 Study by Haber et al. (2014)

Figure 2-10 shows the application of headed coupler (HC) and grouted coupler (GC) in column tested by Haber et al (2014). Their focus of study was to develop a new moment connection at column –footing joints for accelerated bridge construction in regions of high seismicity. Therefore, they conducted a large scale experimental test in four precast models with different column- footing detail. Among them, two were connected directly to the footing without pedestal which was denoted by NP and two others were connected at a top of precast pedestal which was denoted by PP.

Figure 2-10 shows the force-displacement response of four columns test under cyclic loading. The force displacement relationship for column with headed coupler (HC) was approximately similar to the cast in situ (CIP) model. In case of column with grouted coupler (GC) models, they completed one full cycle at the drift ratio of 6%, while cast in situ (CIP) completed one full cycle at 10% drift ratio.

Looking through these test results, they concluded that mechanical bar splices are practical option for use in accelerated bridge construction in seismic zones.

a) Headed Reinforcement Connection b) Grouted coupler Connection

Figure 2-10. Precast column adopting Coupler in column-footing connection tested by Haber, Saiidi and Sanders (2014)

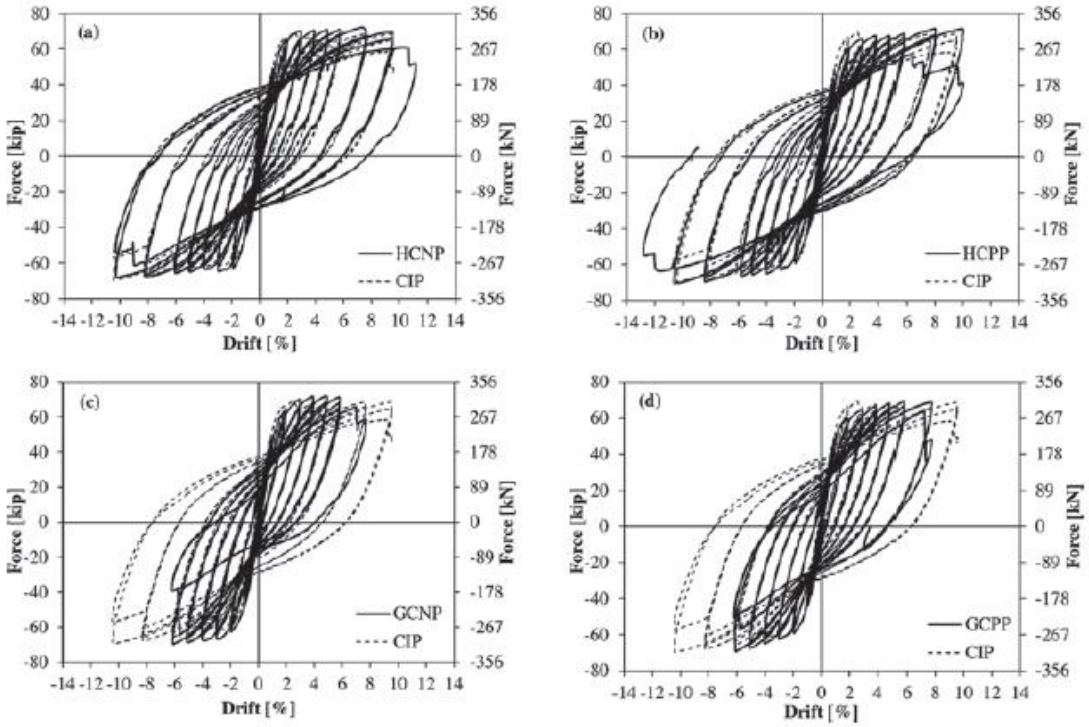

Figure 2-11. Force displacement response of different columns tested by Haber, Saiidi and Sanders (2014)

2.5.3.3 Study by Bompa and Elghazouli (2017)

Figure 2-12 shows a different type of mechanical reinforcement coupling system tested by Bompa and Elghazouli (2017). They tested 511 mechanical bar splices under monotonic -and cyclic loading to failure. Of which, 244 were mechanical interlock type (UHC, PTC, TTC, RTC, BLC, OBLC, SWC, OSWC, MFC) and 267 were grouted sleeve couplers (GSC). They used L_{sp}+ $4d_b$ as the coupler region.

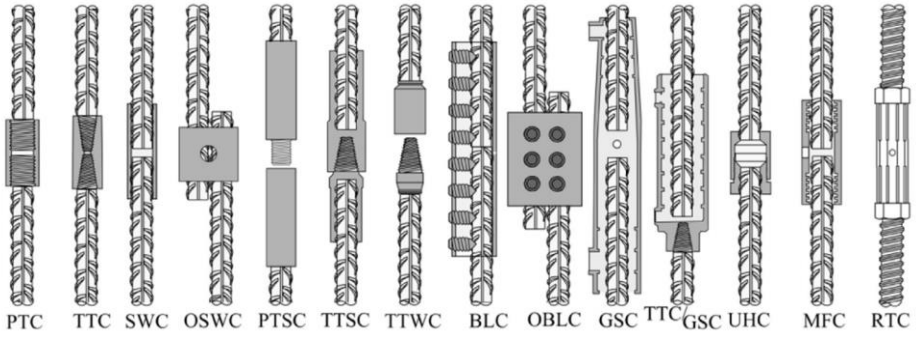

Figure 2-12. Different type of reinforcing coupling system tested by Bompa and Elghazouli (2017)

Figure 2-13 (d) shows the "diameter ratio" as the ratio of the coupler dimeter to the bar diameter. Figure 2-13 (c) shows the "ductility" as the ratio of coupler region ultimate strain to the bar ultimate strain. The ductility was significantly reduced when used with mechanical bar splices.

Figure 2-14 shows a summary of the test results. The strain capacities of the splice bars were up to 50% lower than their reference bar strains.

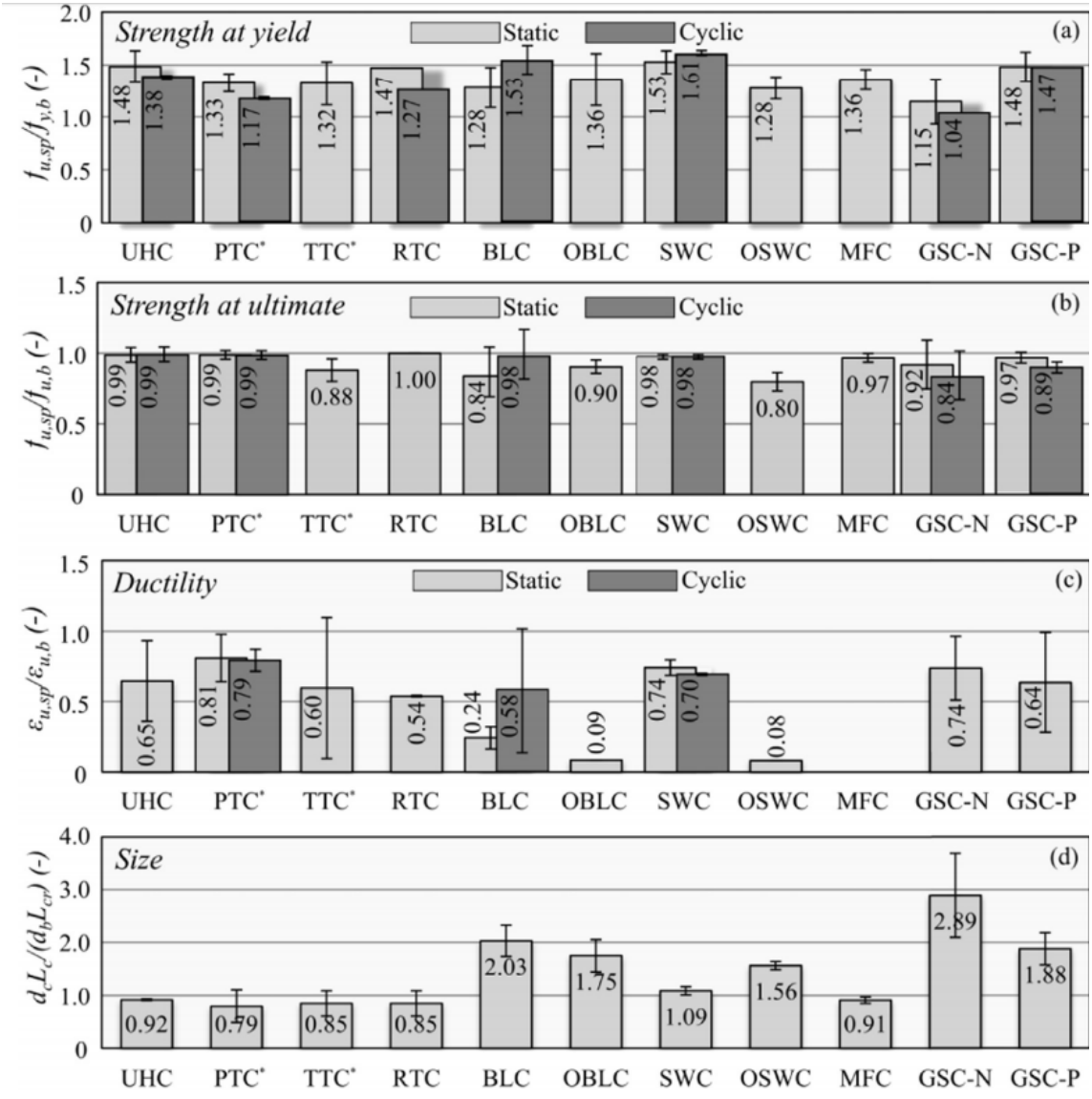

Figure 2-13. Comparative performance of mechanical splices

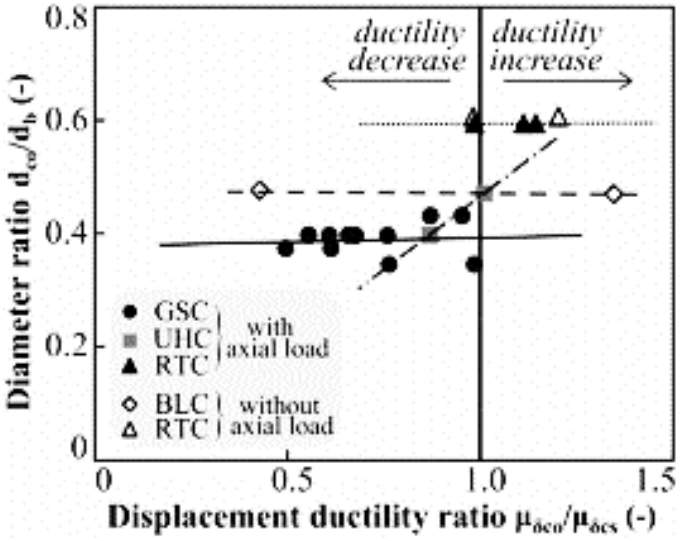

Figure 2-14. Relationship between size and strain capacity of mechanical bar splices tested by Bompa and Elghazouli (2017)

2.6 References

AASHTO LRFD (2014). "AASHTO Guide Specifications for LRFD Seismic Bridge Design," Washington, D.C., American Association of State Highway and Transportation Officials.

AASHTO SGS (2011) "AASHTO Guide Specifications for Seismic Bridge Design," Washington, D.C., American Association of State Highway and Transportation Officials.

ACI 439.3R-07. (2007). "Types of Mechanical Splices for Reinforcing Bars," Reported by American Concrete Institute Committee 439, 24 pp.

ACI 318-14. (2014). "Building Code Requirement for Structural Concrete and Commentary," Reported by American Concrete Institute Committee.

ASTM A1034 (2016). "Standard Test Methods for Testing Mechanical Splices for Steel Reinforcing Bars." ASTM International, West Conshohocken, PA.

ASTM A706 (2009). "Standard Specification for Low-Alloy Steel Deformed and Plain Bars for Concrete Reinforcement." West Conshohocken, PA, 6 pp.

Bompa, D.V and Elghazouli, A.Y (2017). "Ductility considerations for mechanical reinforcement couplers," Structures, pp115-119.

California Test 670. (2004). "Method of Tests for Mechanical and Welded Reinforcing Steel Splices," Sacramento, CA, California Department of Transportation.

Caltrans SDC (2010). "Seismic Design Criteria," Version 1.6. Sacramento, CA, California Department of Transportation.

Caltrans (2015). "Authorized List of Couplers for Reinforcing Steel". Sacramento, CA, California Department of Transportation, September 21.

Eurocode 8 (2004). “Design of Structures for Earthquake Restistance -part 1: General Rules, Seismic Actions and Rules for Buildings” London, UK.

Haber, ZB, Saiidi, MS, and Sanders, DH. (2015), “Behavior and Simplified Modeling of Mechanical Reinforcing Bar Splices.” ACI structure Journal, Vol. 112, No. 2, pp. 179-88

Haber, ZB, Saiidi, MS, and Sanders, DH (2013). “Precast Column Footing Connections for Accelerated Bridge Construction in Seismic Zones.” Rep. No. CCEER 13-08 Center for Civil Engineering Earthquake Research, Dept. of Civil and Environmental Engineering, Univ. of Nevada, Reno. NV.

Hurd, M.K (1998). “Mechanical vs. Lap Splicing” The Aberdeen Group, Publication No. C980683

Taskin, K., and Peker, K (2015). “Assessing and Evaluation of the Mechanical Properties of Reinforcement Coupler Systems in Turkey.” SMAR 2015-Third Conference on Smart Monitoring Assessment and Rehabilitation of Civil Structures

ISO (2009). “Steels for the Reinforcements of Concrete-Reinforcement Couplers for Mechanical Splices of Bars (part-1 and Part- 3),” International Organizationa for Standardization, Geneva, Switzerland.

Scott, M., and Fenves, G. (2006). “Plastic Hinge Integration Methods for Force-Based Beam-Column Elements.” Journal of Structural Engineering, ASCE, 10.1061/ (ASCE) 0733-9445(2006)132:2(244), 244–252.

Tazarv, M. and Saiidi, M.S. (2015). “Design and Construction of Bridge Columns Incorporating Mechanical Bar Splices in Plastic Hinge Zones.” Center for Civil

Engineering Earthquake Research, Department of Civil and Environmental Eng, University of Nevada; 2014. P. 400. Report No. CCEER-14-06.

Tazarv, M. and Saiidi, M.S. (2016). "Seismic Design of Bridge Columns Incorporating Mechanical Bar Splices in Plastic Hinge Regions," Engineering Structures, DOI: 10.1016/j.engstruct.2016.06.041, Vol 124, pp. 507-520.

Yang, Y., Sneed, L.H., Morgan, A., Saiidi, M.S., Belarbi, A. (2014). "Repair of Earthquake-Damaged Bridge Columns with Interlocking Spirals and Fractured Bars," California Department of Transportation Report No. CA 14-2179, 211 pp.

Chapter 3. Test Matrix, Test Setup, and Loading Protocols for Mechanical Bar Splices

3.1 Introduction

Different mechanical bar splices (commonly referred to as bar couplers), their splicing mechanism, minimum code requirements, and acceptance criteria for mechanical bar splices were discussed in Ch. 2. Based on the minimum requirements and their availability, more than 270 couplers including nine different types were collected from six manufacturers. Subsequently, more than 160 of which were tested under uniaxial tensile monotonic and cyclic loading to failure in the Lohr Structures laboratory at South Dakota State University to determine their mechanical properties. This chapter discusses the test matrix, the test setup, specimen preparations, and loading protocols for mechanical bar splices. The test results are presented in the following chapter.

3.2 Test Matrix for Mechanical Bar Splices

The selection process for coupler test specimens and the test matrix are discussed herein.

3.2.1 Selection of Coupler Test Specimens

There are more than ten coupler manufacturers in the United States of America at the time of this writing, whom produces more than 60 coupler products. Furthermore, some

of these manufactures produce the same types of couplers (coupler types were discussed in Sec. 2.4). Therefore, a set of selection criteria was needed to identify couplers that could be potentially used in plastic hinge regions of ductile members.

The minimum requirements of the US codes on mechanical bar splices and the results from previous studies were used to select coupler test specimens in the present study. Different coupler types were categorized in Sec. 2.4. The Caltrans, ACI, and AASHTO requirements on couplers were presented in Sec. 2.4.1. Only those couplers that can potentially fracture bars were selected for testing. Such a coupler may have been labeled as ACI Type 2 coupler, Caltrans Ultimate coupler, and AASHTO Full Mechanical Connection.

All coupler types in the US market were reviewed based on the abovementioned selection criteria and a list was developed as presented in Table 3-1. Note Caltrans has a list of pre-approved couplers (Appendix A) and manufacturers usually include the code certificates in their brochures. Code compliance information in the table was extracted from the Caltrans list or the product datasheets.

Table 3-1. Selected couplers for uniaxial testing

Coupler Type	Coupler Manufacturer	Coupler Model	ACI Coupler Types		Caltrans Coupler Types		AASHTO Coupler Type
			Type 1	Type 2	Service Splice	Ultimate Splice	Full Mechanical Connection (FMC)
Shear Screw Coupler	Erico International Corp.	LENTON® LOCK (B1 Series)		X		X	N.A.
Headed Bar Coupler	Headed Reinforcement Corp.	Xtender® 500/510 Standard Coupler		X		X	N.A.
Grouted Sleeve Coupler	Datyon Superior	D410 Sleeve-Lock® Grout Sleeve		X		X	X
	Splice Sleeve North America	NMB		X	X		N.A.
Threaded Coupler	Dextra America,Inc	Bartec Standard Splice (type A)		X		X	N.A.
	Dextra America,Inc	Bartec Position Splices (Type B)		X		X	N.A.
	Erico International Corp.	LENTON® PLUS, Standard Coupler, (A12)		X		X	X
Swaged Coupler	Bar Splice	BarGrip® XL		X		X	N.A.
Hybrid Coupler	Dextra America, Inc	Griptec®		X		X	N.A.
	Erico International Corp.	Lenton Interlock		X	X		N.A.

3.2.2 Test Matrix

Tables 3-2 to 3-6 present the selected couplers for testing, and include the coupler information, the specimen name, the specimen identification (ID), the bar size, and the loading protocol. The right column of the tables presents the geometry of the test specimen. The specimen naming guide is presented in the following section. Note for each spliced specimen, at least one unspliced bar was tested as the reference sample.

During the period of this study, the selected shear screw coupler (Table 3-1) was not available in the market due to a change/shortage in the supply chain. Therefore, no test

was performed on shear screw couplers. Other available shear screw couplers cannot develop the full strength of the bar.

Table 3-2. Test matrix for headed reinforcement couplers

Product Details	Specimen Name	Specimen ID	Bar Size	Loading Type	Sample Geometry (in.)
Coupler Type: Headed Bar **Manufacturer:** Headed Reinforcement Corp **Model No:** Xtender® 500/510 Standard Coupler	HR-1	HR-5-M(HR-2)	No.5 (16 mm)	Monotonic	L_{sp} = 2.4 L_{cr} = 4.9 L_{tot} = 20
	HR-2	HR-5-M(HR-2)			
	HR-3	HR-5-M(HR-3)			
	HR-4	HR-5-C(HR-4)		Cyclic	L_{sp} = 2.4 L_{cr} = 4.9 L_{tot} = 20
	HR-5	HR-5-C(HR-5)			
	HR-6	HR-5-C(HR-6)			
	HR-7	HR-8-M(HR-7)	No.8 (25 mm)	Monotonic	L_{sp} = 3.25 L_{cr} = 5.75 L_{tot}= 31.25
	HR-8	HR-8-M(HR-8)			
	HR-9	HR-8-M(HR-9)			
	HR-10	HR-8-C(HR-10)		Cyclic	L_{sp} = 3.25 L_{cr} = 5.75 L_{tot} = 31.25
	HR-11	HR-8-C(HR-11)			
	HR-12	HR-8-C(HR-12)			
	HR-13	HR-10-M(HR-13)	No.10 (32 mm)	Monotonic	L_{sp} = 3.88 L_{cr} = 7.00 L_{tot} = 31.875
	HR-14	HR-10-M(HR-14)			
	HR-15	HR-10-M(HR-15)			
	HR-16	HR-10-C(HR-16)		Cyclic	L_{sp} = 3.88 L_{cr} = 7.00 L_{tot} = 31.875
	HR-17	HR-10 -C(HR-17)			
	HR-18	HR-10-C (HR-18)			

Note: L_{sp} is the coupler length, L_{cr} is the coupler region length, and L_{tot} is the grip-to-grip length of the test specimen
1 *in. = 25.4 mm*

Table 3-3. Test matrix for threaded couplers

Product Details	Specimen Name	Specimen ID	Bar Size	Loading Type	Sample Geometry (in.)
Coupler Type: Threaded **Manufacturer:** Dextra America,Inc **Model No:** Bartec Standard Splice (type A)	TH-1	TH-5-M(TH-1)	No.5 (16 mm)	Monotonic	L_{sp} = 1.75 L_{cr} = 4.25 L_{tot} = 21.25
	TH-2	TH-5-M(TH-2)			
	TH-3	TH-5-M(TH-3)			
	TH-4	TH-5-C(TH-4)		Cyclic	L_{sp} = 1.75 L_{cr} = 4.25 L_{tot} = 21.25
	TH-5	TH-5-C(TH-5)			
	TH-6	TH-5-C(TH-6)			
	TH-7	TH-8-M(TH-7)	No.8 (25 mm)	Monotonic	L_{sp} = 2.63 L_{cr} = 5.13 L_{tot} = 30.63
	TH-8	TH-8-M(TH-8)			
	TH-9	TH-8-M(TH-9)			
	TH-10	TH-8-C(TH-10)		Cyclic	L_{sp} = 2.63 L_{cr} = 5.13 L_{tot} = 30.63
	TH-11	TH-8-C(TH-11)			
	TH-12	TH-8-C(TH-12)			
	TH-13	TH-10-M(TH-13)	No.10 (32 mm)	Monotonic	L_{sp} = 3.06 L_{cr} = 6.03 L_{tot} = 31.00
	TH-14	TH-10-M(TH-14)			
	TH-15	TH-10-M(TH-15)			
	TH-16	TH-10-C(TH-16)		Cyclic	L_{sp} = 3.06 L_{cr} = 6.03 L_{tot} = 31.0
	TH-17	TH-10-C(TH-17)			
	TH-18	TH-10-C(TH-18)			
Coupler Type: Threaded **Manufacturer:** Dextra America,Inc **Model No:** Bartec Standard Splice (type B)	TH-19	TH-5-M(TH-19)	No.5 (16 mm)	Monotonic	L_{sp} = 1.75 L_{cr} = 4.25 L_{tot} = 21.25
	TH-20	TH-5-M(TH-20)			
	TH-21	TH-5-M(TH-21)			
	TH-22	TH-5-C(TH-22)		Cyclic	L_{sp} = 1.75 L_{cr} = 4.25 L_{tot} = 21.25
	TH-23	TH-5-C(TH-23)			
	TH-24	TH-5-C(TH-24)			
	TH-25	TH-8-M(TH-25)	No.8 (25 mm)	Monotonic	L_{sp} = 2.63 L_{cr} = 5.13 L_{tot} = 30.63
	TH-26	TH-8-M(TH-26)			
	TH-27	TH-8-M(TH-27)			
	TH-28	TH-8-C(TH-28)		Cyclic	L_{sp} = 2.63 L_{cr} = 5.13 L_{tot} = 30.63
	TH-29	TH-8-C(TH-29)			
	TH-30	TH-8-C(TH-30)			
	TH-31	TH-10-M(TH-31)	No.10 (32 mm)	Monotonic	L_{sp} = 3.06 L_{cr} = 6.03 L_{tot} = 31.00
	TH-32	TH-10-M(TH-32)			
	TH-33	TH-10-M(TH-33)			
	TH-34	TH-10-C(TH-34)		Cyclic	L_{sp} = 3.06 L_{cr} = 6.03 L_{tot} = 31.00
	TH-35	TH-10-C(TH-35)			
	TH-36	TH-10-C(TH-36)			

Note: L_{sp} is the coupler length, L_{cr} is the coupler region length, and L_{tot} is the grip-to-grip length of the test specimen
1in. = 25.4 mm

Table 3-3. Continued…

Coupler Type: Threaded **Manufacturer:** Erico International Corp. **Model No:** LENTON® PLUS Standard Coupler (A12)	TH-37	TH-5-M(TH-37)	No.5 (16 mm)	Monotonic	L_{sp} = 2.38 L_{cr} = 4.88 L_{tot} = 35.5
	TH-38	TH-5-M(TH-38)			
	TH-39	TH-5-M(TH-39)			
	TH-40	TH-5-C(TH-40)		Cyclic	L_{sp} = 2.38 L_{cr} = 4.88 L_{tot} = 21.25
	TH-41	TH-5-C(TH-41)			
	TH-42	TH-5-C(TH-42)			
	TH-43	TH-8-M(TH-43)	No.8 (25 mm)	Monotonic	L_{sp} = 3.75 L_{cr} = 6.25 L_{tot} = 33.5
	TH-44	TH-8-M(TH-44)			
	TH-45	TH-8-M(TH-45)			
	TH-46	TH-8-C(TH-46)		Cyclic	L_{sp} = 3.75 L_{cr} = 6.25 L_{tot} = 33.5
	TH-47	TH-8-C(TH-47)			
	TH-48	TH-8-C(TH-48)			
	TH-49	TH-10-M(TH-49)	No.10 (32 mm)	Monotonic	L_{sp} = 4.20 L_{cr} = 7.38 L_{tot} = 37.00
	TH-50	TH-10-M(TH-50)			
	TH-51	TH-10-M(TH-51)			
	TH-52	TH-10-C(TH-52)		Cyclic	L_{sp} = 4.20 L_{cr} = 7.38 L_{tot} = 37.00
	TH-53	TH-10-C(TH-53)			
	TH-54	TH-10-C(TH-54)			

Note: L_{sp} is the coupler length, L_{cr} is the coupler region length, and L_{tot} is the grip-to-grip length of the test specimen
1in. = 25.4 mm

Table 3-4. Test matrix for swaged couplers

Product Details	Specimen Name	Specimen ID	Bar Size	Loading Type	Sample Geometry (in.)
Coupler Type: Swaged Coupler **Manufacturer:** Bar Splice **Model No:** BarGrip® XL	SW-1	SW-5-M(SW-1)	No.5 (16 mm)	Monotonic	L_{sp} = 5.25 L_{cr} = 7.75 L_{tot} = 21.25
	SW-2	SW-5-M(SW-2)			
	SW-3	SW-5-M(SW-3)			
	SW-4	SW-5-C(SW-4)		Cyclic	L_{sp} = 5.25 L_{cr} = 7.75 L_{tot} = 21.25
	SW-5	SW-5-C(SW-5)			
	SW-6	SW-5-C(SW-6)			
	SW-7	SW-8-M(SW-7)	No.8 (25 mm)	Monotonic	L_{sp} = 7.90 L_{cr} = 10.4 L_{tot}= 39.00
	SW-8	SW-8-M(SW-8)			
	SW-9	SW-8-M(SW-9)			
	SW-10	SW-8-C(SW-10)		Cyclic	L_{sp} = 7.90 L_{cr} = 10.40 L_{tot} = 39.00
	SW-11	SW-8-C(SW-11)			
	SW-12	SW-8-C(SW-12)			
	SW-13	SW-10-M(SW-13)	No.10 (32 mm)	Monotonic	L_{sp} = 9.50 L_{cr} = 12.68 L_{tot} = 40.00
	SW-14	SW-10-M(SW-14)			
	SW-15	SW-10-M(SW-15)			
	SW-16	SW-10-C(SW-16		Cyclic	L_{sp} = 9.50 L_{cr} = 12.68 L_{tot} = 40.00
	SW-17	SW-10-C(SW-17)			
	SW-18	SW-10-C(SW-18)			

Note: L_{sp} is the coupler length, L_{cr} is the coupler region length, and L_{tot} is the grip-to-grip length of the test specimen
1in. = 25.4 mm

Table 3-5. Test matrix for grouted sleeve couplers

Product Details	Specimen Name	Specimen ID	Bar Size	Loading Type	Sample Geometry (in.)
Coupler Type: Splice Sleeve North America **Manufacturer:** Splice Sleeve North America **Model No:** NMB	GS-1	GS-5-M(GS-1)	No.5 (16 mm)	Monotonic	L_{sp} = 9.63 L_{cr} = 12.13 L_{tot} = 36.50
	GS-2	GS-5-M(GS-2)			
	GS-3	GS-5-M(GS-3)			
	GS-4	GS-5-C(GS-4)		Cyclic	L_{sp} = 9.63 L_{cr} = 12.13 L_{tot} = 36.50
	GS-5	GS-5-C(GS-5)			
	GS-6	GS-5-C(GS-6)			
	GS-7	GS-8-M(GS-7)	No.8 (25 mm)	Monotonic	L_{sp} = 14.50 L_{cr} = 17.00 L_{tot} = 38.50
	GS-8	GS-8-M(GS-8)			
	GS-9	GS-8-M(GS-9)			
	GS-10	GS-8-C(GS-10)		Cyclic	L_{sp} = 14.50 L_{cr} = 17.00 L_{tot} = 38.50
	GS-11	GS-8-C(GS-11)			
	GS-12	GS-8-C(GS-12)			
	GS-13	GS-10-M(GS-13)	No.10 (32 mm)	Monotonic	L_{sp} = 18.00 L_{cr} = 21.20 L_{tot} = 43.00
	GS-14	GS-10-M(GS-14)			
	GS-15	GS-10-M(GS-15)			
	GS-16	GS-10-C(GS-16)		Cyclic	L_{sp} = 18.00 L_{cr} = 21.20 L_{tot} = 43.00
	GS-17	GS-10-C(GS-17)			
	GS-18	GS-10-C(GS-18)			
Coupler Type: Splice Sleeve North America **Manufacturer:** Datyon Superior **Model No:** D410 Sleeve-Lock® Grout Sleeve	GS-19	GS-5-M(GS-19)	No.5 (16 mm)	Monotonic	L_{sp} = 9.50 L_{cr} = 12.00 L_{tot} = 36.50
	GS-20	GS-5-M(GS-20)			
	GS-21	GS-5-M(GS-21)			
	GS-22	GS-5-C(GS-22)		Cyclic	L_{sp} = 9.50 L_{cr} = 12.00 L_{tot} = 36.50
	GS-23	GS-5-C(GS-23)			
	GS-24	GS-5-C(GS-24)			
	GS-25	GS-8-M(GS-25)	No.8 (25 mm)	Monotonic	L_{sp} = 9.50 L_{cr} = 12.00 L_{tot} = 36.50
	GS-26	GS-8-M(GS-26)			
	GS-27	GS-8-M(GS-27)			
	GS-28	GS-8-C(GS-28)		Cyclic	L_{sp} = 9.50 L_{cr} = 12.00 L_{tot} = 36.50
	GS-29	GS-8-C(GS-29)			
	GS-30	GS-8-C(GS-30)			
	GS-31	GS-10-M(GS-31)	No.10 (32 mm)	Monotonic	L_{sp} = 9.50 L_{cr} = 12.68 L_{tot} = 40.00
	GS-32	GS-10-M(GS-32)			
	GS-33	GS-10-M(GS-33)			
	GS-34	GS-10-C(GS-34)		Cyclic	L_{sp} = 9.50 L_{cr} = 12.68 L_{tot} = 40.00
	GS-35	GS-10-C(GS-35)			
	GS-36	GS-10-C(GS-36)			

Note: L_{sp} is the coupler length, L_{cr} is the coupler region length, and L_{tot} is the grip-to-grip length of the test specimen
1in. =25.4 mm

Table 3-6. Test matrix for hybrid couplers

Product Details	Specimen Name	Specimen ID	Bar Size	Loading Type	Sample Geometry (in.)
Coupler Type: Hybrid **Manufacturer:** Dextra America**,Inc** **Model No:** Griptec®	HY-1	HY-5-M(HY-1)	No.5 (16 mm)	Monotonic	L_{sp} = 8.13 L_{cr} = 10.63 L_{tot} = 32.12
	HY-2	HY-5-M(HY-2)			
	HY-3	HY-5-M(HY-3)			
	HY-4	HY-5-C(HY-4)		Cyclic	L_{sp} = 8.13 L_{cr} = 10.63 L_{tot} = 32.12
	HY-5	HY-5-C(HY-5)			
	HY-6	HY-5-C(HY-6)			
	HY-7	HY-8-M(HY-7)	No.8 (25 mm)	Monotonic	L_{sp} = 9.31 L_{cr} = 11.81 L_{tot} = 39.25
	HY-8	HY-8-M(HY-8)			
	HY-9	HY-8-M(HY-9)			
	HY-10	HY-8-C(HY-10)		Cyclic	L_{sp} = 9.31 L_{cr} = 11.81 L_{tot} = 39.25
	HY-11	HY-8-C(HY-11)			
	HY-12	HY-8-C(HY-12)			
	HY-13	HY-10-M(HY-13)	No.10 (32 mm)	Monotonic	L_{sp} = 10.63 L_{cr} = 13.8 L_{tot} = 40.00
	HY-14	HY-10-M(HY-14)			
	HY-15	HY-10-M(HY-15)			
	HY-16	HY-10-C(HY-16)		Cyclic	L_{sp} = 10.63 L_{cr} = 13.8 L_{tot} = 40.00
	HY-17	HY-10-C(HY-17)			
	HY-18	HY-10-C(HY-18)			
Coupler Type: Hybrid **Manufacturer:** Erico **International Corp.** **Model No:** Lenton Interlock	HY-19	HY-5-M(HY-19)	No.5 (16 mm)	Monotonic	L_{sp} = 7.88 Lcr = 10.38 L_{tot} = 40.00
	HY-20	HY-5-M(HY-20)			
	HY-21	HY-5-M(HY-21)			
	HY-22	HY-5-C(HY-22)		Cyclic	L_{sp} = 7.88 L_{cr} = 10.38 L_{tot} = 40.00
	HY-23	HY-5-C(HY-23)			
	HY-24	HY-5-C(HY-24)			
	HY-25	HY-8-M(HY-25)	No.8 (25 mm)	Monotonic	L_{sp} = 8.75 L_{cr} = 11.25 Lt_{ot} = 39.25
	HY-26	HY-8-M(HY-26)			
	HY-27	HY-8-M(HY-27)			
	HY-28	HY-8-C(HY-28)		Cyclic	L_{sp} = 8.75 L_{cr} = 11.25 Lt_{ot} = 39.25
	HY-29	HY-8-C(HY-29)			
	HY-30	HY-8-C(HY-30)			
	HY-31	HY-10-M(HY-31)	No.10 (32 mm)	Monotonic	L_{sp} = 10.75 L_{cr} = 13.93 L_{tot} = 40.00
	HY-32	HY-10-M(HY-32)			
	HY-33	HY-10-M(HY-33)			
	HY-34	HY-10-C(HY-34)		Cyclic	L_{sp} = 10.75 L_{cr} = 13.93 L_{tot} = 40.00
	HY-35	HY-10-C(HY-35)			
	HY-36	HY-10-C(HY-36)			

Note: L_{sp} is the coupler length, L_{cr} is the coupler region length, and L_{tot} is the grip-to-grip length of the test specimen
1in. =25.4 mm

3.2.3 Test Specimen Nomenclature System

A naming system including the coupler type, bar size, loading protocol, and a specific ID was developed to quickly identify each test specimen. Figure 3-1 shows the naming system for a coupler.

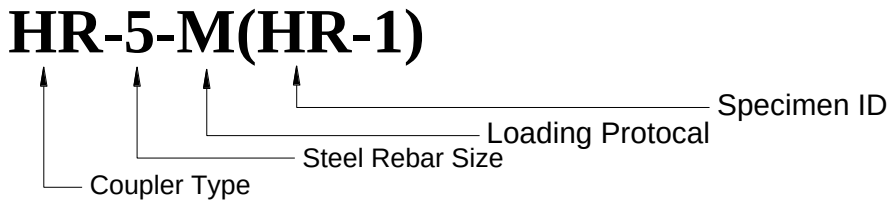

Figure 3-1. Coupler test specimen name guide

The following describes each portion of the specimen name:

- The first term indicates the coupler type as:

  SS: Shrew Screw coupler

  HR: Headed Reinforcement coupler

  SW: Swaged coupler

  TH: Threaded coupler

  GS: Grouted Sleeve coupler

  HY: Hybrid coupler

- The second term refers to the bar size which can be No. 5 (16 mm), No. 8 (25 mm), or No. 10 (32 mm).
- The third term indicates the loading type, which can be monotonic (M) or cyclic (C).
- The term in the parenthesis is a specific ID assigned to each coupler type as presented in Tables 3-2 to 3-6.

Note for each spliced specimen, at least one unspliced bar was tested as a reference sample, which were named similar to the corresponding coupler but adding Ref. at the end (e.g., HR-5-M(HR-1)-Ref).

3.3 Test Setup for Mechanical Bar Splices

Figure 3-2 shows the test setup for mechanical bar splices including a static universal testing machine, its hydraulic system and controller, and one test specimen with an extensometer specifically developed for couplers.

The universal testing machine can accommodate samples with a maximum length of 43 in. (110 cm). The total stroke of the machine is 7 in. (18 cm). The machine force capacity is 135 kips (600 kN) both in tension and compression.

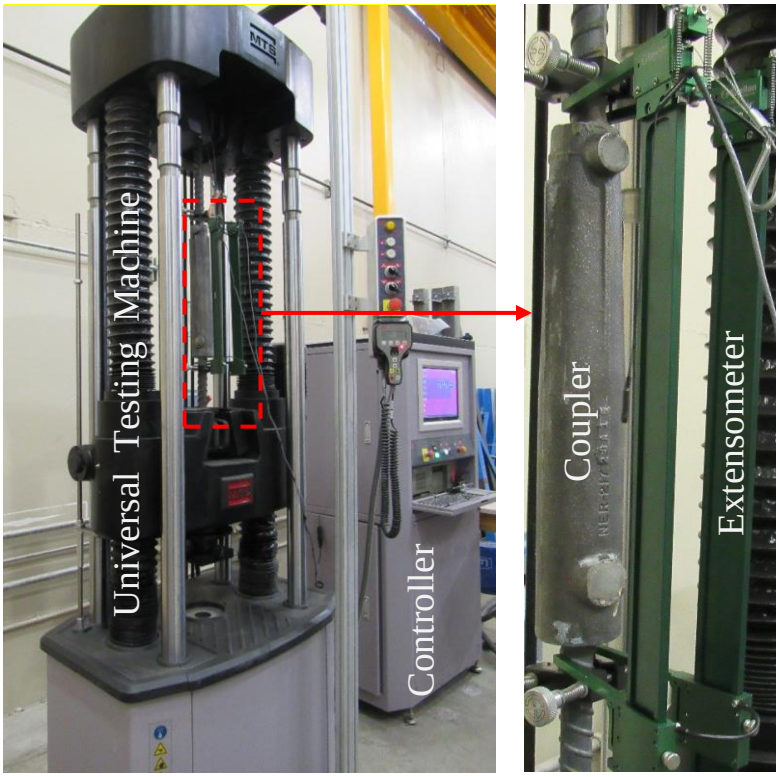

Figure 3-2. Test setup for mechanical bar splices

A unified geometry was needed for all test specimens to minimize variations in the results. Figure 3-3 shows the selected geometry for reference unspliced bars (according to ASTM E8, 2012) and spliced specimens, which was developed based on the requirements presented in ASTM A1034 (2015) and Caltrans 670 (2004). The total specimen length (L_{tot}) depends on the size of the bar and the length of the mechanical bar splice (L_{sp}). The coupler region length (L_{cr}) is defined as the coupler length plus α times the bar diameter ($\alpha . d_b$) from each side of the coupler ends. Alpha was not more than twice the bar diameter in the present study according to the ASTM A1034 (2015). The bar length outside the coupler region to the grip was at least six times the bar diameter to avoid localized failure. ASTM E8 (2011) requires at least $5d_b$ clear length for testing of a regular bar.

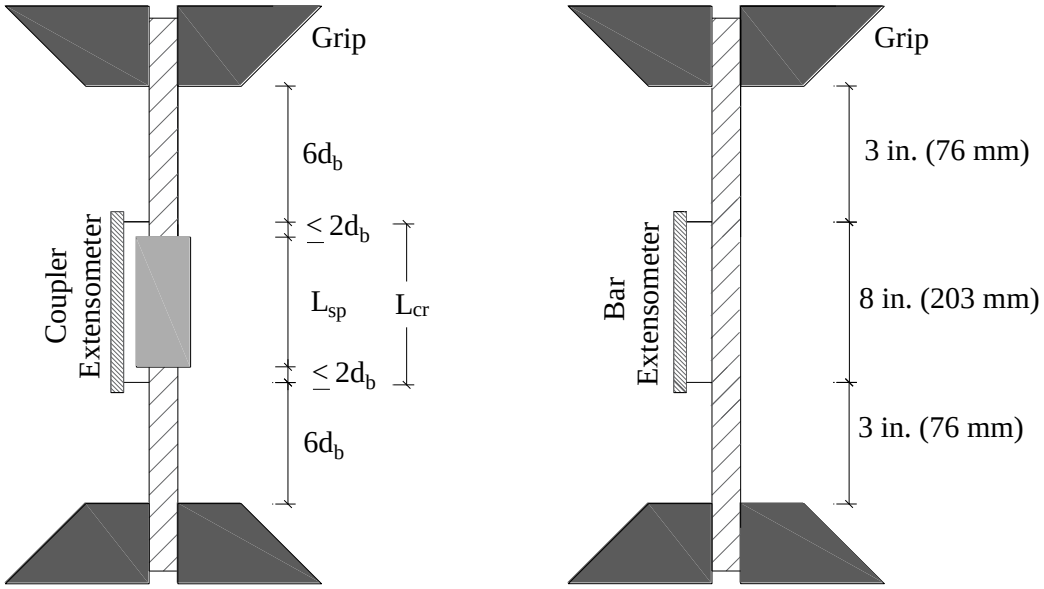

Figure 3-3. Geometry of spliced and unspliced specimen

3.3.1 Instrumentation

Figure 3-4 shows two different types of extensometers that were used to measure the strains of spliced and unspliced specimens. The bar extensometer (Fig. 3-4a) had a 4-in. (100-mm) stroke and could measure strains until the fracture of the bar. The accuracy of the bar extensometer was A-1 according to ASTM E83 (2010). The coupler extensometer (Fig. 3-4b), which was a new product by Epsilon, was specifically made for mechanical bar splices and its properties were modified based on the findings of the present study. The main modification was to increase the measuring length of the device from 0.5 in. (12 mm) to 1.5 in. (38 mm) to include long couplers. The accuracy of this extensometer meets the requirements of a B-1 device according to ASTM E83 (2010).

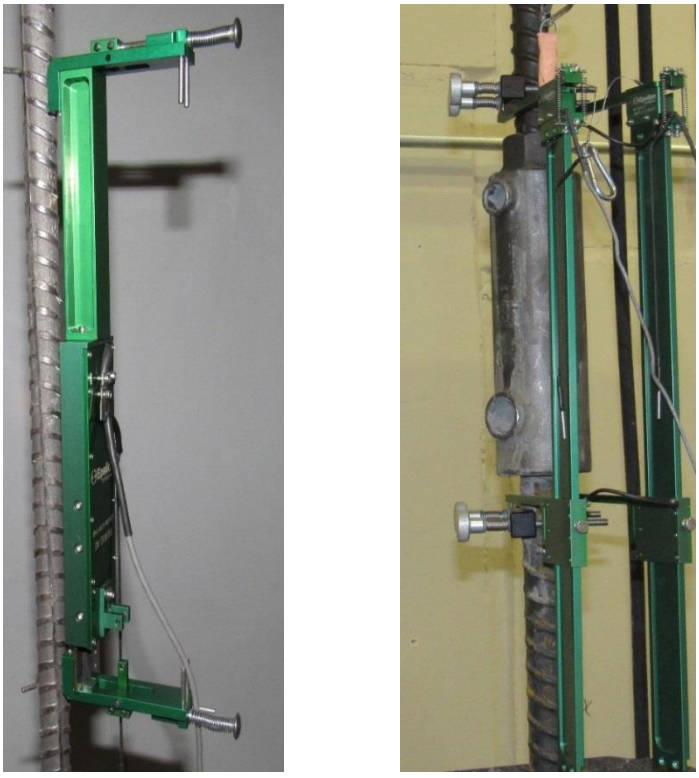

a. Bar extensometer b. Coupler extensometer

Figure 3-4. Extensometers used for unspliced and spliced specimens

Furthermore, the universal testing machine provides loads with an accuracy of 0.224 lb. (1.0 N) and head displacements with an accuracy of 3.9×10^{-6} in. (0.0001 mm).

3.4 Mechanical Bar Splice Preparation

Figures 3-5 to 3-13 show the mechanical bar splice specimens before and after the full assembly. Bar end preparation and coupler assembly are different for each product, and the manufacturer's requirements should be followed. Depending on the type, the coupler preparation time may vary from a few minutes to a few days. For example, a threaded coupler, which may not need any field bar end preparation, can be assembled within a few minutes. While, a grouted sleeve coupler may need at least four days for the grout to cure and to gain a sufficient bond strength. Chapter 2 presents more discussion on the anchoring mechanism for each coupler type.

a. Unassembled

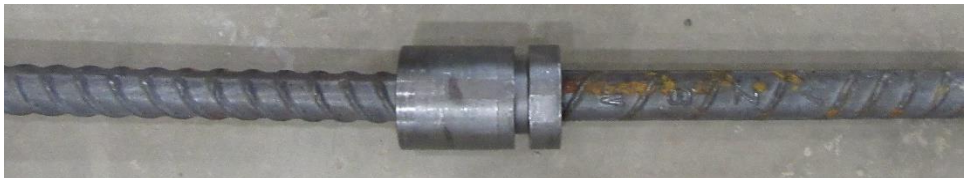

b. Assembled

Figure 3-5. Sample preparation for headed reinforcement coupler

a. Unassembled

b. Assembled

Figure 3-6. Sample preparation grouted sleeve coupler

a. Unassembled

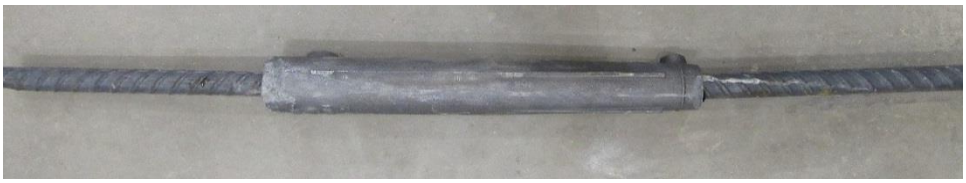

b. Assembled

Figure 3-7. Sample preparation for grouted sleeve coupler

a. Unassembled

b. Assembled

Figure 3-8. Sample preparation for threaded coupler (Type A)

a. Unassembled

b. Assembled

Figure 3-9. Sample preparation for threaded coupler (Type B)

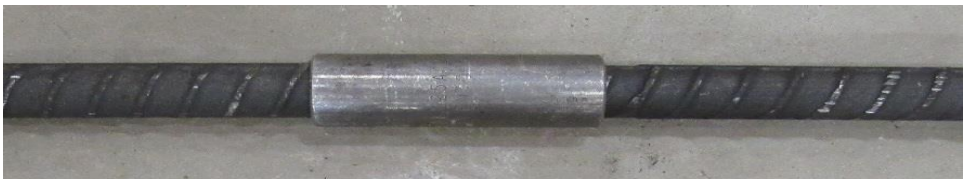

a. Unassembled

b. Assembled

Figure 3-10. Sample preparation for threaded coupler

a. Unassembled

b. Assembled

Figure 3-11. Sample preparation for swaged coupler

a. Unassembled

b. Assembled

Figure 3-12. Sample preparation for hybrid coupler (swaged and threaded)

a. Unassembled

b. Assembled

Figure 3-13. Sample preparation for hybrid Coupler (threaded and grouted)

3.5 Loading Protocols for Mechanical Bar Splices

Each type of the selected mechanical bar splices was tested under both uniaxial tensile monotonic and cyclic loading to failure.

3.5.1 Monotonic Loading

Monotonic testing of unspliced and spliced specimens was performed according to ASTM E8 (2012) by pulling the specimen to failure with a constant strain rate of 0.019

in./in./min, which was within the ASTM rate of 0.015 ± 0.006 in./in./min. This ASTM standard allows two speeds before and after the yielding of a bar to expedite the testing. Nevertheless, only the prior-to-yielding strain rate was used in the present study for all specimens during the entire test to minimize the test variables since the anchoring mechanism of a coupler may change its yield strain. The data sampling rate was 10 Hz.

3.5.2 Cyclic Loading

Cyclic testing of mechanical bar splices is challenging since couplers alter the hysteretic behavior compared to unspliced bars. Current codes do not specify any provisions for post-yield loading of couplers. Nevertheless, this is an essential piece of information in the present study to comment whether a coupler is suitable for the use in plastic hinge regions of bridge columns.

To overcome this shortcoming, a cyclic loading protocol based on the data from an initial monotonic testing is proposed (Fig. 3-14.) After testing a mechanical bar splice under the aforementioned monotonic loading protocol, the coupler stress-strain relationship is available and can be used as the input for the cyclic loading. A few target stresses can be selected (e.g. 10 points from zero stress to 100% of the peak stress with an interval of 10% of the peak stress) then the strains corresponding to these stresses can be determined from the measured monotonic data. These strains are the target strains for cyclic loading.

The next challenge for the cyclic loading was to determine the number of load cycles. The Caltrans test procedure for couplers (2004) requires four cycles per amplitude but the Caltrans cyclic test is mainly in the elastic strain range. In the present study, four tensile cycles per strain amplitude were selected for all mechanical bar splices to conservatively

investigate their behavior under extreme loading. A minimum of 5000 psi stress was selected as the lower tensile stress limit to avoid buckling of the bars in compression. After completion of all target cycles where the specimen did not fail, it was then monotonically pulled to failure. One sample of cyclic loading history used in a coupler test is shown in Fig. 3-15. The speed of the cyclic loading was the same as that in the monotonic loading, which was 0.019 in./in./min.

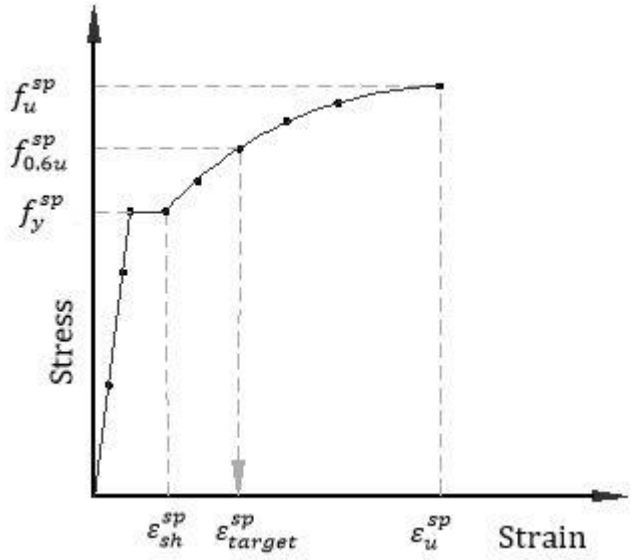

Figure 3-14. Identification of target strains for cyclic testing of mechanical bar splices

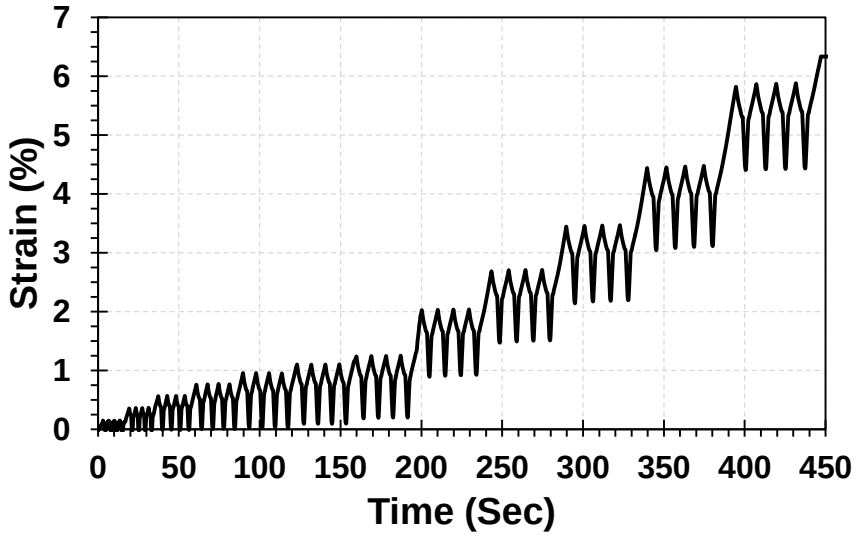

Figure 3-15. A sample cyclic loading history for mechanical bar splices

3.6 References

AASHTO. (2014). "AASHTO Guide Specifications for LRFD Seismic Bridge Design," Washington, D.C., American Association of State Highway and Transportation Officials.

ACI 439.3R-07. (2007). "Types of Mechanical Splices for Reinforcing Bars," Reported by American Concrete Institute Committee 439, 24 pp.

ASTM A1034 (Sep. 2016). "Standard Test Methods for Testing Mechanical Splices for Steel Reinforcing Bars." ASTM International, West Conshohocken, PA.

ASTM A706 (2009). "Standard specification for Low-Alloy Steel Deformed and Plain Bars for Concrete Reinforcement." West Conshohocken, PA, 6 pp.

ASTM E8 (2012). "Standard Test Methods for Tension Testing of Metallic Materials." ASTM International, West Conshohocken, PA.

ASTM E83 (2010). "Standard Practice for Verification and Classification of Extensometer Systems." ASTM International, West Conshohocken, PA.

California Test 670. (2004). “Method of Tests for Mechanical and Welded Reinforcing Steel Splices,” Sacramento, CA, California Department of Transportation.

Caltrans (2015). “Authorized List of Couplers for Reinforcing Steel”. Sacramento, CA, California Department of Transportation, September 21.

Tazarv, M. and Saiidi, M.S. (2016). “Seismic Design of Bridge Columns Incorporating Mechanical Bar Splices in Plastic Hinge Regions,” Engineering Structures, DOI: 10.1016/j.engstruct.2016.06.041, Vol 124, pp. 507-520.

Chapter 4. Results of Experimental Studies on Mechanical Bar Splices

4.1 Introduction

Using the loading protocols and test setup discussed in Chapter 3, 162 mechanical bar splices were tested to failure at the Lohr Structures Laboratory at South Dakota State University. Of 162 specimens, 81 couplers were tested using the monotonic loading protocol and 81 couplers were tested using the cyclic loading protocol. Furthermore, more than 170 unspliced bars were tested to failure to serve as reference specimens. Acceptance criteria for mechanical bar splices proposed by Tazarv and Saiidi (2016) (Sec. 2.5.3.1) were adopted in the present study to identify "seismic couplers" for the use in the plastic hinge region of bridge columns. Measured coupler stress-strain relationships, coupler failure modes, and a summary of test results are presented in this chapter.

4.2 Coupler Monotonic Testing

Tables 3.2 to 3.6 presents the test matrix for all mechanical bar splices used in the present study. A total of 81 mechanical bar splices consisting of No. 5 (16 mm), No. 8 (25 mm), and No. 10 (32 mm) splices were tested using the monotonic loading protocol detailed in Sec. 3.5. Five different types of couplers (headed, threaded, swaged, grouted, and hybrid) consisting of nine different products were included in this experimental

program. Three spliced specimens were tested per product, and at least one unspliced bar was tested per product as the reference sample. This section presents the detailed findings of the monotonic testing for each coupler type and then concludes with a summary of the findings for all specimens.

4.2.1 Headed Reinforcement Couplers

Figures 4-1 to 4-3 show the measured stress-strain relationships for the No. 5 (16-mm), No. 8 (25-mm), and No. 10 (32-mm) headed reinforcement couplers, respectively. The unspliced reference bar data and the coupler failure mode are also included in these figures for completeness. All headed reinforcement couplers failed by "bar fracture" outside the coupler region, thus they are "seismic couplers".

The splices with the same-size bars showed consistent stress-strain behavior. The average modulus of elasticity of the No. 5, No. 8, and No. 10 headed bar couplers was respectively 76%, 76%, and 63% lower than the conventional steel bar modulus of elasticity, which is 29000 ksi (200,000 MPa). Furthermore, it can be seen that the strain at the peak stress, which is also known as the ultimate strain, was approximately the same for the couplers with the same bar sizes. The average ultimate strain of the No. 5, No. 8, and No. 10 spliced specimens was respectively 44%, 41%, and 42% lower than that for the corresponding unspliced reference bars.

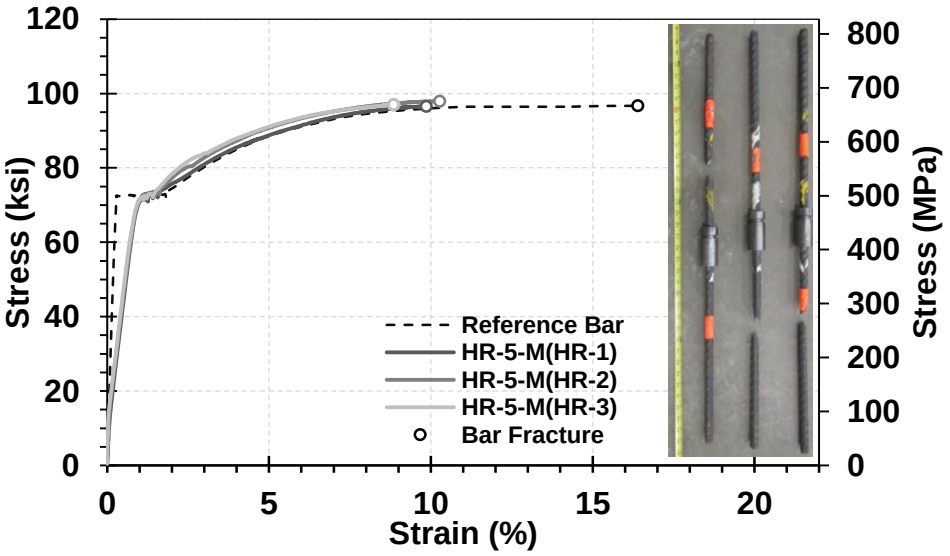

Figure 4-1. Monotonic test results for No. 5 (16-mm) headed reinforcement couplers

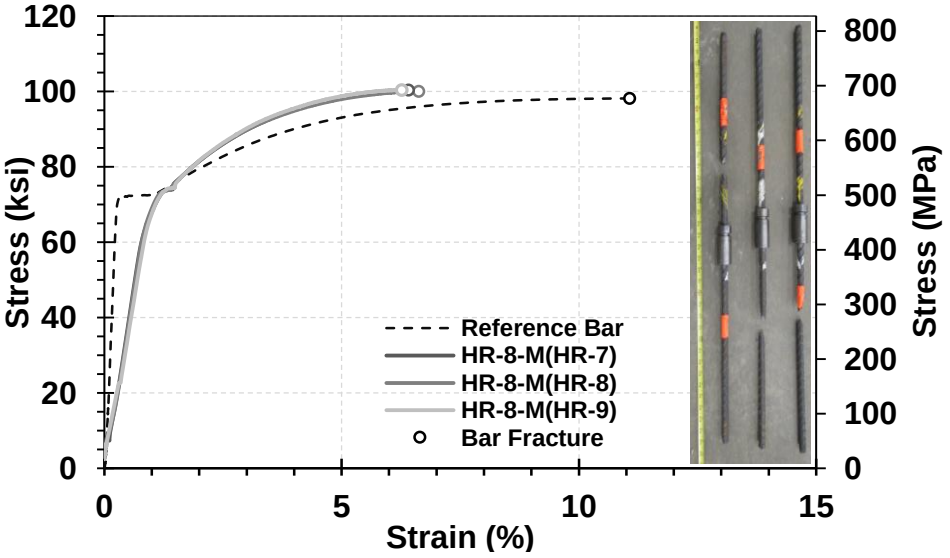

Figure 4-2. Monotonic test results of No. 8 (25-mm) headed reinforcement couplers

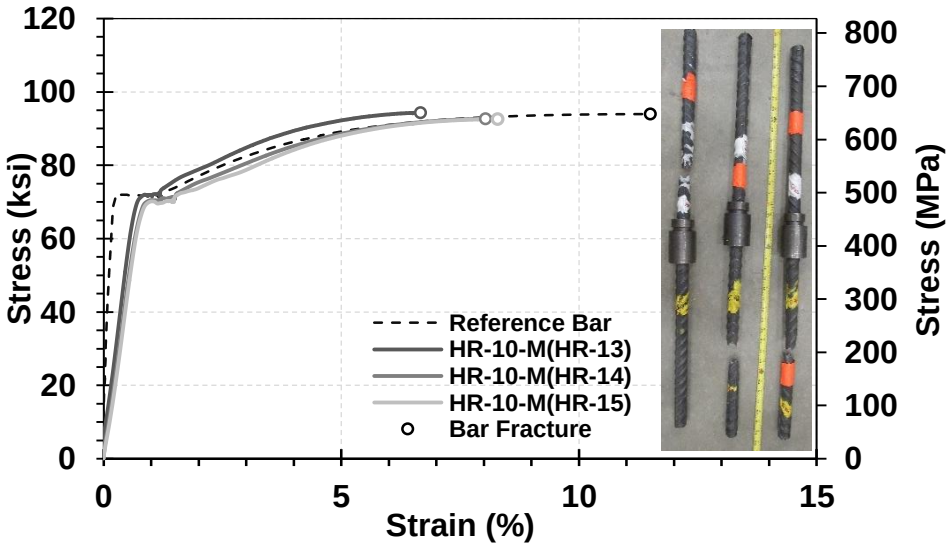

Figure 4-3. Monotonic test results of No. 10 (32-mm) headed reinforcement couplers

4.2.2 Threaded Couplers

Three different products were categorized as the threaded coupler (Table 3-3) and three samples of each product per bar size were monotonically tested to failure.

4.2.2.1 Threaded Coupler (Type A by Dextra)

Figures 4-4 to 4-6 show the measured stress-strain relationships for the No. 5 (16-mm), No. 8 (25-mm), and No. 10 (32-mm) threaded couplers (Type A), respectively. The unspliced reference bar data and the coupler failure mode are also included in these figures for completeness. All threaded couplers failed by "bar fracture". However, the reinforcing steel bar of only one No. 10 splice fractured inside the coupler region. Overall, it can be concluded that this coupler type is a "seismic coupler".

The splices with the same-size bars showed consistent stress-strain behavior. The average modulus of elasticity of the No. 5, No. 8, and No. 10 threaded couplers (Type A), couplers were respectively 13%, 41%, and 35% lower than the conventional steel bar modulus of elasticity. Furthermore, it can be seen that the strain at the peak stress was

approximately the same for the couplers with the same bar sizes. The average ultimate strain of the No. 5, No. 8, and No. 10 spliced specimens was respectively 78%, 77%, and 87% lower than that for the corresponding unspliced reference bars. Another observation was that this coupler did not show any strain plateau after yielding.

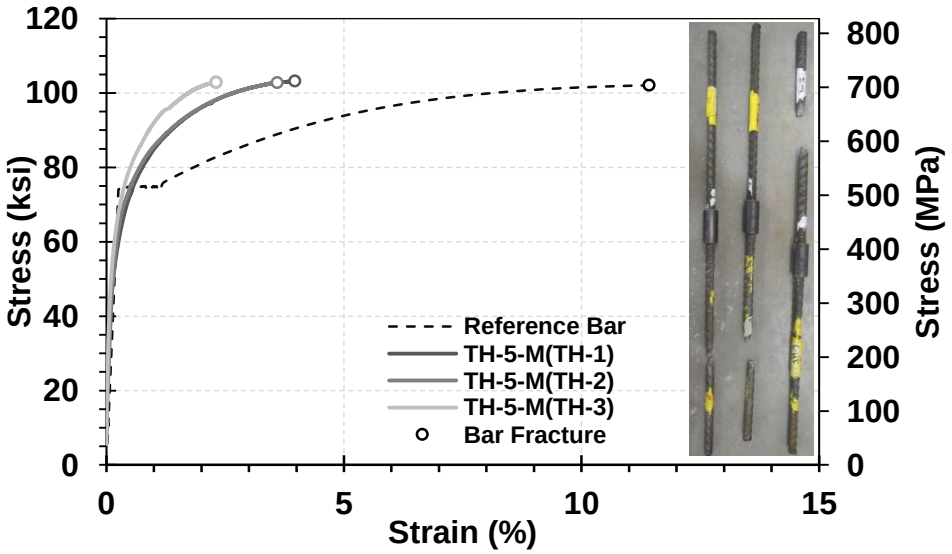

Figure 4-4. Monotonic test results for No.5 (16-mm) threaded couplers (Type A)

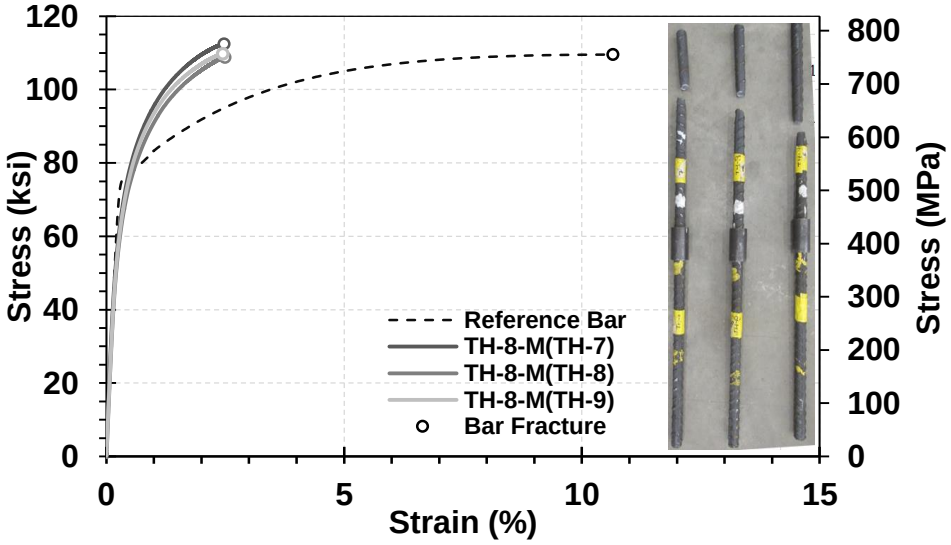

Figure 4-5. Monotonic test results for No.8 (24-mm) threaded couplers (Type A)

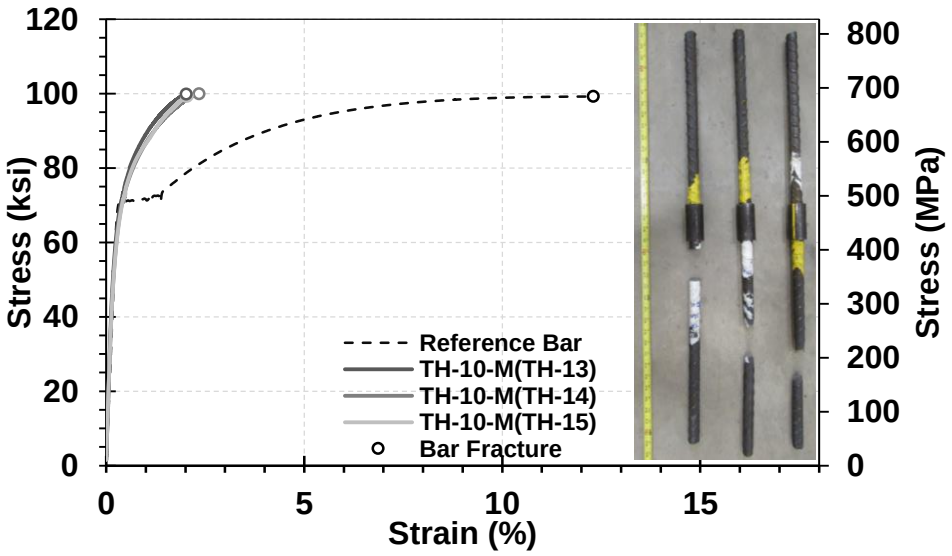

Figure 4-6. Monotonic test results for No.10 (32-mm) threaded couplers (Type A)

4.2.2.2 Threaded Coupler (Type B by Dextra)

Figures 4-7 to 4-9 show the measured stress-strain relationships for the No. 5 (16-mm), No. 8 (25-mm), and No. 10 (32-mm) threaded couplers (Type B), respectively. The unspliced reference bar data and the coupler failure mode are also included in these figures for completeness. All threaded couplers failed by "bar fracture" outside the coupler region, thus they are "seismic couplers".

The splices with the same-size bars showed consistent stress-strain behavior. The average modulus of elasticity of the No. 5, No. 8, and No. 10 threaded couplers (Type B) is respectively 42%, 30%, and 26% lower than the conventional steel bar modulus of elasticity. Furthermore, it can be seen that the ultimate strain was approximately the same for the couplers with the same bar sizes. The average ultimate strain of the No. 5, No. 8, and No. 10 spliced specimens was respectively 78%, 80%, and 78% lower than that for the corresponding unspliced reference bars. Further, this coupler did not exhibit any strain plateau after yielding even when the reference bar had strain plateau.

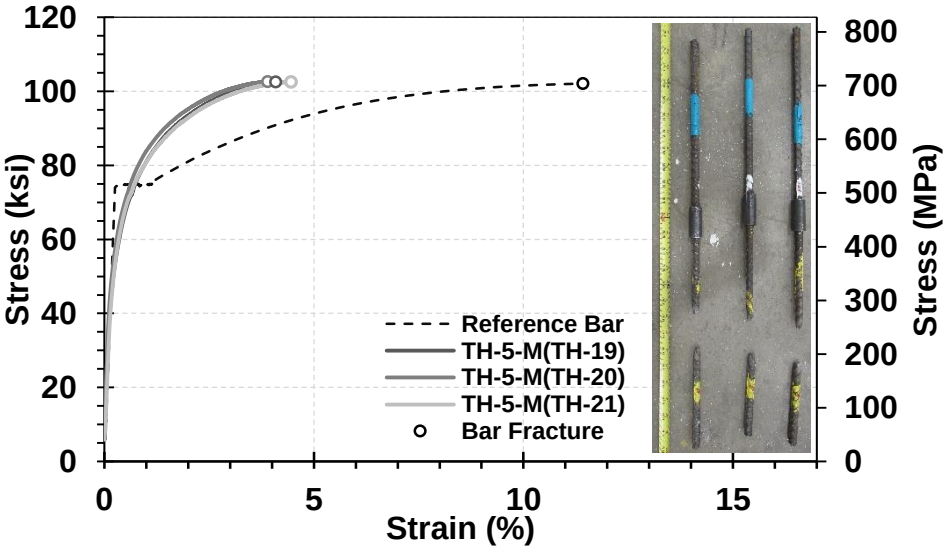

Figure 4-7. Monotonic test results for No.5 (16-mm) threaded couplers (Type B)

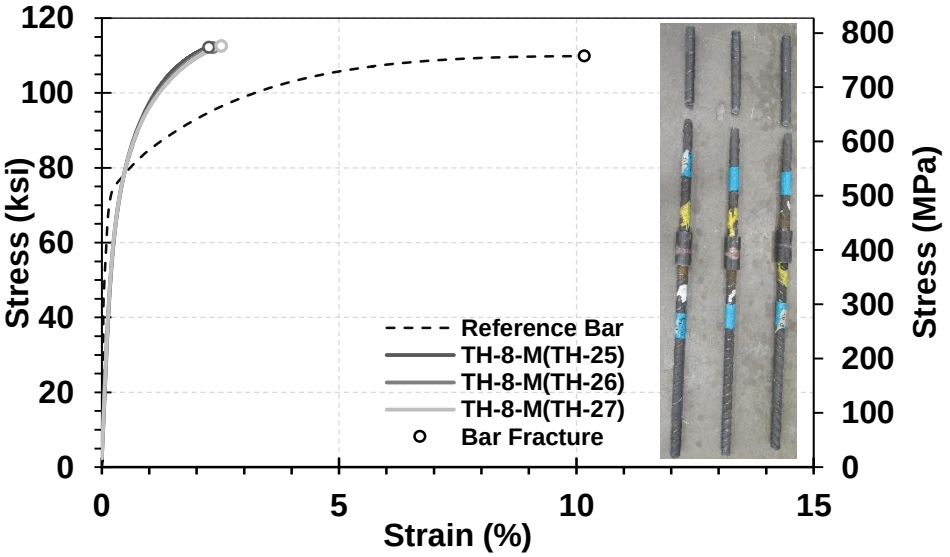

Figure 4-8. Monotonic test results for No.8 (24-mm) threaded couplers (Type B)

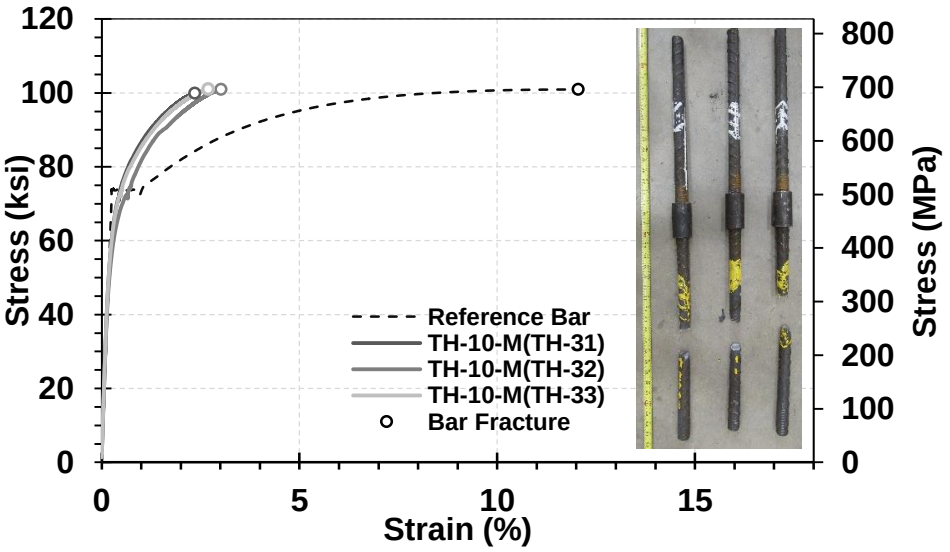

Figure 4-9. Monotonic test results for No.10 (32-mm) threaded couplers (Type B)

4.2.2.3 Threaded Coupler (Tapered by Erico)

Figures 4-10 to 4-12 show the measured stress-strain relationships for the No. 5 (16-mm), No. 8 (25-mm), and No. 10 (32-mm) tapered threaded couplers, respectively. Similar to previous sections, the unspliced reference bar data and the coupler failure mode are included in the figures for completeness. It can be seen that all tapered threaded couplers failed by "bar fracture" outside the coupler region, thus they are "seismic couplers".

The splices with the same-size bars showed consistent stress-strain behavior. The average modulus of elasticity of the No. 5, No. 8, and No. 10 tapered threaded couplers is respectively 3%, 12%, and 37% lower than the conventional steel bar modulus of elasticity. Furthermore, the ultimate strain was approximately the same for the couplers with the same bar sizes. The average ultimate strain of the No. 5, No. 8, and No. 10 spliced specimens was respectively 47%, 68%, and 67% lower than that for the corresponding unspliced reference bars.

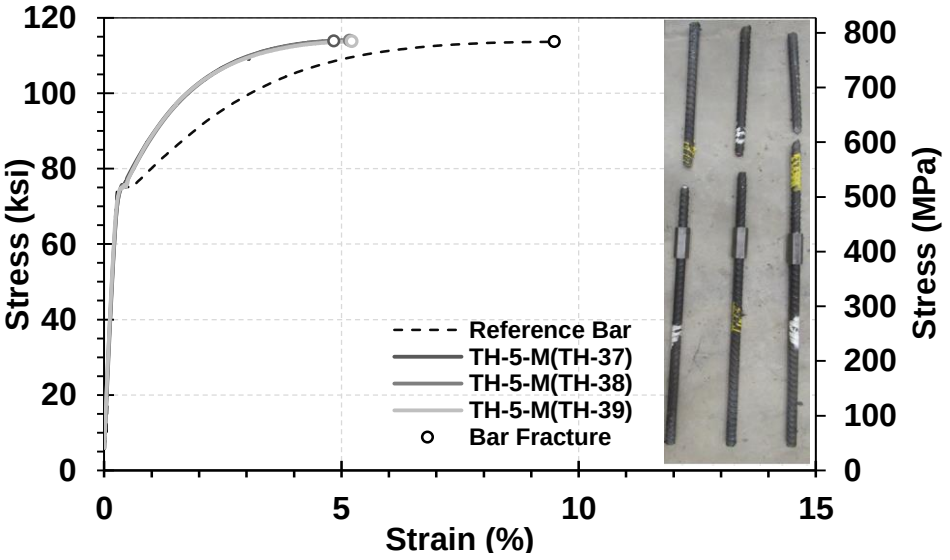

Figure 4-10. Monotonic test results for No.5 (16-mm) tapered threaded couplers

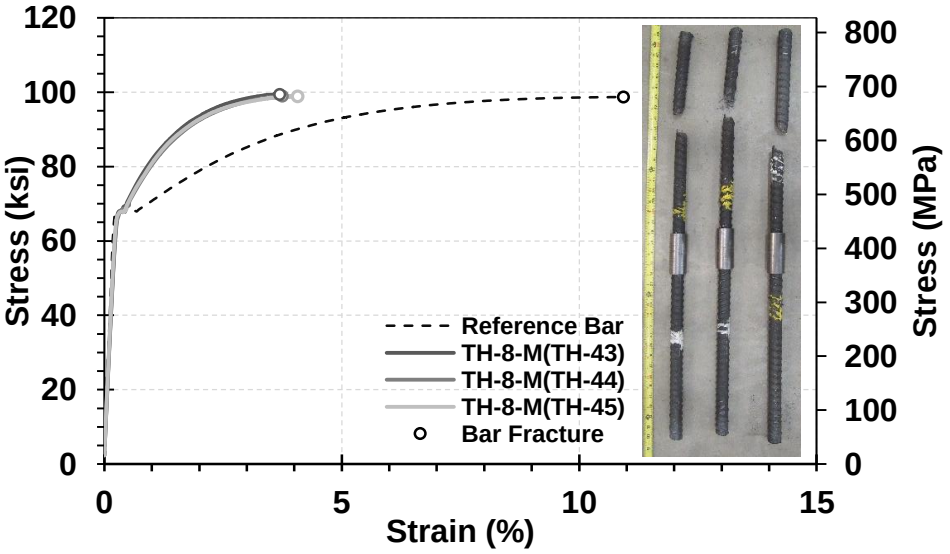

Figure 4-11. Monotonic test results for No.5 (16-mm) tapered threaded couplers

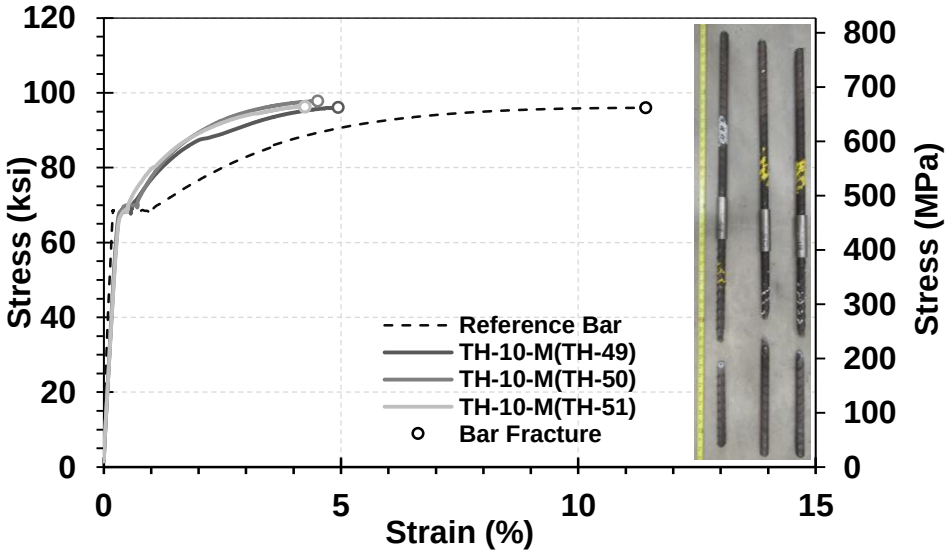

Figure 4-12. Monotonic test results for No.10 (32-mm) tapered threaded couplers

4.2.3 Swaged Couplers

Figures 4-13 to 4-15 show the measured stress-strain relationships for the No. 5 (16-mm), No. 8 (25-mm), and No. 10 (32-mm) swaged couplers, respectively. One No.5 (16-mm) swaged coupler (SW-2) failed by "coupler failure", and bar fractured in other eight specimens outside the coupler region. Caltrans test standard 670 (2004) accepts couplers in which one out of four samples does not fail by bar fracture. Note only three samples per bar size were tested in this project. Therefore, one may say that No. 5 swaged couplers are not "seismic couplers" since 33% of the test specimens did not fail by bar fracture outside the coupler region. However, the measured data shows that the strain capacity of SW-2 is comparable to other two in which bar fractures. Therefore, it was concluded that all swaged couplers tested in this study including No. 5 are "seismic couplers".

The splices with the same-size bars showed consistent stress-strain behavior. The average modulus of elasticity of the No. 5, No. 8, and No. 10 swaged couplers was respectively 11%, 31%, and 32% lower than the conventional steel bar modulus of elasticity. Furthermore, the ultimate strain was approximately the same for the couplers with the same bar sizes. The average ultimate strain of the No. 5, No. 8, and No. 10 spliced specimens was respectively 56%, 72%, and 67% lower than that for the corresponding unspliced reference bars.

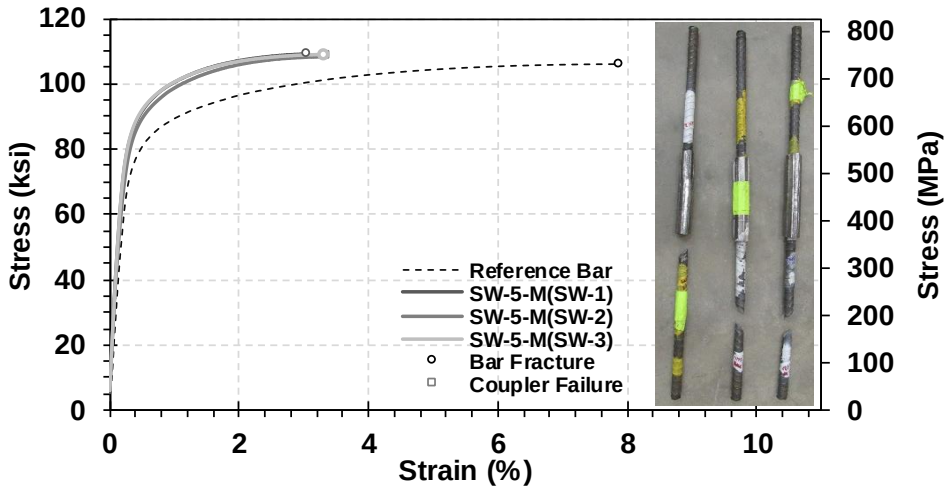

Figure 4-13. Monotonic test results for No.5 (16-mm) swaged couplers

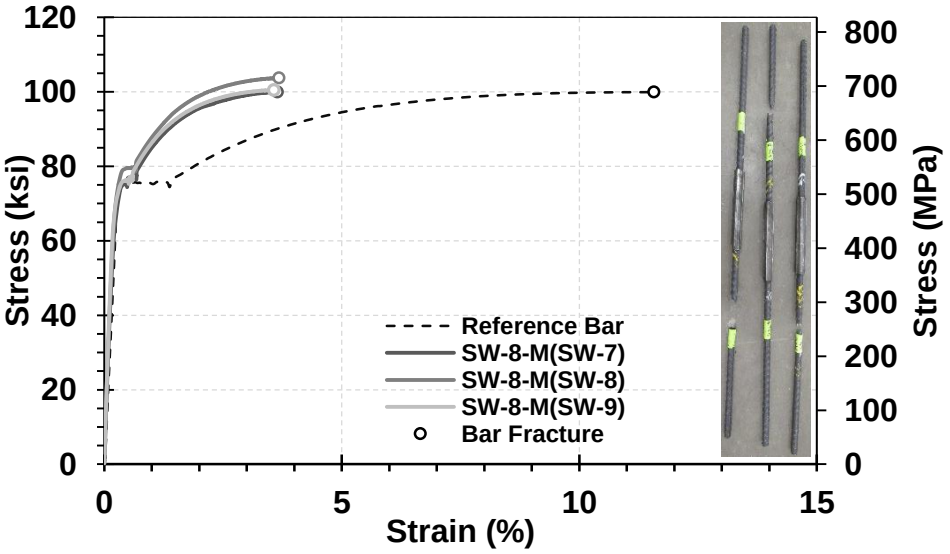

Figure 4-14. Monotonic test results for No.8 (24-mm) swaged couplers

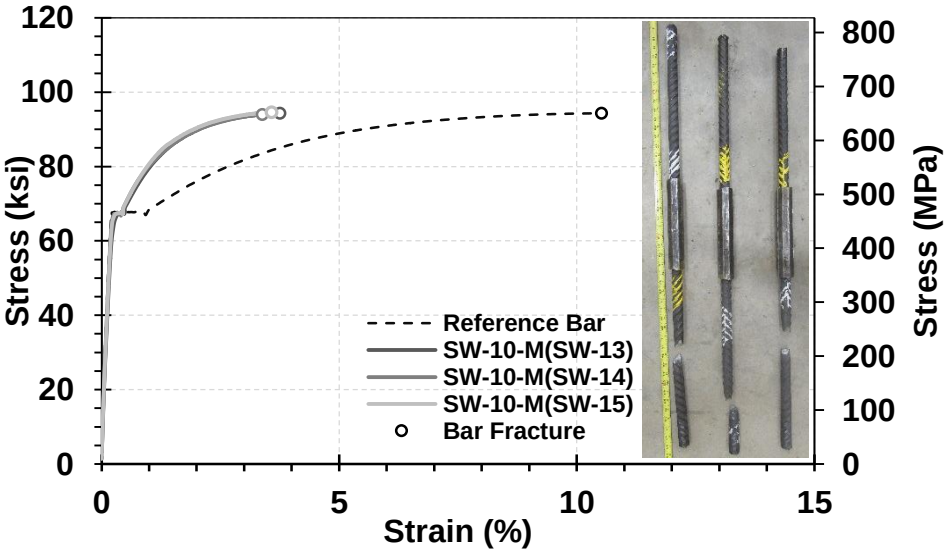

Figure 4-15. Monotonic test results for No.10 (32-mm) swaged couplers

4.2.4 Grouted Sleeve Couplers

Two products were categorized as the grouted sleeve coupler and three samples of each product per bar size were monotonically tested to failure.

4.2.4.1 Grouted Sleeve Couplers (by Splice Sleeve North America, NMB)

Figures 4-16 to 4-18 show the measured stress-strain relationships for the No. 5 (16 mm), No. 8 (25 mm), and No. 10 (32 mm) grouted sleeve couplers (NMB), respectively. Table 4-1 presents the compressive strength of grout used in this type of coupler, which were measured at different days in accordance to ASTM C109 (2012).

It can be seen that all No. 5 grouted sleeve couplers failed by "bar pullout", bar fractured in all No. 8 splices, and one No. 10 coupler failed (GC-13) at the coupler. Bar fractured outside the coupler region in the other two No. 10 splices (GC-14 and GC-15). Therefore, No. 5 (16-mm) NMB grouted sleeve couplers are not "seismic couplers". No. 8 (25-mm) NMB grouted sleeve couplers are "seismic couplers". Similar to the discussion provided for swaged couplers, it can be concluded that the No. 10 (32-mm) NMB grouted sleeve couplers are also "seismic couplers".

The splices with the same-size bars generally showed consistent stress-strain behavior. The average modulus of elasticity of the No. 5, No. 8, and No. 10 couplers was respectively 21%, 36%, and 31% lower than the conventional steel bar modulus of elasticity. Furthermore, the ultimate strain was approximately the same for the couplers with the same bar sizes. The average ultimate strain of the No. 5, No. 8, and No. 10 spliced specimens was respectively 56%, 72%, and 67% lower than that for the corresponding unspliced reference bars.

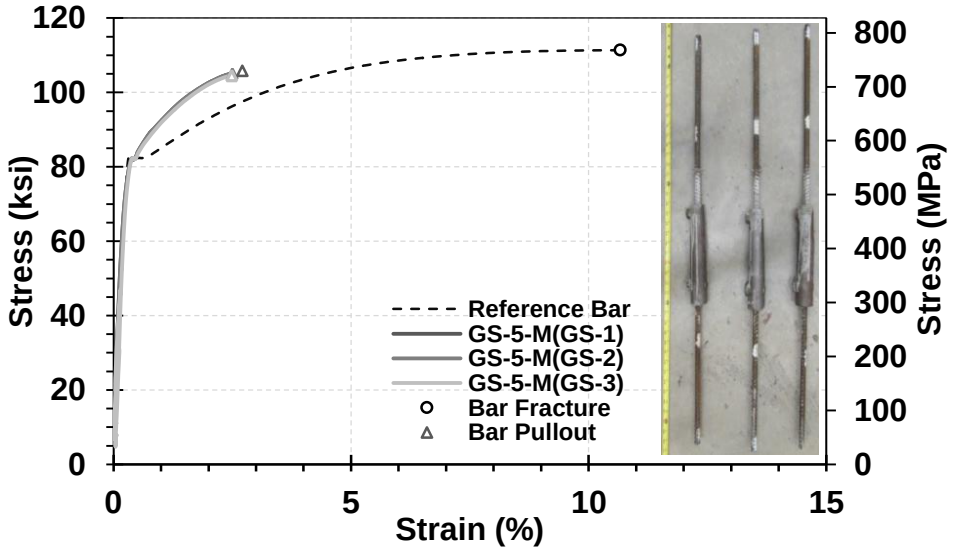

Figure 4-16. Monotonic test results for No.5 (16-mm) grouted sleeve couplers (NMB)

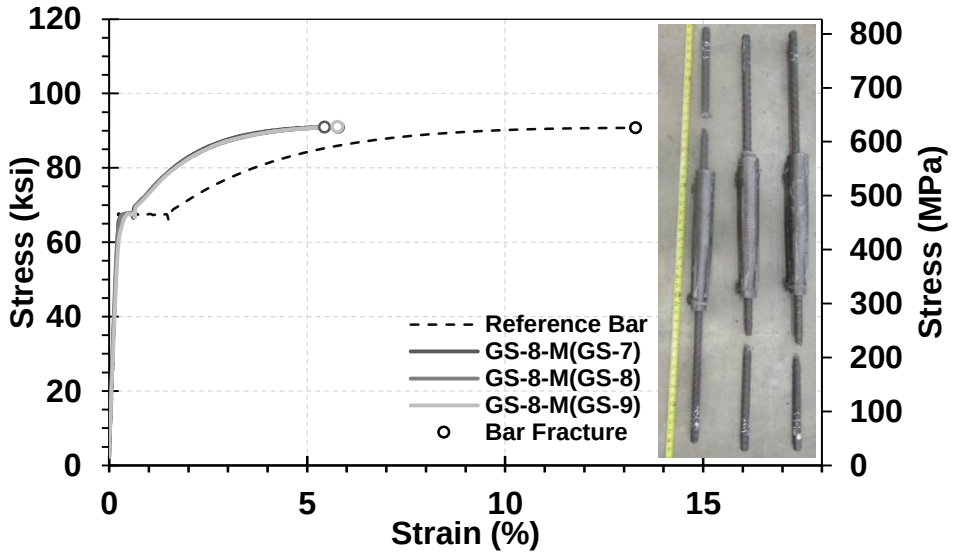

Figure 4-17. Monotonic test results for No.8 (25-mm) grouted sleeve couplers (NMB)

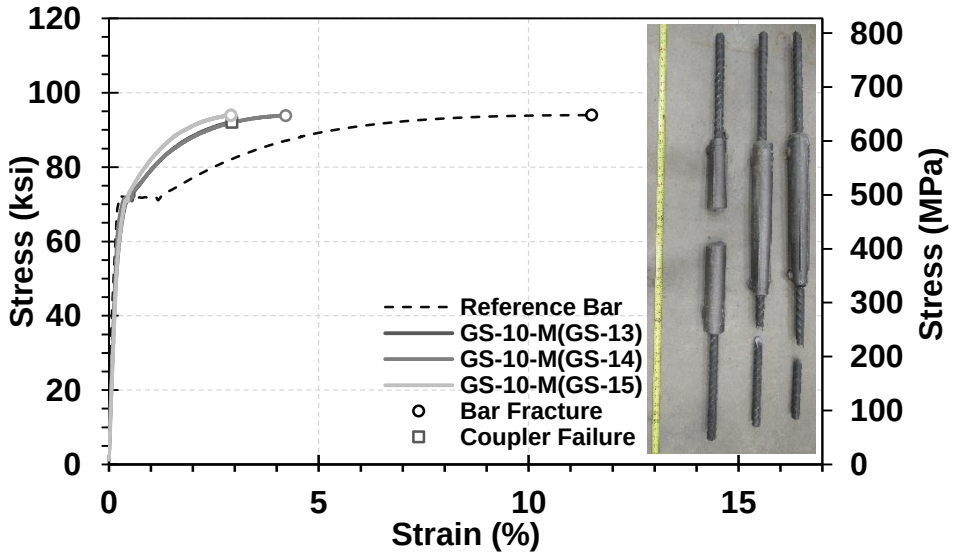

Figure 4-18. Monotonic test results for No.5 (16-mm) grouted sleeve couplers (NMB)

Table 4-1. Measured compressive strength for grout used in grouted sleeve couplers (NMB)

Coupler Size	7 days, psi (MPa)	28 days, psi (MPa)	First Coupler Test Day, psi (MPa)	Last Coupler Test Day, psi (MPa)
No. 5 (16 mm)	6,675 (46.0)	14145 (97.5)	15630 (107.8)	15545 (107.2)
No.8 (25 mm)	6,675 (46.0)	14145 (97.5)	15630 (107.8)	15545 (107.2)
No. 10 (32 mm)	8700 (60.0)	14350 (99.0)	14530 (100.2)	14605 (100.7)

4.2.4.2 Grouted Sleeve Coupler (by Dayton Superior)

Figures 4-19 to 4-21 show the measured stress-strain relationships for the No. 5 (16-mm), No. 8 (25-mm), and No. 10 (32-mm) grouted sleeve couplers (Dayton Superior), respectively. Table 4-2 presents the compressive strength of the grout used in this type of coupler, which were measured at different days in accordance to ASTM C109 (2012). Two No. 5 (16-mm) grouted sleeve couplers failed by "bar pullout" and one with "bar fracture" outside the coupler region, thus No. 5 (16-mm) grouted sleeve couplers (by Dayton Superior) are not "seismic couplers". Bar fractured outside the coupler region for

No. No. 8 (25-mm), and No. 10 (32-mm) grouted sleeve couplers (by Dayton Superior) thus they are “seismic couplers”.

The average modulus of elasticity of the No. 5, No. 8, and No. 10 grouted sleeve couplers (Dayton Superior) was respectively 33%, 9%, and 8% lower than the conventional steel bar modulus of elasticity. Furthermore, the ultimate strain of same-size couplers with the mode of failure of “bar fracture” was approximately the same. The average ultimate strain of the No. 5, No. 8, and No. 10 spliced specimens was respectively 64%, 62%, and 56% lower than that for the corresponding unspliced reference bars.

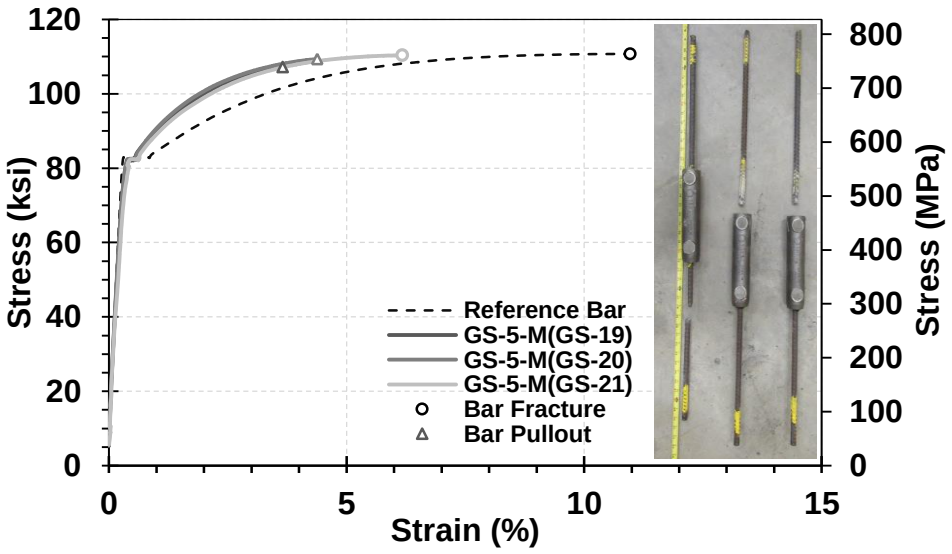

Figure 4-19. Monotonic test results for No.5 (16-mm) grouted sleeve couplers (Dayton Superior)

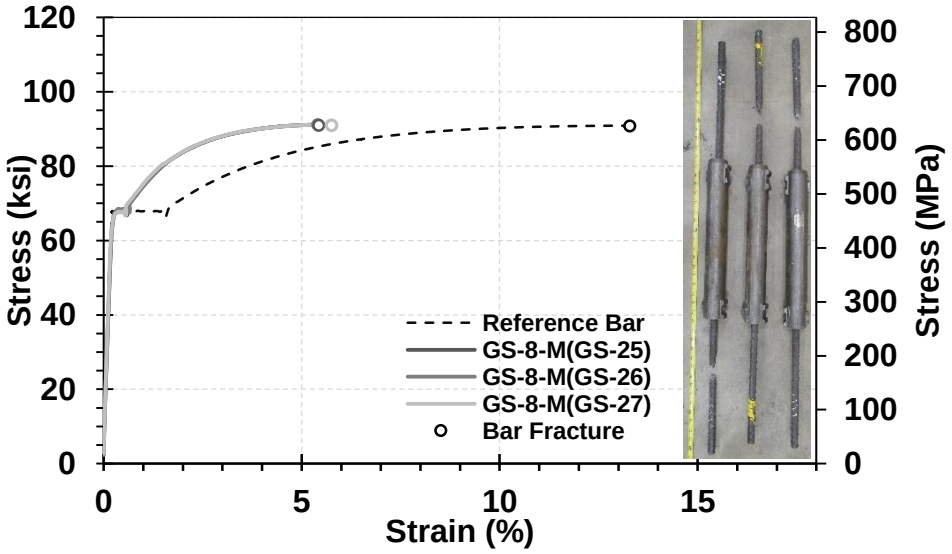

Figure 4-20. Monotonic test results for No.8 (24-mm) grouted sleeve couplers (Dayton Superior)

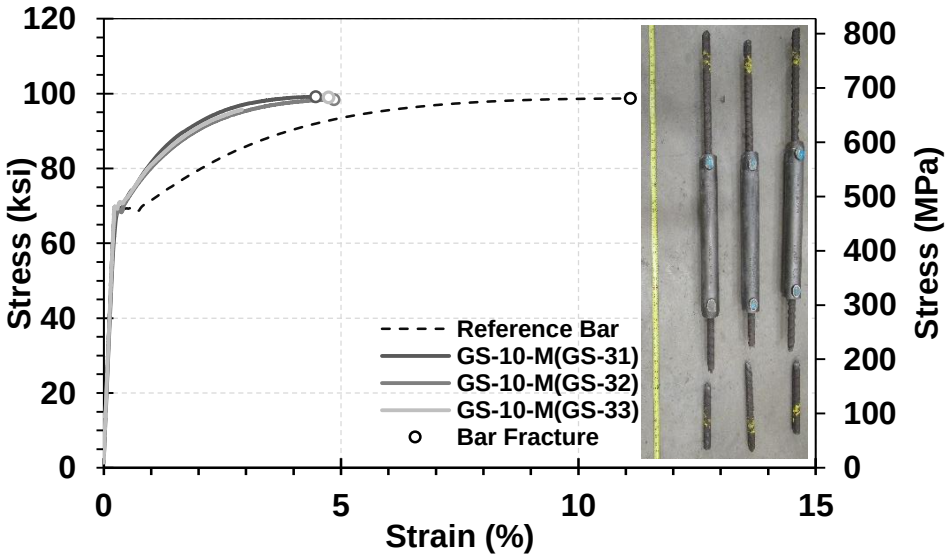

Figure 4-21. Monotonic test results for No.10 (32-mm) grouted sleeve couplers (Dayton Superior)

Table 4-2. Measured compressive strength for grout used in grouted sleeve coupler (by Dayton)

Coupler Size	7 days, psi (MPa)	28 days, psi (MPa)	First Coupler Test Day, psi (MPa)	Last Coupler Test Day, psi (MPa)
No. 5 (16 mm)	10630 (73.3)	11220 (77.4)	12430 (85.7)	14275 (98.4)
No.8 (25 mm)	10630 (73.3)	11220 (77.4)	12430 (85.7)	14275 (98.4)
No. 10 (32 mm)	12860 (88.7)	13300 (91.7)	13380 (92.2)	13915 (95.9)

4.2.5 Hybrid Couplers

Two products were categorized as the hybrid coupler and three samples of each product per bar size were monotonically tested to failure. In one of the products, bars were spliced through grouted and threaded mechanisms at the ends of the coupler. In the second hybrid coupler, bars were spliced using threaded and swaged mechanisms at the ends.

4.2.5.1 Hybrid Coupler (Threaded & Swaged):

Figures 4-22 to 4-24 show the measured stress-strain relationships for the No. 5 (16-mm), No. 8 (25-mm), and No. 10 (32-mm) hybrid couplers (threaded and swaged), respectively. All threaded-swaged hybrid couplers failed by "bar fracture" outside the coupler region, thus they are "seismic couplers".

The splices with the same-size bars generally showed consistent stress-strain behavior. The average modulus of elasticity of the No. 5, No. 8, and No. 10 threaded-swaged hybrid couplers was respectively 5%, 3%, and 25% lower than the conventional steel bar modulus of elasticity. Furthermore, the ultimate strain was almost the same for couplers with the same bar sizes. The average ultimate strain of the No. 5, No. 8, and No. 10 spliced specimens was respectively 60%, 74%, and 64% lower than that for the corresponding unspliced reference bars.

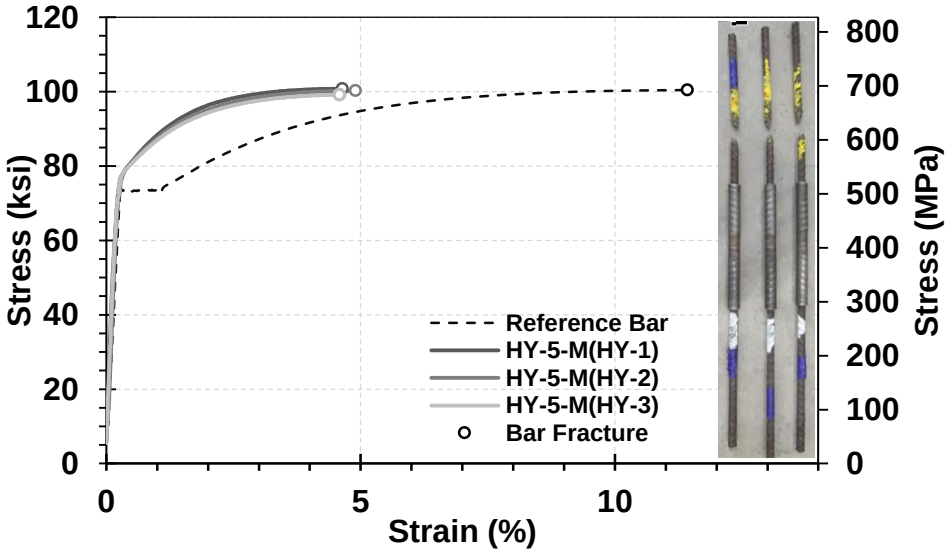

Figure 4-22. Monotonic test results for No.5 (16-mm) threaded-swaged hybrid couplers.

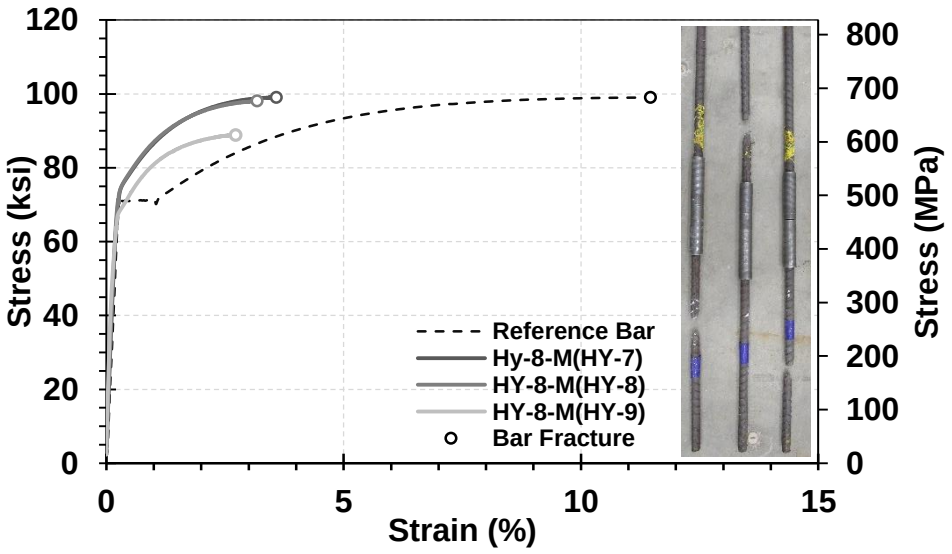

Figure 4-23. Monotonic test results for No.8 (24-mm) threaded-swaged hybrid couplers

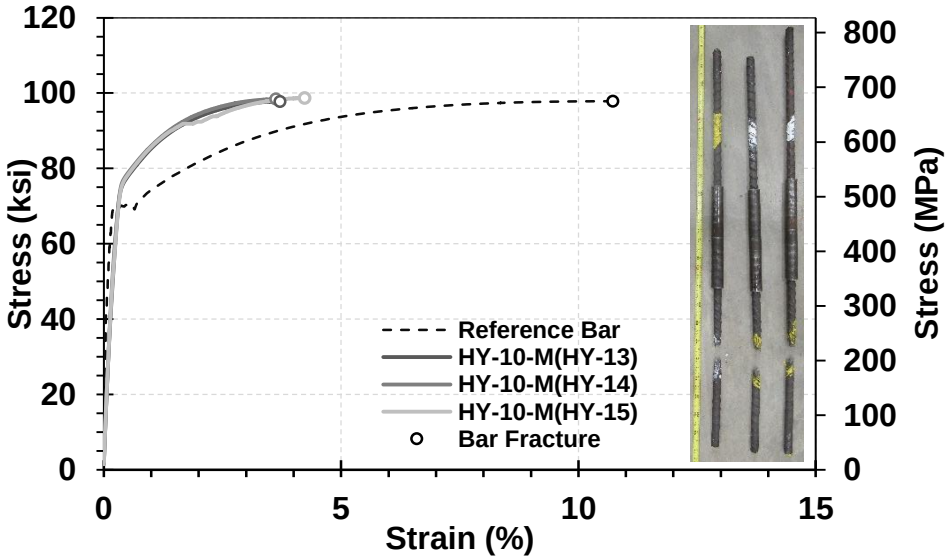

Figure 4-24. Monotonic test results for No.10 (32-mm) threaded-swaged hybrid couplers

4.2.5.1 Hybrid Coupler (Grouted & Threaded):

Figures 4-25 to 4-27 show the measured stress-strain relationships for the No. 5 (16-mm), No. 8 (25-mm), and No. 10 (32-mm) hybrid couplers (grouted and threaded), respectively. Table 4-3 presents the compressive strength of grout used in this type of coupler, which were measured at different days in accordance to ASTM C109 (2012). All grouted-threaded hybrid couplers failed by "bar fracture" outside the coupler region, thus they are "seismic couplers".

The splices with the same-size bars generally showed consistent stress-strain behavior. The average modulus of elasticity of the No. 5, No. 8, and No. 10 hybrid couplers (grouted-threaded) is respectively 14%, 67%, and 33% lower than the conventional steel bar modulus of elasticity. Furthermore, the ultimate strain was approximately the same for couplers with the same bar sizes. The average ultimate strain

of the No. 5, No. 8, and No. 10 spliced specimens was respectively 67%, 74%, and 68% lower than that for the corresponding unspliced reference bars.

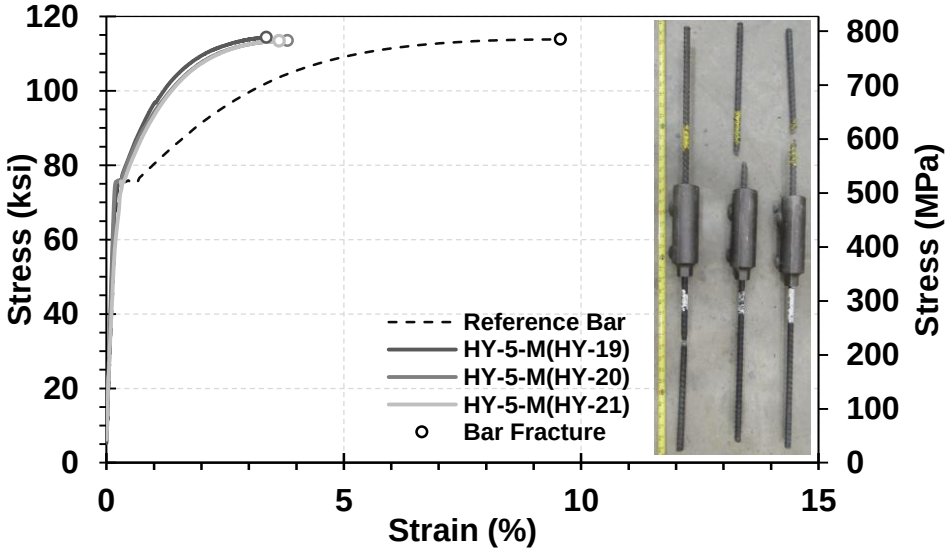

Figure 4-25. Monotonic test results for No.5 (16-mm) grouted-threaded hybrid couplers

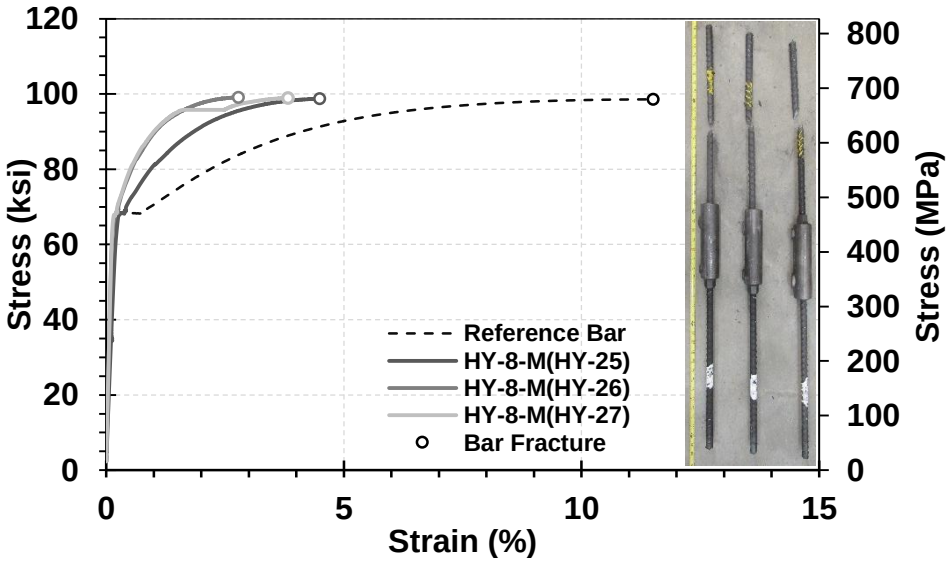

Figure 4-26. Monotonic test results for No.8 (24-mm) grouted-threaded hybrid couplers

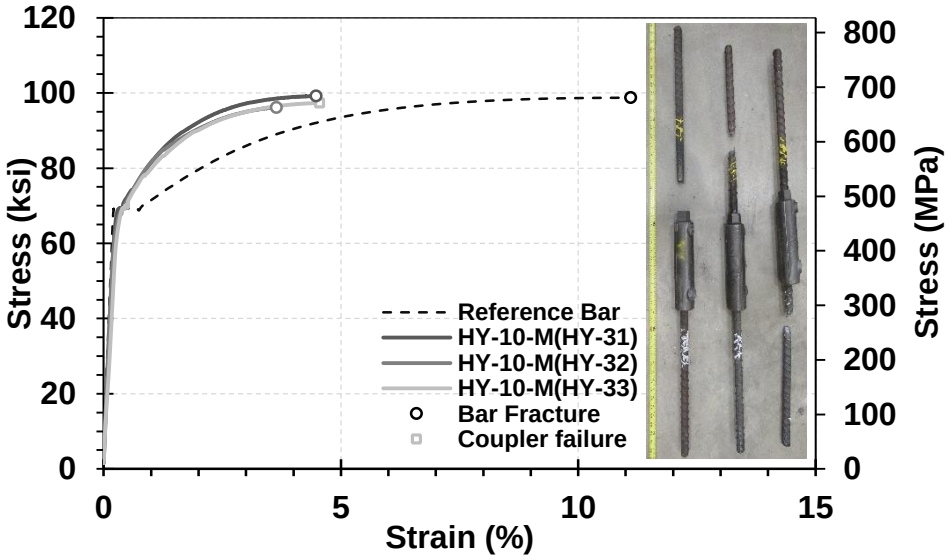

Figure 4-27. Monotonic test results for No.10 (32-mm) grouted-threaded hybrid couplers

Table 4-3. Measured compressive strength for grout used in grouted-threaded hybrid couplers

Coupler Size	7 days, psi (MPa)	28 days, psi (MPa)	First Coupler Test Day, psi (MPa)	Last Coupler Test Day, psi (MPa)
No. 5 (16 mm)	13805 (95.2)	19920 (137.4)	23760 (163.8)	24105 (166.2)
No.8 (25 mm)	13805(95.2)	19920 (137.4)	23760 (163.8)	24105 (166.2)
No. 10 (32 mm)	14720(101.5)	21080 (145.3)	16280 (112.2)	22480 (155)

4.3 Summary of Coupler Monotonic Test Results

The experimental findings presented in the previous sections indicate that different couplers exhibit different stress-strain behavior depending on their size, type, and product. Tazarv and Saiidi (2016) proposed a generic stress-strain material model for couplers as discussed in Sec. 2.5.3.1. The key input of this model is the coupler "rigid length factor, β" and the mechanical properties of splicing bars. The coupler rigid length factor should be determined from test data. They recommended to use the ultimate strains of the spliced and unspliced specimens in the calculation of β. However, one may obtain this factor using multiple points and report the average as the design value.

In an attempt to explore the best way of obtaining the coupler rigid length factor, three methods were followed. In the first method, this factor (β_u) was calculated using the ultimate strain of the spliced and unspliced specimens (Eq. 2.1). In the second and third methods, the stress range from the yield to the peak was divided into ten equally spaced stress levels (Fig. 4-28) then the spliced and unspliced specimen strains corresponding to these stresses were used in the β calculation. β_{3p} was the average of these factors using the last three points and β_{10p} was the average of these factors using 10 points.

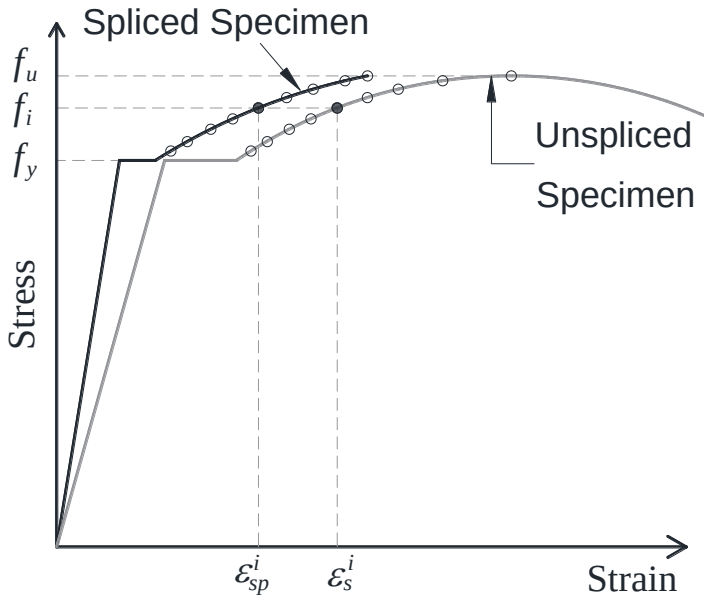

Figure 4-28. Calculation of coupler rigid length factor using measured strain data

4.3.1 Coupler Rigid Length Factors Obtained from Test Data

Table 4-4 presents the coupler rigid length factor obtained for each of 81 couplers tested under the monotonic loading. The three different rigid length factors discussed above, the error between the measured and calculated ultimate strains per method of the

calculation of beta, and the coefficient of determination were included in the table. The R^2 shows the correlation between the measured and calculated stress-strain relationships using each beta. An R^2 of 1.0 (or 100 in the table) indicates a perfect match between the measured and calculated stress-strain relationships. Figure 4-29 shows the measured and calculated stress-strain relationships for different coupler types using three values of beta. It can be inferred that all of the three proposed methods of calculation of beta are viable. Nevertheless, the beta using the ultimate point (β_u) resulted in minimal errors between the measured and calculated ultimate strains for all splices and could reproduce the measured stress-strain behavior with a reasonable accuracy. β_u might be used as the design value for bar couplers.

It should be noted that the main use of this coupler model will be to quantify the coupler effect on the seismic performance of mechanically spliced bridge columns. As discussed in Chapter 2, previous studies found that couplers usually reduce the displacement capacity of bridge columns. Thus, in a displacement-based design, the ultimate strains of couplers would be more important than the initial behavior to accurately calculate the bridge ultimate displacements. The error in the prior-to-yielding branch of the coupler calculated stress-strain relationship has minimal effect on the column seismic behavior especially since the coupler length is insignificant relative to the column length.

Table 4-4. Measured coupler rigid length factors

Specimen	L_{sp}	α	L_{cr}	β_u	β_{3p}	β_{10p}	Error in Ultimate Strain, (R^2) (%)		
							β_u	β_{3p}	β_{10p}
Headed Reinforcement Coupler									
HR-5-M(HR-1)	2.40	2.00	4.90	0.81	0.26	0.15	0.06, (86.59)	45.39, (93.31)	54.11, (92.86)
HR-5-M(HR-2)	2.40	2.00	4.90	0.90	0.55	0.27	0.07, (88.07)	30.80, (92.78)	55.25, (94.12)
HR-5-M(HR-3)	2.40	2.00	4.90	0.68	0.58	0.42	0.07, (91.11)	7.40, (91.68)	19.09, (92.22)
HR-8-M(HR-7)	3.25	1.25	5.75	0.74	0.70	0.37	0.07, (75.43)	3.88, (76.58)	36.46, (81.53)
HR-8-M(HR-8)	3.25	1.25	5.75	0.72	0.67	0.35	0.07, (73.07)	4.63, (74.42)	35.58, (74.30)
HR-8-M(HR-9)	3.25	1.25	5.75	0.78	0.73	0.39	0.07, (72.69)	4.91, (74.49)	38.96, (79.63)
HR-10-M(HR-13)	3.88	1.25	7.00	0.76	0.57	0.36	0.45, (73.17)	18.68, (78.36)	38.64, (82.21)
HR-10-M(HR-14)	3.88	1.25	7.00	0.48	0.00	0.00	0.20, (68.01)	44.46, (81.05)	53.88, (82.61)
HR-10-M(HR-15)	3.88	1.25	7.00	0.44	0.00	0.00	0.17, (68.36)	45.26, (77.44)	60.75, (80.30)
Threaded Coupler (Type A)									
TH-5-M(TH-1)	1.75	2.00	4.25	1.57	1.83	1.71	0.07, (91.33)	31.04, (88.83)	16.20, (90.74)
TH-5-M(TH-2)	1.75	2.00	4.25	1.68	1.92	1.85	0.07, (94.67)	35.58, (86.86)	32.20, (90.94)
TH-5-M(TH-3)	1.75	2.00	4.25	1.93	2.09	2.01	0.07, (95.38)	31.75, (88.68)	15.41, (93.63)
TH-8-M(TH-7)	2.63	1.25	5.13	1.49	1.41	1.07	0.08, (74.43)	18.22, (78.70)	93.92, (73.63)
TH-8-M(TH-8)	2.63	1.25	5.13	1.49	1.20	0.85	0.08, (75.21)	63.11, (77.80)	139.44, (72.89)
TH-8-M(TH-9)	2.63	1.25	5.13	1.47	1.21	0.94	0.08, (71.17)	39.11, (78.24)	110.17, (72.95)
TH-10-M(TH-13)	3.06	1.25	6.25	1.64	1.40	1.31	1.09, (76.89)	28.59, (88.14)	57.97, (93.14)
TH-10-M(TH-14)	3.06	1.25	6.25	1.52	1.33	1.11	0.89, (77.96)	57.32, (88.14)	80.69, (93.14)
TH-10-M(TH-15)	3.06	1.25	6.25	1.58	1.43	1.28	1.07, (75.26)	75.62, (82.49)	107.15, (88.39)
Threaded Coupler (Type B)									
TH-5-M(TH-19)	1.75	2.00	4.25	1.58	1.80	1.53	0.07, (95.38)	25.72, (88.68)	5.72, (93.63)
TH-5-M(TH-20)	1.75	2.00	4.25	1.63	1.85	1.64	0.07, (93.72)	28.07, (85.90)	1.67, (93.52)
TH-5-M(TH-21)	1.75	2.00	4.25	1.52	1.70	1.51	0.07, (87.16)	19.46, (77.97)	1.37, (88.07)
TH-8-M(TH-25)	2.63	1.25	5.13	1.51	1.43	1.01	0.08, (70.81)	19.40, (76.16)	115.70, (74.93)
TH-8-M(TH-26)	2.63	1.25	5.13	1.46	1.34	0.72	0.08, (76.194)	25.34, (78.76)	151.94, (74.93)
TH-8-M(TH-27)	2.63	1.25	5.13	1.48	1.39	1.06	0.08, (75.91)	19.44, (79.33)	89.50, (70.94)
TH-10-M(TH-31)	3.06	1.25	6.25	1.70	1.60	1.50	0.89, (65.17)	59.29, (77.32)	81.91, (83.13)
TH-10-M(TH-32)	3.06	1.25	6.25	1.64	1.40	1.32	0.67, (62.78)	37.81, (83.05)	81.34, (86.45)
TH-10-M(TH-33)	3.06	1.25	6.25	1.69	1.43	1.32	0.75, (65.36)	32.46, (79.54)	64.65, (83.92)

Table 4-4. Continued

Specimen	L_{sp}	α	L_{cr}	β_u	β_{3p}	β_{10p}	Error in Ultimate Strain, (R^2) (%)		
							β_u	β_{3p}	β_{10p}
Threaded Coupler (Erico)									
TH-5-M(TH-37)	2.38	2.00	4.88	1.00	0.94	0.89	0.11, (95.94)	5.87, (95.93)	10.71, (95.73)
TH-5-M(TH-38)	2.38	2.00	4.88	0.89	0.83	0.80	0.08, (96.58)	5.63, (95.84)	8.30, (96.13)
TH-5-M(TH-39	2.38	2.00	4.88	0.96	0.85	0.83	0.08, (96.68)	10.13, (96.01)	11.80, (95.91)
TH-8-M(TH-43)	3.75	1.25	6.25	1.10	1.09	0.99	0.08, (91.56)	2.75, (92.18)	19.12, (94.64)
TH-8-M(TH-44)	3.75	1.25	6.25	1.13	0.98	0.92	0.08, (88.10)	28.00, (93.99)	38.60, (95.05)
TH-8-M(TH-45)	3.75	1.25	6.25	1.06	0.98	0.89	0.07, (93.86)	13.37, (95.58)	27.81, (96.45)
TH-10-M(TH-49)	4.20	1.25	7.38	0.99	0.84	0.87	0.07, (80.90)	16.90, (84.21)	19.36, (83.95)
TH-10-M(TH-50)	4.20	1.25	7.38	1.04	0.79	0.75	0.06, (75.09)	41.14, (81.13)	34.31, (81.58)
TH-10-M(TH-51)	4.20	1.25	7.38	1.10	1.03	1.00	0.07, (70.08)	13.13, (73.68)	10.83, (73.15)
Swaged Coupler									
SW-5-M(SW1-1)	5.25	2.00	7.75	0.91	1.06	0.91	0.08, (84.91)	27.29, (77.75)	1.6, (84.27)
SW-5-M(SW2-1)	5.25	2.00	7.75	0.92	0.78	0.69	0.09, (84.68)	26.59, (91.76)	42.23, (94.20)
SW-5-M(SW-3)	5.25	2.00	7.75	0.95	0.87	0.78	0.09, (82.69)	15.70, (92.28)	32.16, (88.33)
SW-8-M(SW-7)	7.90	1.25	10.40	0.90	0.86	0.83	0.09, (92.26)	10.40, (93.75)	18.20, (94.5)
SW-8-M(SW-8)	7.90	1.25	10.40	0.89	0.93	0.87	0.08, (92.99)	9.01, (93.75)	6.41, (94.50)
SW-8-M(SW-9)	7.90	1.25	10.40	0.90	0.95	0.91	0.08, (94.14)	12.53, (92.06)	2.73, (93.77)
SW-10-M(SW-13)	9.50	1.25	12.68	0.86	0.85	0.81	0.07, (93.22)	1.25, (93.43)	9.60, (94.48)
SW-10-M(SW-14)	9.50	1.25	12.68	0.97	0.83	0.82	0.07, (89.15)	37.45, (94.92)	39.50, (95.05)
SW-10-M(SW-15)	9.50	1.25	12.68	0.96	0.86	0.83	0.06, (89.18)	25.68, (93.64)	35.67, (94.51)
Grouted Sleeve Coupler (NMB)									
GS-5-M(GS-1)	9.63	2.00	12.13	0.94	0.56	0.57	Not Seismic Coupler		
GS-5-M(GS-2)	9.63	2.00	12.13	0.96	0.58	0.58			
GS-5-M(GS-3)	9.63	2.00	12.13	0.97	0.56	0.55			
GS-8-M(GS-7)	14.50	1.25	17.00	0.69	0.68	0.67	0.07, (95.55)	2.05, (95.78)	5.27, (96.08)
GS-8-M(GS-8)	14.50	1.25	17.00	0.66	0.65	0.65	0.07, (96.45)	1.90, (96.58)	1.92, (96.58)
GS-8-M(GS-9)	14.50	1.25	17.00	0.66	0.66	0.65	0.07, (95.48)	1.05, (95.86)	3.49, (95.61)
GS-10-M(GS-13)	18.00	1.25	21.20	0.88	0.67	0.67	0.43, (77.62)	71.56, (92.39)	71.12, (92.35)
GS-10-M(GS-14)	18.00	1.25	21.20	0.75	0.67	0.67	0.26, (89.00)	18.28, (93.34)	17.19, (93.17)
GS-10-M(GS-15)	18.00	1.25	21.20	0.88	0.81	0.78	0.41, (77.49)	24.58, (77.31)	32.26, (79.55)

Table 4-4. Continued

Specimen	L_{sp}	α	L_{cr}	β_u	β_{3p}	β_{10p}	Error in Ultimate Strain, (R^2) (%)		
							β_u	β_{3p}	β_{10p}
Grouted Sleeve Coupler (Dayton)									
GS-5-M(GS-19)	9.50	2.00	12.00	0.84	0.47	0.49	Not Seismic Coupler		
GS-5-M(GS-20)	9.50	2.00	12.00	0.76	0.51	0.52			
GS-5-M(GS-21)	9.50	2.00	12.00	0.55	0.42	0.42			
GS-8-M(GS-25)	16.50	1.25	19.00	0.67	0.69	0.69	0.07, (95.95)	3.82, (95.63)	3.97, (95.61)
GS-8-M(GS-26)	16.50	1.25	19.00	0.70	0.70	0.69	0.07, (95.29)	0.05, (95.42)	1.21, (95.31)
GS-8-M(GS-27)	16.50	1.25	19.00	0.67	0.69	0.70	0.08, (95.45)	3.61, (96.19)	5.17, (96.05)
GS-10-M(GS-31)	18.00	1.25	21.20	0.70	0.70	0.67	0.24, (92.57)	0.48, (92.54)	7.09, (93.63)
GS-10-M(GS-32)	18.00	1.25	21.20	0.66	0.57	0.59	0.20, (94.26)	17.97, (96.29)	13.22, (95.92)
GS-10-M(GS-33)	18.00	1.25	21.20	0.66	0.57	0.59	0.20, (94.83)	17.97, (95.49)	13.22, (95.83)
Hybrid Coupler (Dextra Company)									
HY-5-M(HY-1)	8.13	2.00	10.63	0.78	0.86	0.92	0.08, (94.63)	15.04, (92.76)	26.15, (90.24)
HY-5-M(HY-2)	8.13	2.00	10.63	0.74	0.82	0.89	0.08, (88.54)	13.04, (83.75)	25.81, (75.81)
HY-5-M(HY-3)	8.13	2.00	10.63	0.80	0.84	0.90	0.08, (93.44)	7.28, (87.12)	19.69, (91.84)
HY-8-M(HY-7)	9.31	1.25	11.81	0.87	0.85	0.88	0.03, (86.79)	5.15, (88.36)	0.98, (86.48)
HY-8-M(HY-8)	9.31	1.25	11.81	0.93	0.91	0.92	0.02, (83.59)	7.12, (85.98)	2.37, (84.44)
HY-8-M(HY-9)	9.31	1.25	11.81	0.95	0.89	0.93	0.02, (91.95)	18.86, (95.15)	5.04, (93.02)
HY-10-M(HY-13)	10.63	1.25	13.80	0.85	0.79	0.80	0.08, (70.07)	13.63, (76.10)	10.25, (74.78)
HY-10-M(HY-14)	10.63	1.25	13.80	0.90	0.88	0.91	0.08, (75.29)	4.42, (77.74)	1.86, (74.25)
HY-10-M(HY-15)	10.63	1.25	13.80	0.79	0.72	0.79	0.07, (77.95)	12.78, (82.62)	0.63, (77.71)
Hybrid Coupler (Erico International)									
HY-5-M(HY-19)	7.88	2.00	10.38	0.80	0.79	0.73	0.10, (92.30)	4.03, (93.08)	11.66, (94.00)
HY-5-M(HY-20)	7.88	2.00	10.38	0.85	0.83	0.80	0.11, (95.32)	2.91, (96.31)	13.37, (96.92)
HY-5-M(HY-21)	7.88	2.00	10.38	0.79	0.72	0.70	0.10, (93.27)	12.26, (94.26)	16.92, (94.33)
HY-8-M(HY-25)	8.75	1.25	11.25	0.78	0.75	0.73	0.08, (94.37)	6.81, (95.58)	10.38, (96.10)
HY-8-M(HY-26)	8.75	1.25	11.25	0.77	0.78	0.76	0.08, (95.05)	1.08, (94.86)	1.25, (95.29)
HY-8-M(HY-27)	8.75	1.25	11.25	0.86	0.84	0.93	0.08, (98.02)	4.83, (97.87)	16.59, (97.49)
HY-10-M(HY-31)	10.75	1.25	13.93	0.77	0.77	0.73	0.07, (91.65)	0.31, (91.60)	7.25, (92.91)
HY-10-M(HY-32)	10.75	1.25	13.93	0.88	0.82	0.81	0.07, (84.77)	16.07, (89.02)	16.52, (89.12)
HY-10-M(HY-33)	10.75	1.25	13.93	0.78	0.81	0.79	0.06, (84.89)	6.69, (83.13)	1.75, (84.47)

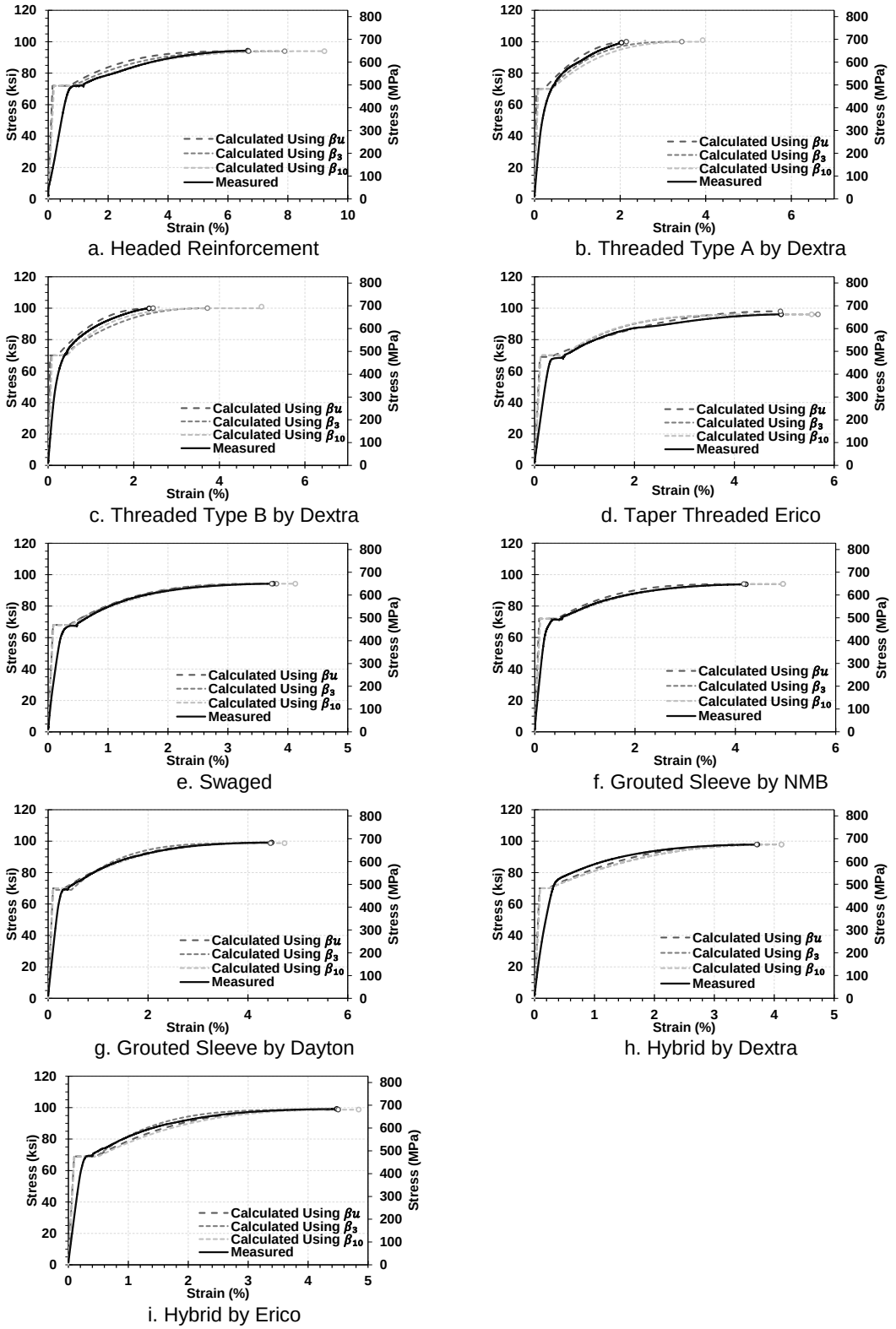

Figure 4-29. Calculated and measured stress-strain relationships for No.10 (32-mm) couplers using different Beta

Table 4-5 presents the failure mode for all 81 couplers tested under the monotonic loading. It can be concluded that bar fractured in most of these splices except No. 5 (16-mm) grouted sleeve couplers. Small size bars are not usually used as the longitudinal reinforcement of bridge columns. Therefore, the selected No. 8 (25-mm) and No. 10 (32-mm) couplers in the present study are seismic couplers and may be used in the plastic hinge region of bridge columns following the column design methods proposed by Tazarv and Saiidi (2016).

Table 4-5. Coupler failure modes in monotonic testing

Coupler Type	Size	Failure Mode			Remarks
		Bar Fracture	Bar Pullout	Coupler Failure	
Headed Bar Coupler	No. 5 (16 mm)	XXX			Seismic Coupler
	No. 8 (24 mm)	XXX			Seismic Coupler
	No. 10 (32 mm)	XXX			Seismic Coupler
Swaged Coupler	No. 5 (16 mm)	XXX			Seismic Coupler
	No. 8 (24 mm)	XX		x	Seismic Coupler
	No. 10 (32 mm)	XXX			Seismic Coupler
Threaed Coupler (Type A)	No. 5 (16 mm)	XXX			Seismic Coupler
	No. 8 (24 mm)	XXX			Seismic Coupler
	No. 10 (32 mm)	XXX			Seismic Coupler
Threaed Coupler (Type B)	No. 5 (16 mm)	XXX			Seismic Coupler
	No. 8 (24 mm)	XXX			Seismic Coupler
	No. 10 (32 mm)	XXX			Seismic Coupler
Threaded Coupler (Taper)	No. 5 (16 mm)	XXX			Seismic Coupler
	No. 8 (24 mm)	XXX			Seismic Coupler
	No. 10 (32 mm)	XXX			Seismic Coupler
Grouted Coupler (NMB)	No. 5 (16 mm)		XXX		Not Seismic Coupler
	No. 8 (24 mm)	XXX			Seismic Coupler
	No. 10 (32 mm)	XXX			Seismic Coupler
Grouted Coupler (Dayton)	No. 5 (16 mm)	X	XX		Not Seismic Coupler
	No. 8 (24 mm)	XXX			Seismic Coupler
	No. 10 (32 mm)	XXX			Seismic Coupler
Hybrid Coupler (Swaged and Thredad)	No. 5 (16 mm)	XXX			Seismic Coupler
	No. 8 (24 mm)	XXX			Seismic Coupler
	No. 10 (32 mm)	XX		X	Seismic Coupler
Hybrid Coupler (Grouted and Thredad)	No. 5 (16 mm)	XXX			Seismic Coupler
	No. 8 (24 mm)	XXX			Seismic Coupler
	No. 10 (32 mm)	XXX			Seismic Coupler

X = one sample

4.3.2 Recommended Coupler Rigid Length Factor (β)

Table 4-6 presents the proposed rigid length factor for different coupler types and sizes. These values are based on the average of three β_u rounded up to the nearest 0.05.

Table 4-6. Recommended rigid length factor (β)

Coupler Type	No. 5 (16 mm)	No. 8 (24 mm)	No. 10 (32 mm)
Headed Reinforcement	0.80	0.75	0.55
Threaded (Dextra-Type A)	1.70	1.5	1.60
Threaded (Dextra-Type B)	1.60	1.5	1.65
Threaded (Erico)	0.95	1.10	1.05
Swaged	0.90	0.90	0.95
Grouted Sleeve (NMB)	0.95	0.65	0.85
Grouted Sleeve (Dayton)	0.70	0.70	0.65
Hybrid (Dextra)	0.80	0.90	0.85
Hybrid (Erico)	0.80	0.80	0.80

Figure 4-30 shows the stress-strain relationships for spliced and unspliced No. 10 ASTM A706 Grade 60 (2009) reinforcing steel bars using the AASHTO Guide Specifications for LRFD Seismic Bridge Design (2011) expected properties. The spliced specimen behavior was based on the recommended β presented in Table 4-6. It can be seen the headed coupler exhibits the highest strain capacity (66.7% of the unspliced bar) and the threaded coupler shows the lowest strain capacity (10% of the unspliced bar) compared to other coupler types. Furthermore, the strain capacity of swaged, grouted, and hybrid couplers are in the range of 25%-40% of the unspliced reinforcing steel bar ultimate strain. It should be note that the coupler length, the coupler location, and the coupler rigid length factor are needed to successfully quantify the coupler effect on the seismic performance of bridge columns based on the methods proposed in Tazarv and Saiidi (2016). Therefore, an extreme rigid length factor for a coupler does not necessarily mean that the displacement capacity of a bridge column incorporating that coupler is

significantly affected. The other two parameters should also be included in the analysis and design.

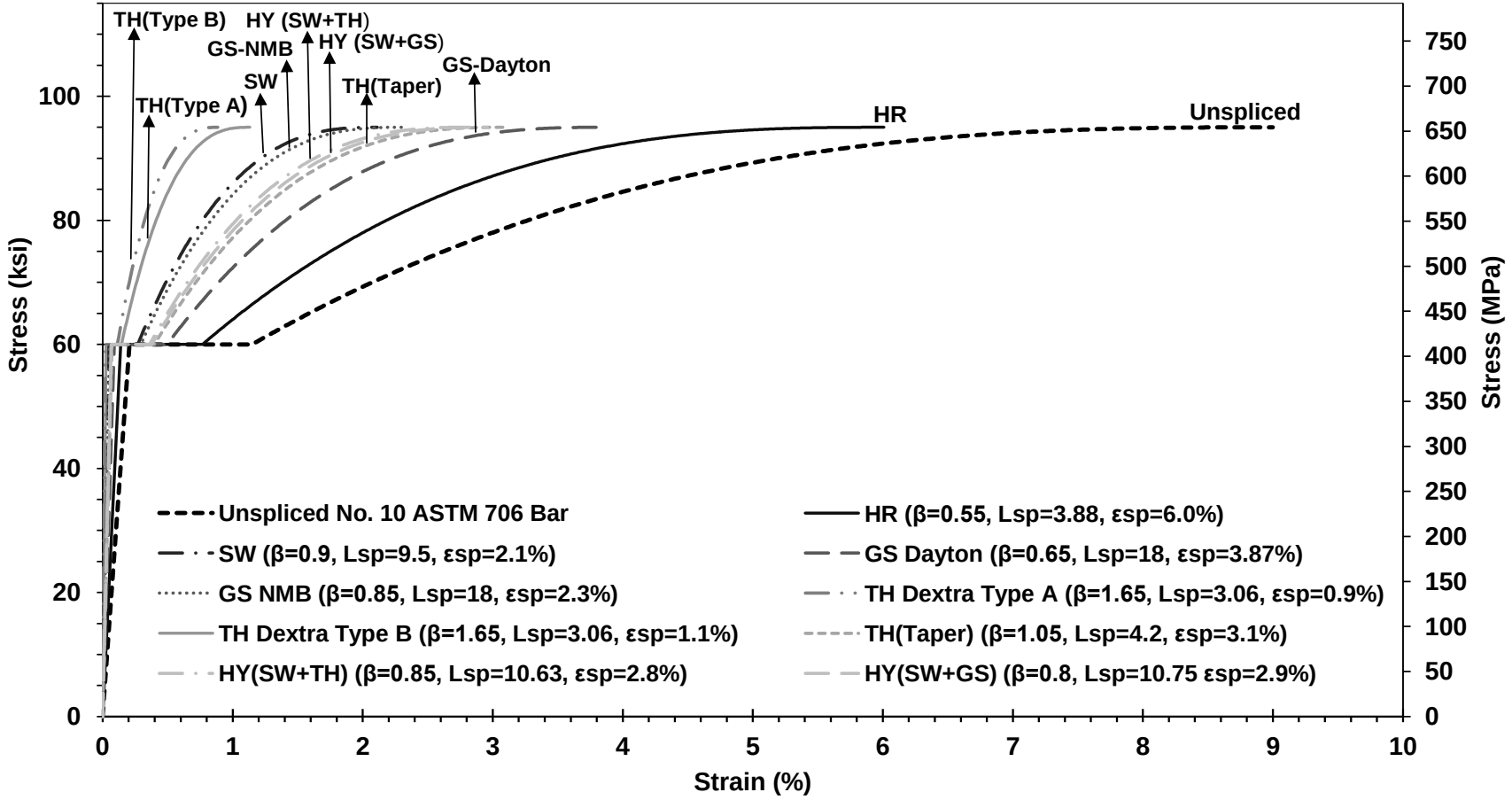

Figure 4-30. Stress-strain relationships for spliced and unspliced No.10 (32-mm) ASTM A706 reinforcing steel bars

4.3.3 Material Model Verification

Figures 4-31 shows the calculated and measured stress- strain relationships for different mechanical bar splices using the recommended "coupler rigid length factor" (Table 4-6). The measured data for all three specimens tested per coupler product was included in the figure for comparison. It can be seen that the coupler model using the recommended rigid length factors could reproduce the measured behavior with a good accuracy. The calculated ultimate strains were no more than 15% different than the average measured ultimate strains per product (shown in subfigures). The splice prior-to-yielding behavior could not be well predicted and mainly overestimated since the model proposed by Tazarv and Saiidi (2016) is calibrated for the ultimate strains, which are important in the displacement-based design of bridge columns. The higher initial stiffness seen in this coupler model is expected to have insignificant effect on the seismic performance of bridge columns due to the relatively small size of couplers compared to the column length.

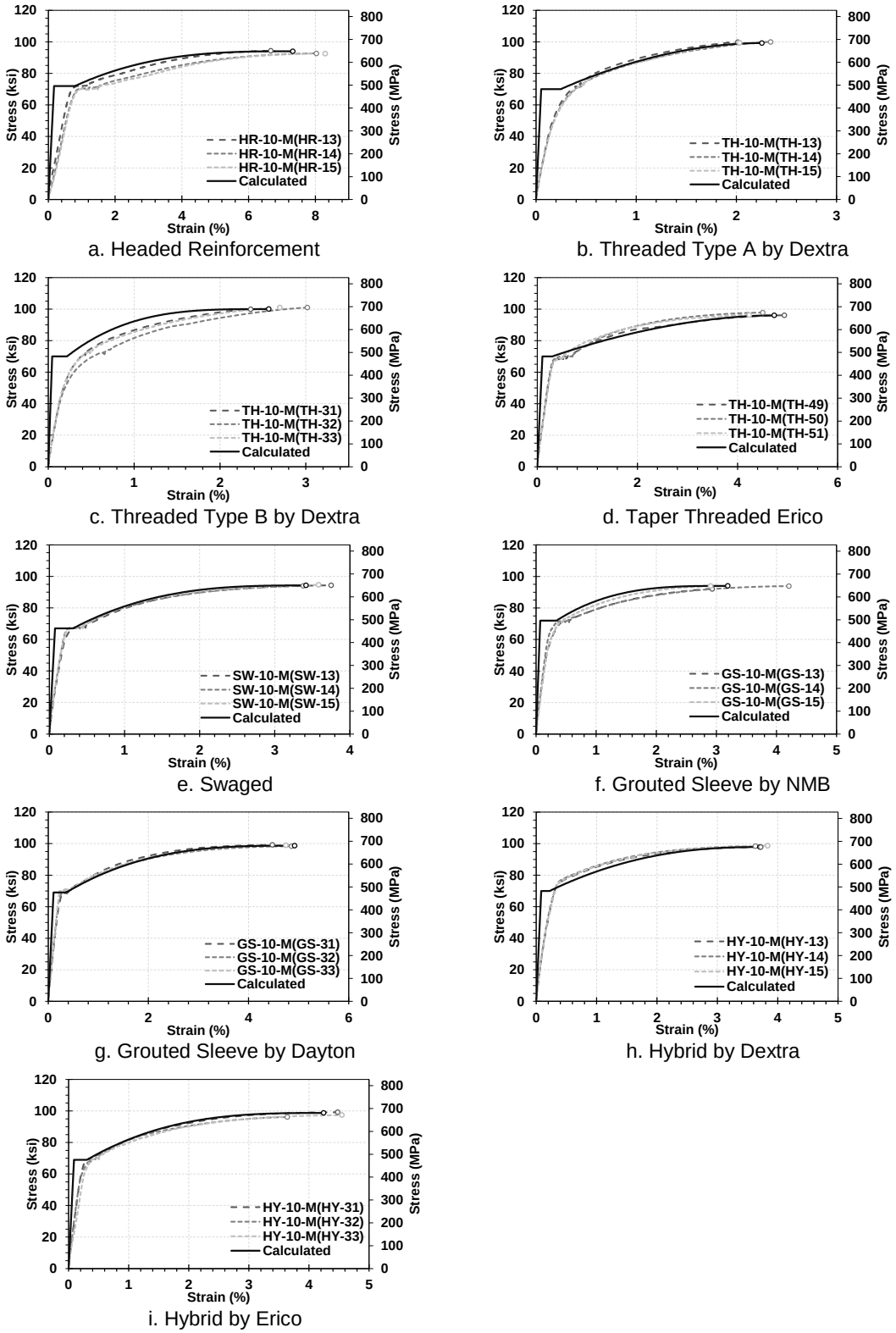

Figure 4-31. Calculated and measured stress-strain relationships for No.10 (32-mm) couplers using recommended Beta

4.4 Coupler Cyclic Testing

Cyclic testing of 81 mechanical bar splices was performed using the loading protocol described in Sec. 3.5.2. The measured stress-strain relationship from the monotonic testing of the same coupler type and size was utilized as the reference data for the cyclic testing. In some of cyclic tests, coupler extensometer strains (Fig. 3-2) were not reliable. Furthermore, the coupler extensometer was removed before the rupture of the splice to avoid any damage of the device. Due to these issues, strains from both the extensometer and the actuator were included in the following sections for completeness and for better understanding of the coupler cyclic performance.

4.4.1 Headed Reinforcement Couplers

Nine headed reinforcement couplers were tested under cyclic loading, three samples per bar size. Figures 4-32 to 34 show the measured cyclic stress-strain hysteresis for the No. 5 (16-mm), No. 8 (25-mm), and No. 10 (32-mm) headed reinforcement couplers, respectively. In all cases, the envelope of the splice cyclic behavior was the same as the monotonic behavior. The hysteretic loop was close to what is expected for a steel bar but sometimes with a minor pinching at the reloading stresses (e.g. Fig. 4-32), which could be because of a small gap between the headed bars inside the coupler.

Figure 4-35 shows the mode of failure for these samples after completion of the cyclic testing. Bar fractured in all of the headed reinforcement couplers outside the coupler region, thus they are seismic couplers under cyclic loads.

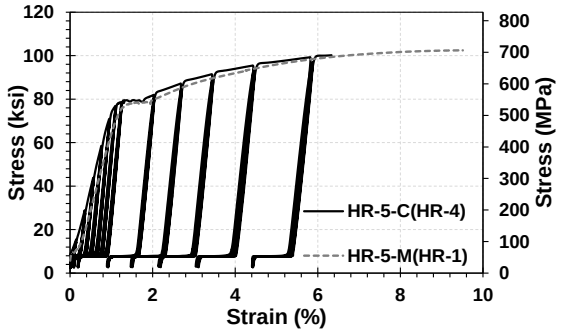

a. Coupler region strains using extensometer displacements

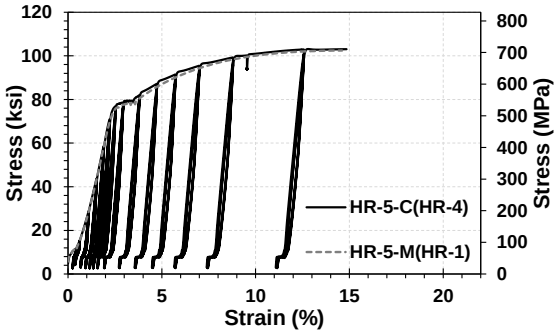

b. Specimen total strains using actuator displacements

Figure 4-32. Cyclic test results for No. 5 (16-mm) headed reinforcement couplers

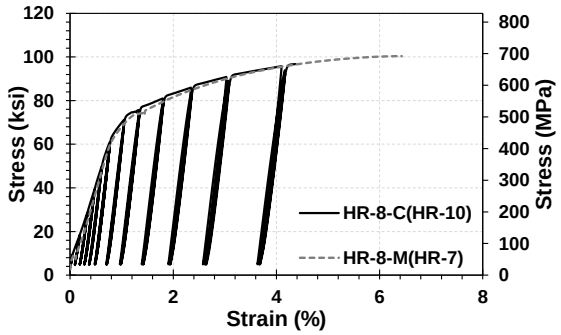

a. Coupler region strains using extensometer displacements

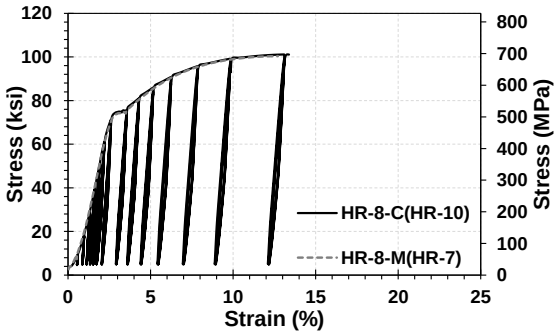

b. Specimen total strains using actuator displacements

Figure 4-33. Cyclic test results for No. 8 (24-mm) headed reinforcement couplers

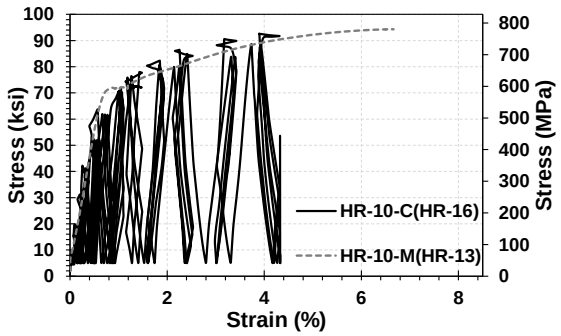

a. Coupler region strains using extensometer displacements

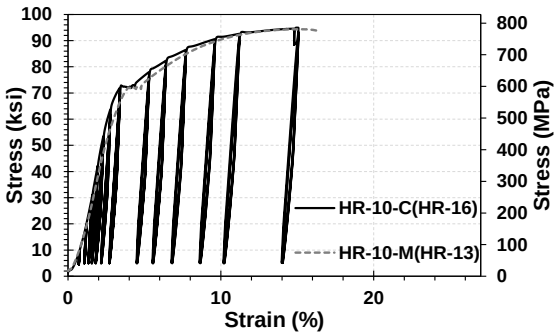

b. Specimen total strains using actuator displacements

Figure 4-34. Cyclic test results for No. 10 (32-mm) headed reinforcement couplers

a. No.5 (16 mm) b. No.8 (25 mm) c. No.10 (32 mm)

Figure 4-35. Failure of headed reinforcement couplers under cyclic loading

4.4.2 Threaded Couplers

Three products were categorized as the threaded coupler and three samples of each product per bar size were cyclically tested to failure.

4.4.2.1 Threaded Coupler (Type A by Dextra)

Nine threaded couplers (Type A) were tested under cyclic loading, three samples per bar size. Figures 4-36 to 4-38 show the measured cyclic stress-strain hysteresis for the No. 5 (16-mm), No. 8 (25-mm), and No. 10 (32-mm) threaded (Type A) couplers, respectively. In all cases, the envelope of the splice cyclic behavior was approximately the same as the monotonic behavior. The hysteretic loop was close to what is expected for a steel bar.

Figure 4-39 shows the mode of failure for these samples after completion of the cyclic testing. Bar fractured in all threaded couplers (Type A) outside the coupler region, thus they are seismic couplers under cyclic loads.

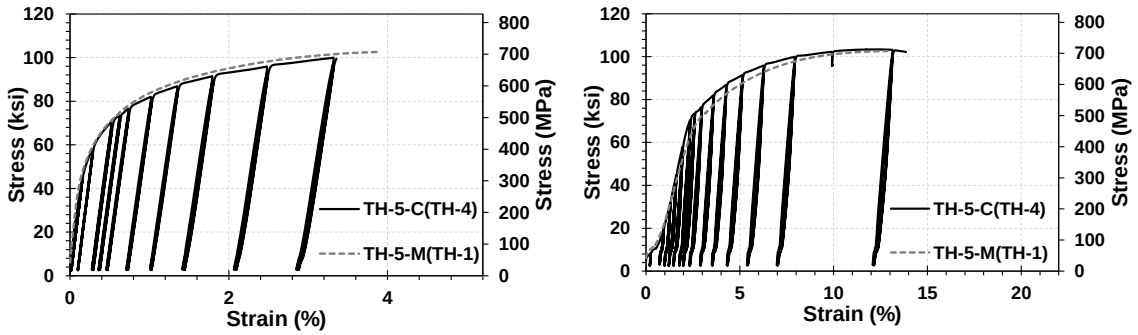

a. Coupler region strains using extensometer displacements

b. Specimen total strains using actuator displacements

Figure 4-36. Cyclic test results for No. 5 (16-mm) threaded couplers (Type A)

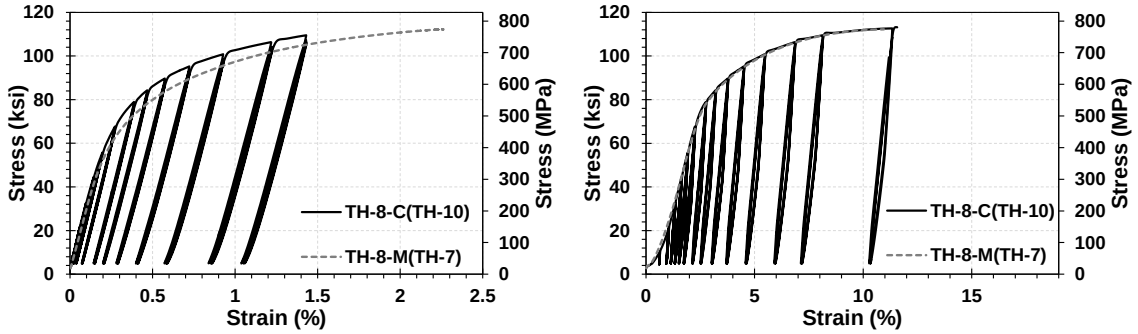

a. Coupler region strains using extensometer displacements

b. Specimen total strains using actuator displacements

Figure 4-37. Cyclic test results for No. 8 (24-mm) threaded couplers (Type A)

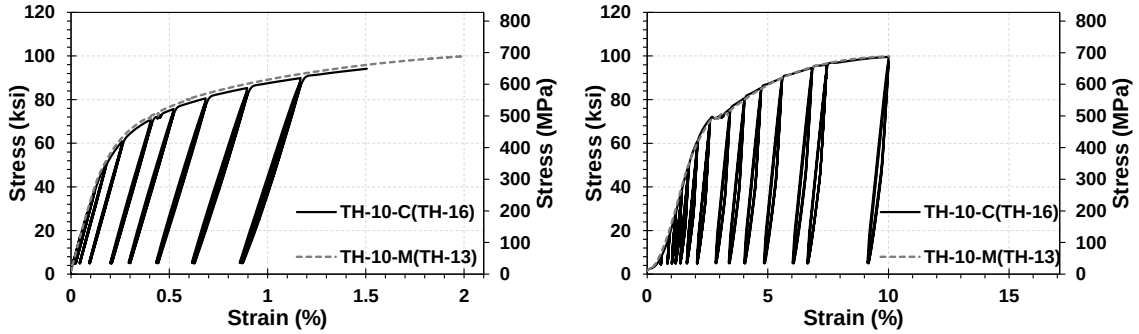

a. Coupler region strains using extensometer displacements

b. Specimen total strains using actuator displacements

Figure 4-38. Cyclic test results for No. 10 (32-mm) threaded couplers (Type A)

a. No.5 (16 mm)

b. No.8 (25 mm)

c. No.10 (32 mm)

Figure 4-39. Failure of threaded couplers (Type A) under cyclic loading

4.4.2.2 Threaded Coupler (Type B by Dextra)

Nine threaded couplers (Type B) were tested under cyclic loading, three samples per bar size. Figures 4-40 to 4-42 show the measured cyclic stress-strain hysteresis for the No. 5 (16-mm), No. 8 (25-mm), and No. 10 (32-mm) threaded couplers (Type B),

respectively. In all cases, the envelope of the splice cyclic behavior was the same as the monotonic behavior. The hysteretic loop was close to what is expected for a steel bar.

Figure 4-43 shows the mode of failure for these samples after completion of the cyclic testing. Bar fractured in all the threaded couplers (Type B) outside the coupler region, thus they are seismic couplers under cyclic loads.

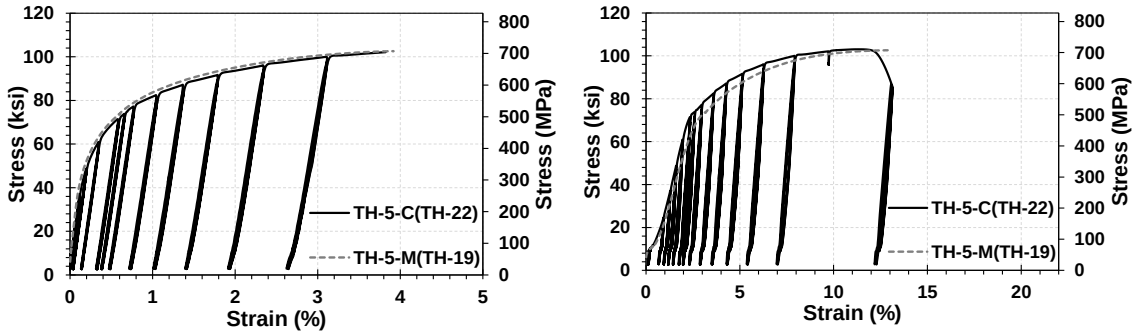

a. Coupler region strains using extensometer displacements

b. Specimen total strains using actuator displacements

Figure 4-40. Cyclic test results for No. 5 (16-mm) threaded couplers (Type B)

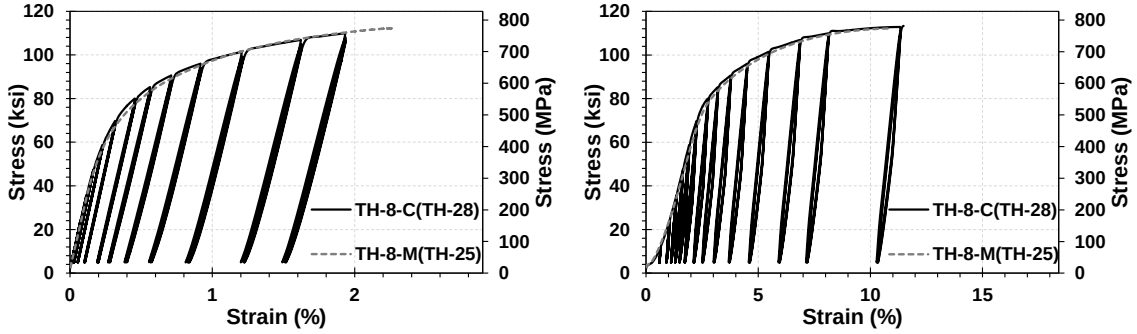

a. Coupler region strains using extensometer displacements

b. Specimen total strains using actuator displacements

Figure 4-41. Cyclic test results for No. 8 (24-mm) threaded couplers (Type B)

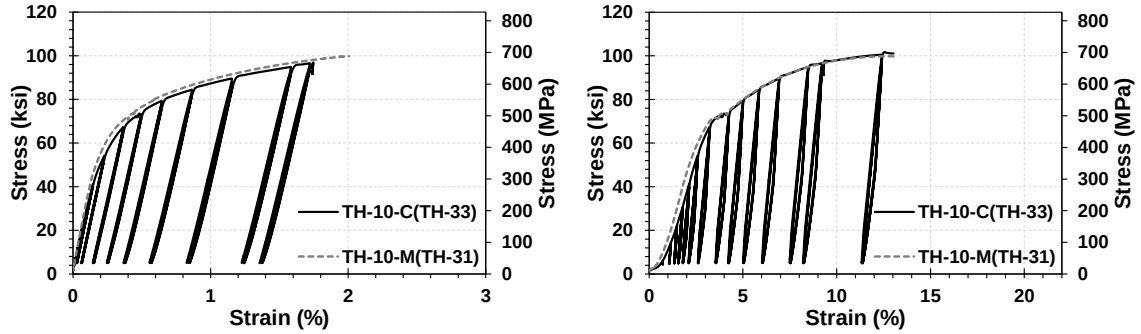

a. Coupler region strains using extensometer displacements

b. Specimen total strains using actuator displacements

Figure 4-42. Cyclic test results for No. 10 (32-mm) threaded couplers (Type B)

a. No.5 (16 mm)

b. No.8 (25 mm)

c. No.10 (32 mm)

Figure 4-43. Failure of threaded couplers (Type B) under cyclic loading

4.4.2.3 Threaded Coupler (Tapered by Erico)

Nine tapered threaded couplers were tested under cyclic loading, three samples per bar size. Figures 4-44 to 4-46 show the measured cyclic stress-strain hysteresis for the No. 5 (16-mm), No. 8 (25-mm), and No. 10 (32-mm) tapered threaded couplers,

respectively. In all cases, the envelope of the splice cyclic behavior was approximately the same as the monotonic behavior. The hysteretic loop was close to what is expected for a steel bar

Figure 4-47 shows the mode of failure for these samples after completion of the cyclic testing. Bar fractured in all the tapered threaded couplers outside the coupler region, thus they are seismic couplers under cyclic loads.

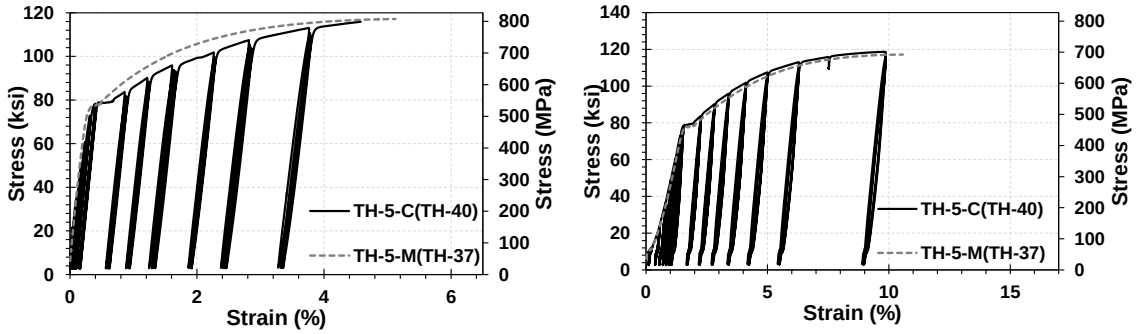

a. Coupler region strains using extensometer displacements

b. Specimen total strains using actuator displacements

Figure 4-44. Cyclic test results for No. 5 (16-mm) tapered threaded couplers

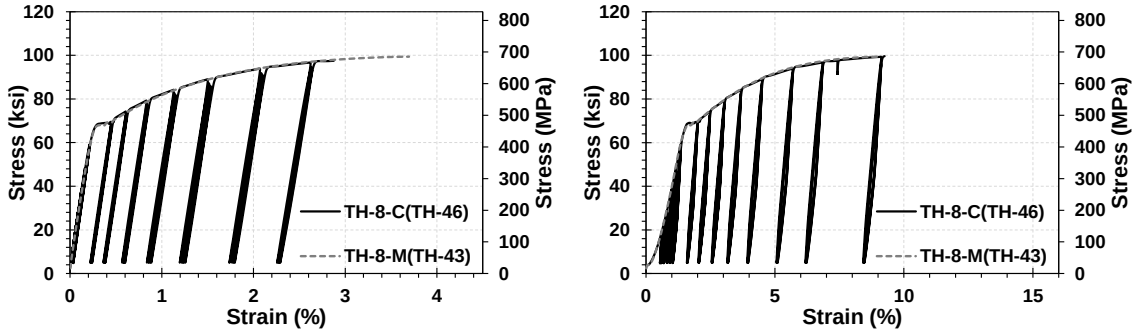

a. Coupler region strains using extensometer displacements

b. Specimen total strains using actuator displacements

Figure 4-45. Cyclic test results for No. 8 (24-mm) tapered threaded couplers

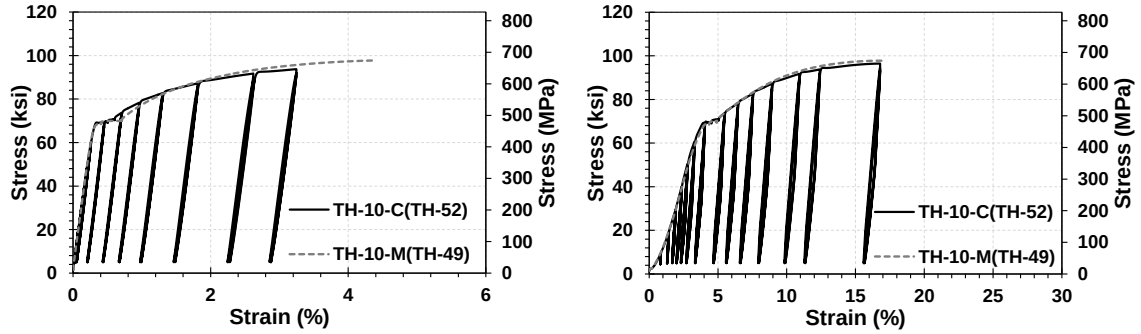

a. Coupler region strains using extensometer displacements

b. Specimen total strains using actuator displacements

Figure 4-46. Cyclic test results for No. 10 (32-mm) tapered threaded couplers

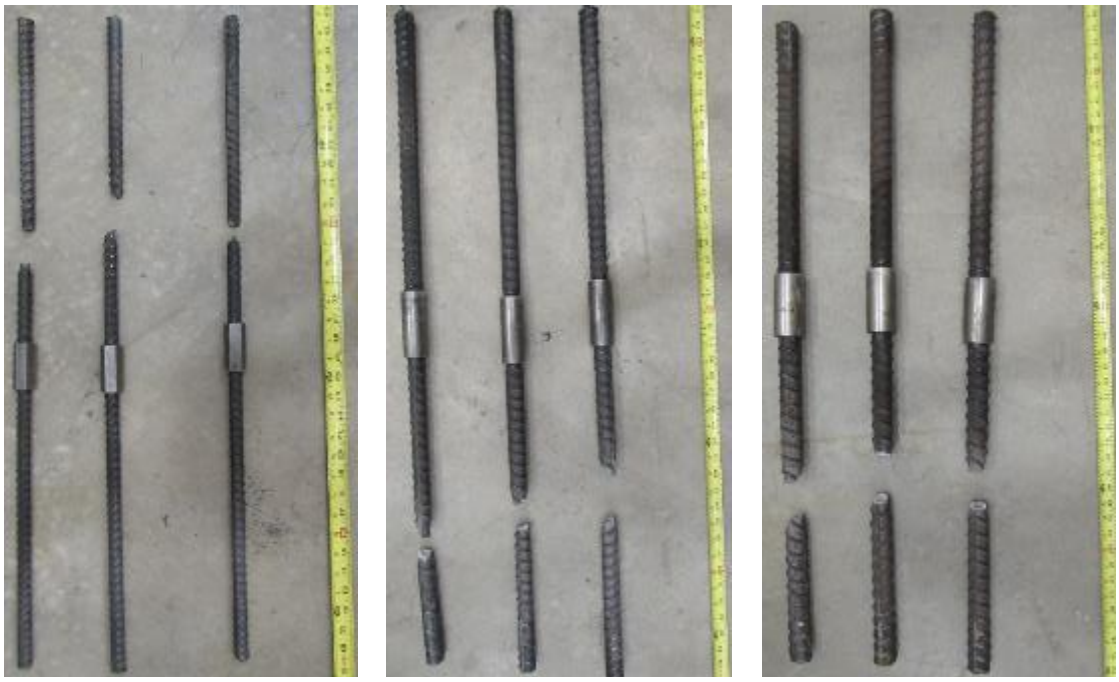

a. No.5 (16 mm)

b. No.8 (25 mm)

c. No.10 (32 mm)

Figure 4-47. Failure of tapered threaded couplers under cyclic loading

4.4.3 Swaged Couplers

Nine swaged couplers were tested under cyclic loading, three samples per bar size. Figures 4-48 to 4-50 show the measured cyclic stress-strain hysteresis for the No. 5 (16-mm), No. 8 (25-mm), and No. 10 (32-mm) swaged couplers, respectively. In all cases,

the envelope of the splice cyclic behavior was approximately the same as the monotonic behavior. The hysteretic loop was close to what is expected for a steel bar.

Figure 4-51 shows the mode of failure for these samples after completion of the cyclic testing. Bar fractured in all of the swaged couplers outside the coupler region, thus they are seismic couplers under cyclic loads.

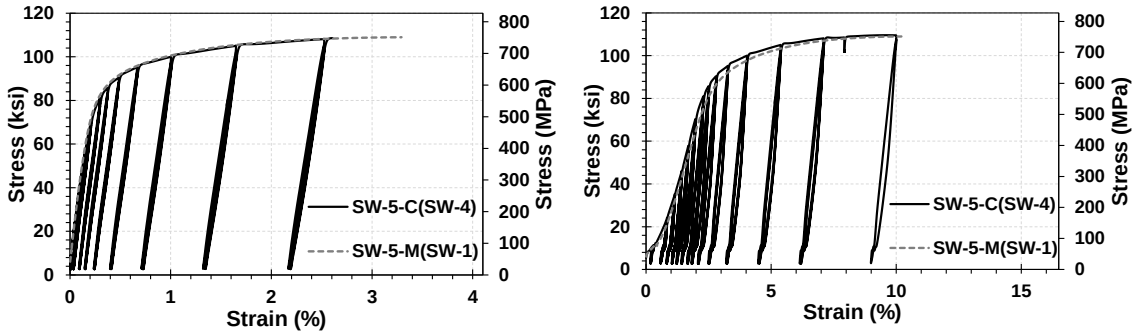

a. Coupler region strains using extensometer displacements

b. Specimen total strains using actuator displacements

Figure 4-48. Cyclic test results for No. 5 (16-mm) Swaged couplers

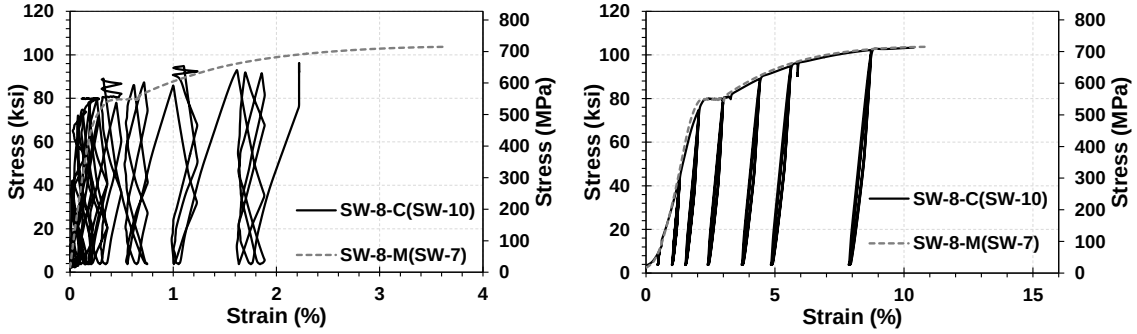

a. Coupler region strains using extensometer displacements

b. Specimen total strains using actuator displacements

Figure 4-49. Cyclic test results for No. 8 (24-mm) Swaged couplers

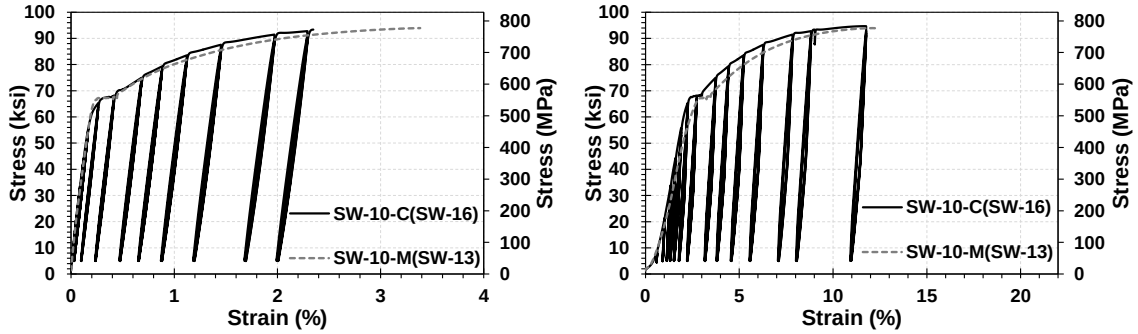

a. Coupler region strains using extensometer displacements

b. Specimen total strains using actuator displacements

Figure 4-50. Cyclic test results for No. 10 (32-mm) Swaged couplers

a. No.5 (16 mm)

b. No.8 (25 mm)

c. No.10 (32 mm)

Figure 4-51. Failure of Swaged couplers under cyclic loading

4.4.4 Grouted Sleeve Couplers

Two products were categorized as the grouted sleeve coupler and three samples of each product per bar size were cyclically tested to failure.

4.4.4.1 Grouted Sleeve Couplers (by Splice Sleeve North America, NMB)

Nine swaged couplers were tested under cyclic loading, three samples per bar size. Figures 4-52 to 4-54 show the measured cyclic stress-strain hysteresis for the No. 5 (16-mm), No. 8 (25-mm), and No. 10 (32-mm) NMB grouted sleeve couplers, respectively. In all cases, the envelope of the splice cyclic behavior was approximately the same as the monotonic behavior. The hysteretic loop was close to what is expected for a steel bar.

Figure 4-55 shows the mode of failure for these samples after completion of the cyclic testing. Bar fractured in all the No. 8 (25-mm), and No. 10 (32-mm) NMB grouted sleeve couplers outside the coupler region, thus they are seismic couplers under cyclic loads. Bar pulled out from the sleeve in No. 5 (16-mm) NMB couplers. Therefore, they are not seismic couplers.

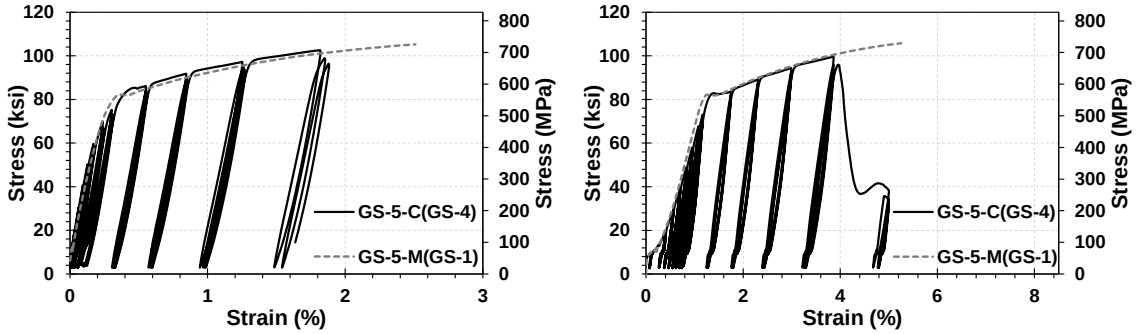

a. Coupler region strains using extensometer displacements

b. Specimen total strains using actuator displacements

Figure 4-52. Cyclic test results for No. 5 (16-mm) grouted sleeve couplers (NMB)

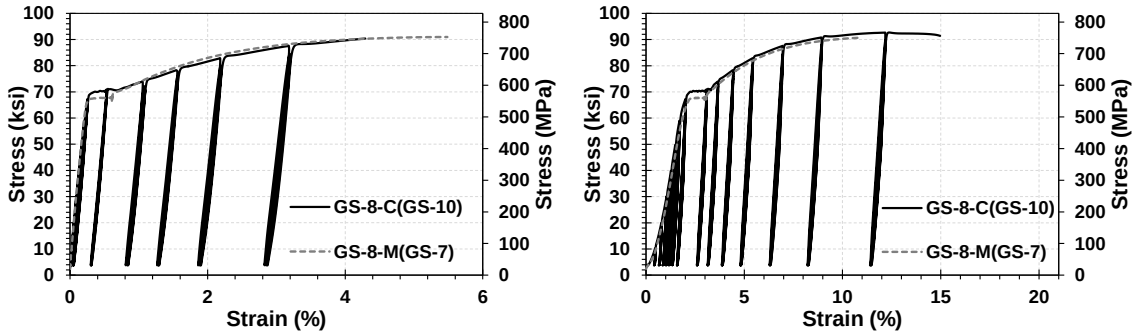

a. Coupler region strains using extensometer displacements

b. Specimen total strains using actuator displacements

Figure 4-53. Cyclic test results for No. 8 (24-mm) grouted sleeve couplers (NMB)

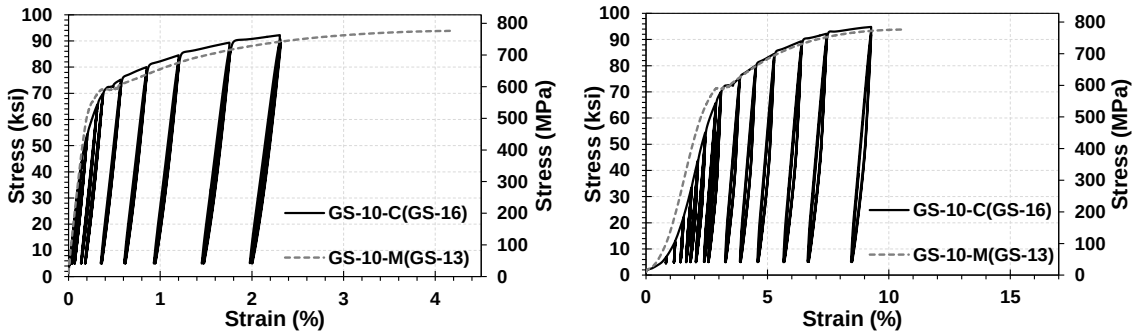

a. Coupler region strains using extensometer displacements

b. Specimen total strains using actuator displacements

Figure 4-54. Cyclic test results for No. 10 (32-mm) grouted sleeve couplers (NMB)

a. No.5 (16 mm) b. No.8 (25 mm) c. No.10 (32 mm)

Figure 4-55. Failure of NMB Grouted Sleeve couplers under cyclic loading

4.4.4.2 Grouted Sleeve Coupler (by Dayton Superior)

Nine grouted sleeve couplers (by Dayton Superior) were tested under cyclic loading, three samples per bar size. Figures 4-56 to 4-58 show the measured cyclic stress-strain hysteresis for the No. 5 (16-mm), No. 8 (25-mm), and No. 10 (32-mm) grouted sleeve couplers (Dayton Superior), respectively. In all cases, the envelope of the splice cyclic behavior was the same as the monotonic behavior. The hysteretic loop was close to what is expected for a steel bar.

Figure 4-59 shows the mode of failure for these samples after completion of the cyclic testing. Bar fractured in all of No. 8 (25-mm), and No. 10 (32-mm) grouted sleeve couplers (Dayton Superior) outside the coupler region, thus they are seismic couplers under cyclic loads. Bar pulled out from the sleeve in No. 5 (16-mm), couplers. Therefore, they are not seismic couplers.

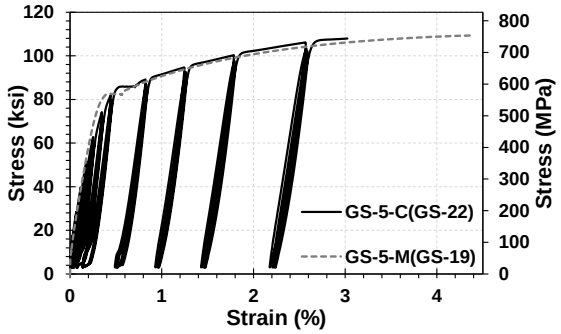

a. Coupler region strains using extensometer displacements

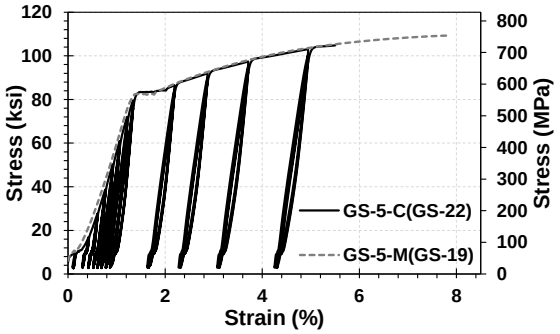

b. Specimen total strains using actuator displacements

Figure 4-56. Cyclic test results for No. 5 (16-mm) grouted sleeve couplers (Dayton Superior)

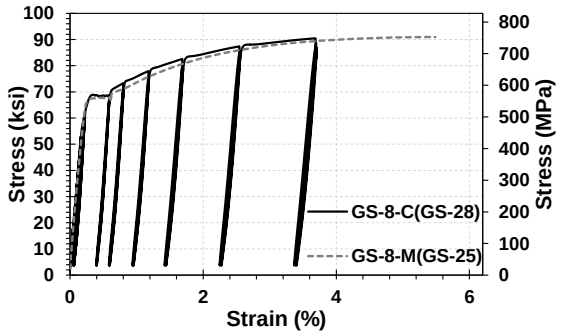

a. Coupler region strains using extensometer displacements

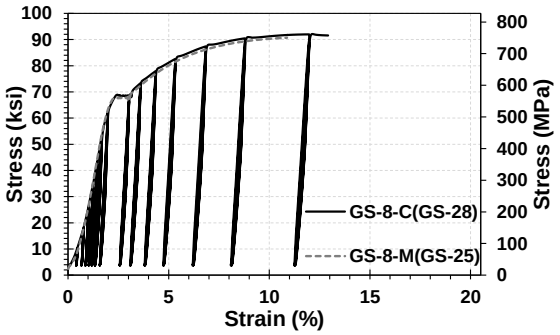

b. Specimen total strains using actuator displacements

Figure 4-57. Cyclic test results for No. 8 (24-mm) grouted sleeve couplers (Dayton Superior)

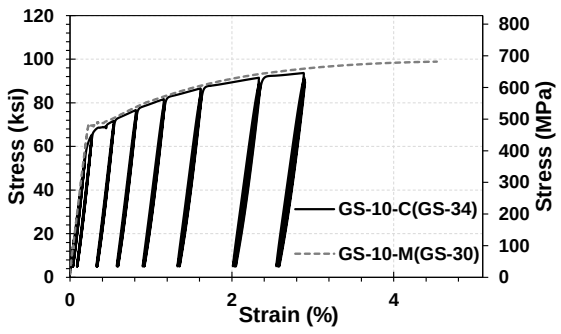

a. Coupler region strains using extensometer displacements

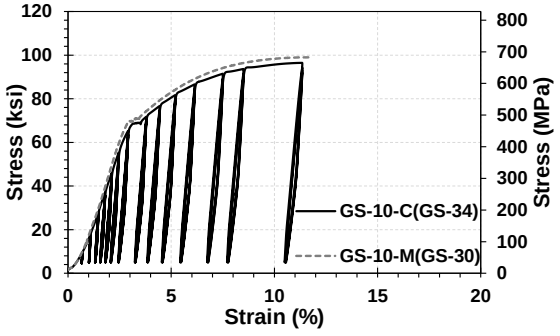

b. Specimen total strains using actuator displacements

Figure 4-58. Cyclic test results for No. 10 (32-mm) grouted sleeve couplers (Dayton Superior)

a. No.5 (16 mm) b. No.8 (25 mm) c. No.10 (32 mm)

Figure 4-59. Failure of grouted sleeve couplers (Dayton Superior) under cyclic loading

4.4.5 Hybrid couplers

Two products were categorized as the hybrid coupler and three samples of each product per bar size were cyclically tested to failure. In one of the products, bars were spliced through grouted and threaded mechanisms at the ends of the coupler. In the second hybrid coupler, bars were spliced using threaded and swaged mechanisms at the ends.

4.4.4.1 Hybrid Coupler (Swaged & Threaded)

Nine swaged-threaded hybrid couplers were tested under cyclic loading, three samples per bar size. Figures 4-60 to 4-62 show the measured cyclic stress-strain hysteresis for the No. 5 (16-mm), No. 8 (25-mm), and No. 10 (32-mm) swaged-threaded hybrid couplers, respectively. In all cases, the envelope of the splice cyclic behavior was approximately the same as the monotonic behavior. The hysteretic loop was close to what is expected for a steel bar.

Figure 4-63 shows the mode of failure for these samples after completion of the cyclic testing. Bar fractured in all swaged-threaded hybrid couplers outside the coupler region, thus they are seismic couplers under cyclic loads.

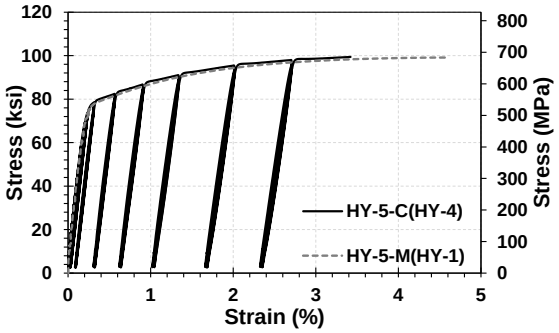

a. Coupler region strains using extensometer displacements

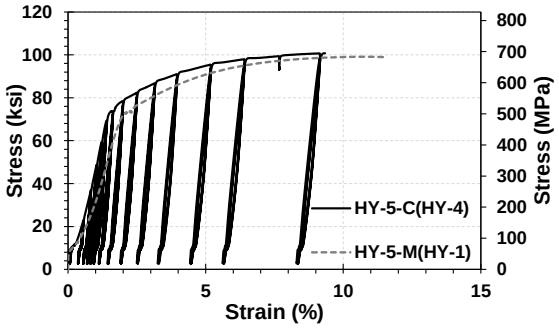

b. Specimen total strains using actuator displacements

Figure 4-60. Cyclic test results for No. 5 (16-mm) swaged-threaded hybrid couplers

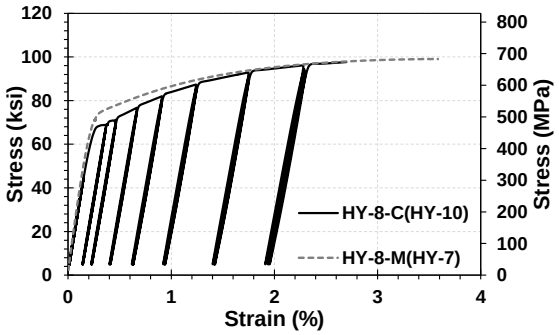

a. Coupler region strains using extensometer displacements

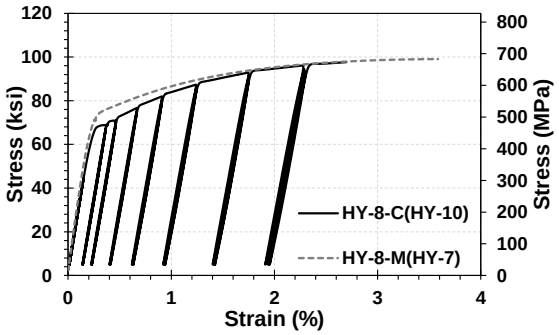

b. Specimen total strains using actuator displacements

Figure 4-61. Cyclic test results for No. 8 (24-mm) swaged-threaded hybrid couplers

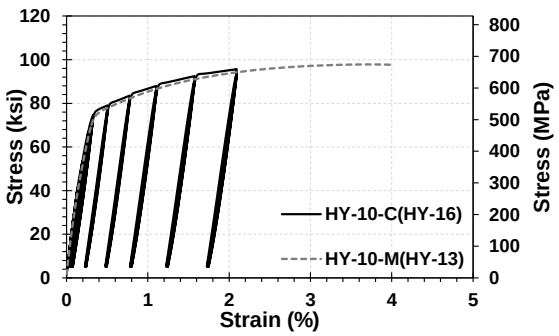

a. Coupler region strains using extensometer displacements

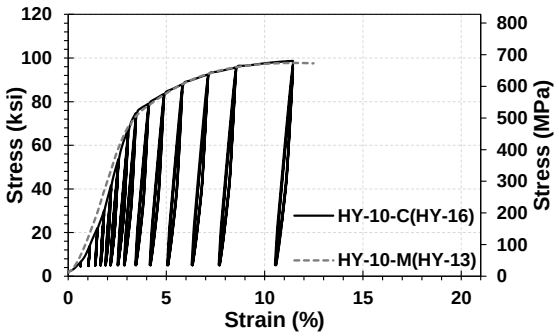

b. Specimen total strains using actuator displacements

Figure 4-62. Cyclic test results for No. 10 (32-mm) swaged-threaded hybrid couplers

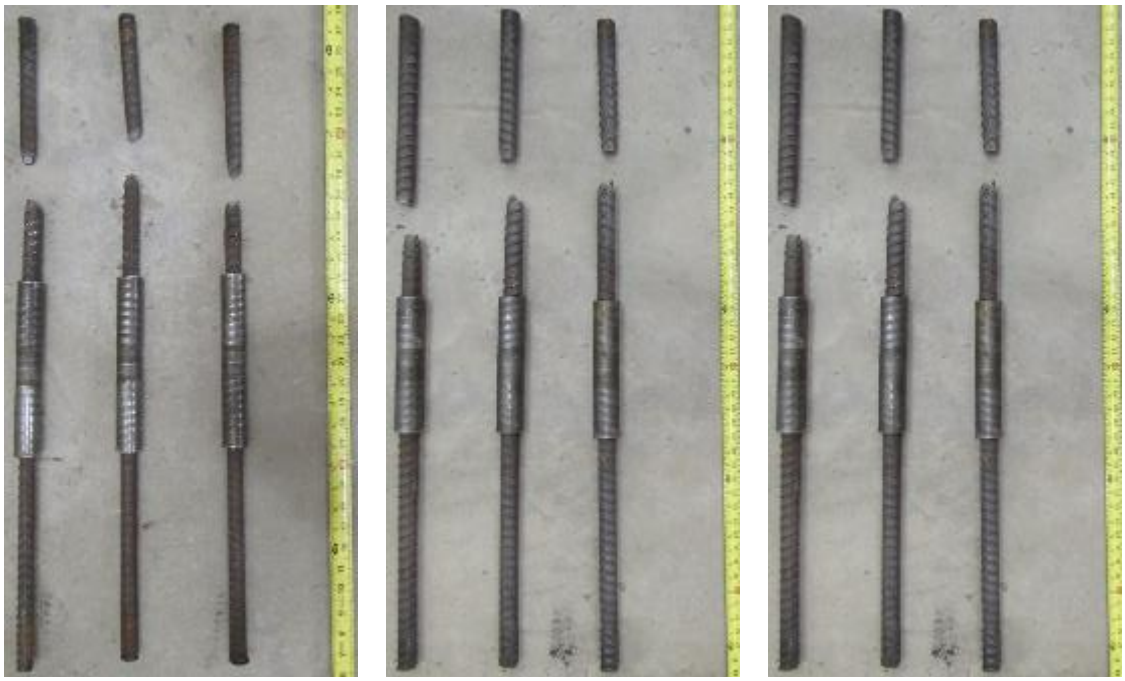

a. No.5 (16 mm) b. No.8 (25 mm) c.No.10 (32 mm)

Figure 4-63. Failure of swaged-threaded hybrid couplers under cyclic loading

4.4.5.2 Hybrid Coupler (Grouted & Threaded)

Nine grouted-threaded hybrid couplers were tested under cyclic loading, three samples per bar size. Figures 4-64 to 4-66 show the measured cyclic stress-strain hysteresis for the No. 5 (16 mm), No. 8 (25 mm), and No. 10 (32 mm) grouted threaded hybrid couplers respectively. In all cases, the envelope of the splice cyclic behavior was approximately the same as the monotonic behavior. The hysteretic loop was close to what is expected for a steel bar.

Figure 4-67 shows the mode of failure for these samples after completion of the cyclic testing. Bar fractured in all of the grouted-threaded hybrid couplers outside the coupler region, thus they are seismic couplers under cyclic loads.

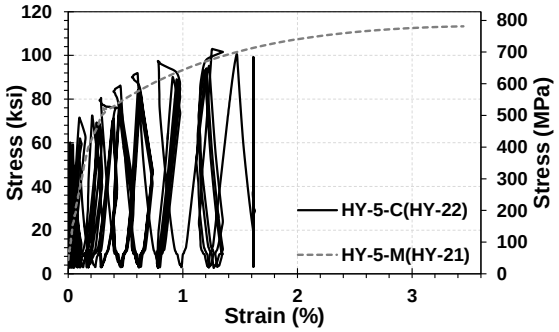

a. Coupler region strains using extensometer displacements

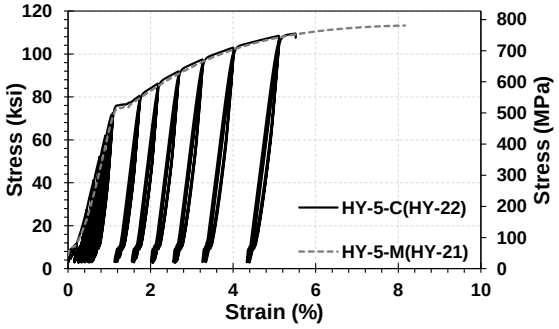

b. Specimen total strains using actuator displacements

Figure 4-64. Cyclic test results for No. 5 (16-mm) grouted-threaded hybrid couplers

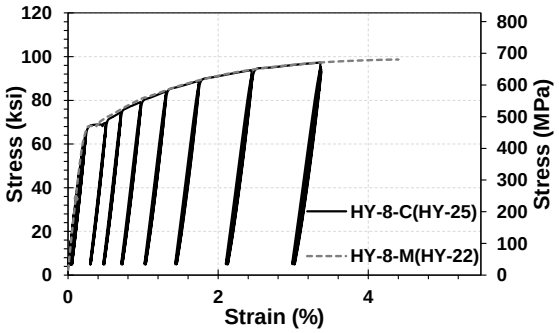

a. Coupler region strains using extensometer displacements

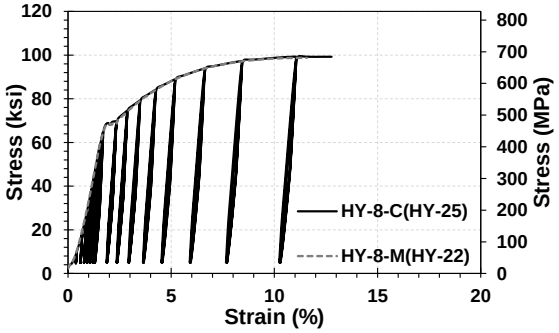

b. Specimen total strains using actuator displacements

Figure 4-65. Cyclic test results for No. 8 (24-mm) grouted-threaded hybrid couplers

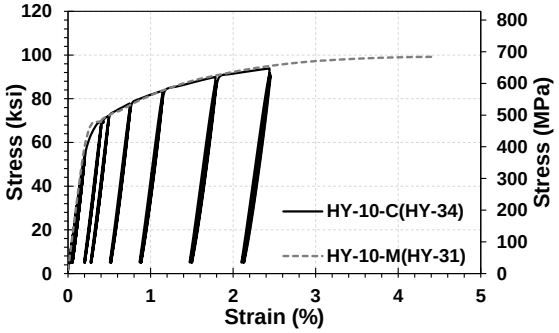

a. Coupler region strains using extensometer displacements

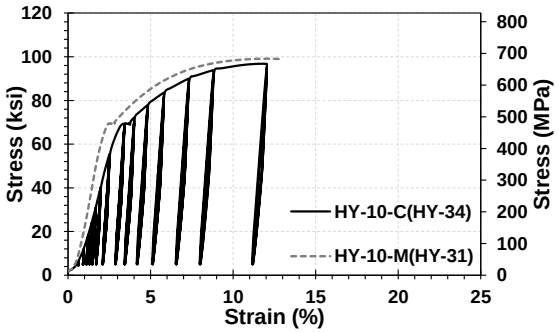

b. Specimen total strains using actuator displacements

Figure 4-66. Cyclic test results for No. 10 (32-mm) grouted-threaded hybrid couplers

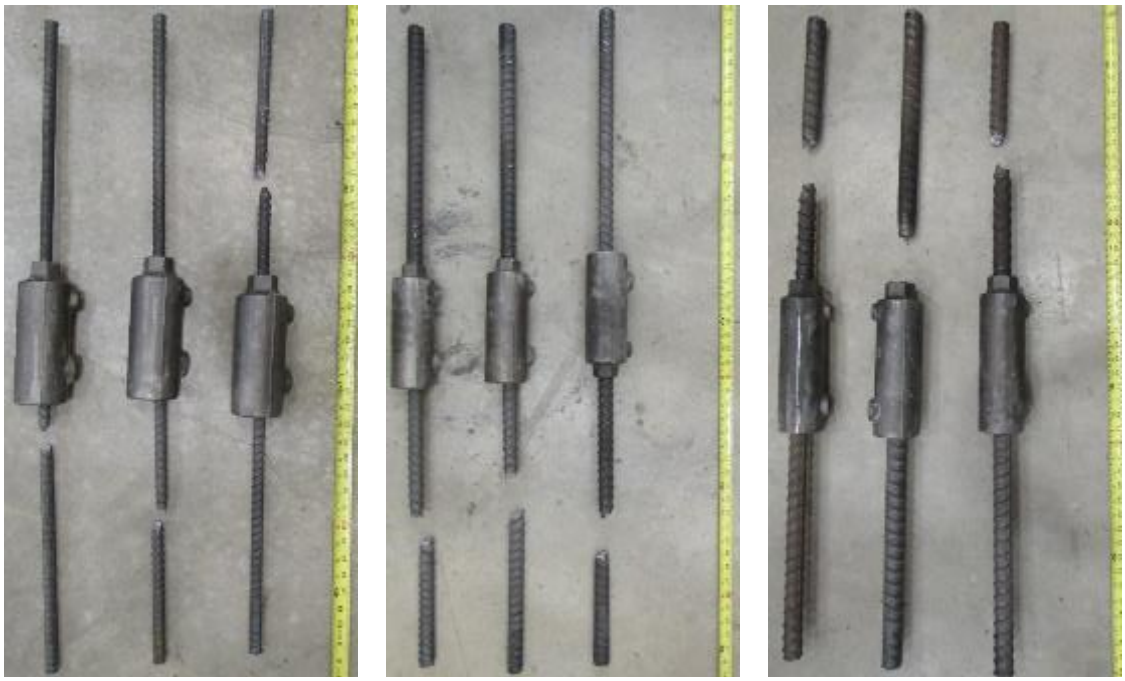

a. No.5 (16 mm) b. No.8 (25 mm) c. No.10 (32 mm)

Figure 4-67. Failure of grouted-threaded hybrid couplers under cyclic loading

4.5 Summary of Coupler Cyclic Test Results

Table 4-7 presents a summary of the failure modes for all cyclic tests on couplers. It can be inferred that all No. 8 (24 mm) and No. 10 (32 mm) couplers tested in the present study can be categorized as the seismic coupler. Nevertheless, No. 5 (16-mm) grouted sleeve couplers provided by two manufacturers failed by bar pullout thus they are not seismic couplers.

Table 4-7. Coupler failure modes in cyclic testing

Coupler Type	Size	Failure Mode			Remarks
		Bar Fracture	Bar Pullout	Coupler Failure	
Headed Bar Coupler	No. 5 (16 mm)	XXX			Seismic Coupler
	No. 8 (24 mm)	XXX			Seismic Coupler
	No. 10 (32 mm)	XXX			Seismic Coupler
Swaged Coupler	No. 5 (16 mm)	XXX			Seismic Coupler
	No. 8 (24 mm)	XXX			Seismic Coupler
	No. 10 (32 mm)	XXX			Seismic Coupler
Threaed Coupler (Type A)	No. 5 (16 mm)	XXX			Seismic Coupler
	No. 8 (24 mm)	XXX			Seismic Coupler
	No. 10 (32 mm)	XXX			Seismic Coupler
Threaed Coupler (Type B)	No. 5 (16 mm)	XXX			Seismic Coupler
	No. 8 (24 mm)	XXX			Seismic Coupler
	No. 10 (32 mm)	XXX			Seismic Coupler
Threaded Coupler (Taper)	No. 5 (16 mm)	XXX			Seismic Coupler
	No. 8 (24 mm)	XXX			Seismic Coupler
	No. 10 (32 mm)	XXX			Seismic Coupler
Grouted Coupler (NMB)	No. 5 (16 mm)		XXX		Not Seismic Coupler
	No. 8 (24 mm)	XXX			Seismic Coupler
	No. 10 (32 mm)	XXX			Seismic Coupler
Grouted Coupler (Dayton)	No. 5 (16 mm)		XXX		Not Seismic Coupler
	No. 8 (24 mm)	XXX			Seismic Coupler
	No. 10 (32 mm)	XXX			Seismic Coupler
Hybrid Coupler (Swaged and Thredad)	No. 5 (16 mm)	XXX			Seismic Coupler
	No. 8 (24 mm)	XXX			Seismic Coupler
	No. 10 (32 mm)	XX		X	Seismic Coupler
Hybrid Coupler (Grouted and Thredad)	No. 5 (16 mm)	XXX			Seismic Coupler
	No. 8 (24 mm)	XXX			Seismic Coupler
	No. 10 (32 mm)	XXX			Seismic Coupler

X = one sample

4.6 References

AASHTO. (2011). "AASTHO Guide Specification for LRFD Seismic Bridge Design".2nd Edition, with 2012, 2014, and 2015 Interim Revisions'. < https://bookstore.transportation.org/item_details.aspx?id=1915>

ASTM A706 (2009). "Standard specification for Low-Alloy Steel Deformed and Plain Bars for Concrete Reinforcement." West Conshohocken, PA, 6 pp.

ASTM C109 (2012). "Standard Test Method for Compressive Strength of Hydraulic Cement Mortars (Using 2-in. or [50 mm] cube Specimens)". West Conshohocken, PA.

Tazarv, M. and Saiidi, M.S. (2016). "Seismic Design of Bridge Columns Incorporating Mechanical Bar Splices in Plastic Hinge Regions," Engineering Structures, DOI: 10.1016/j.engstruct.2016.06.041, Vol 124, pp. 507-520.

Chapter 5. Analytical Study of Mechanically Spliced Bridge Columns

5.1 Introduction

Mechanical properties of nine different coupler products were investigated through tensile testing of more than 160 mechanical bar splices at the Lohr Structures Laboratory at South Dakota State University, and the results were presented in Chapter 4. Coupler rigid length factor, which is a key parameter to establish a coupler stress-strain behavior, was recommended for the nine coupler products based on the test data. Previous experimental studies (e.g. Haber et al., 2013; Tazarv and Saiidi, 2014; Ameli and Pantelides, 2015) have shown that bar couplers usually reduce the displacement capacity of bridge columns when they are used in plastic hinge regions. This is mainly because a splice strain capacity is usually less than an unspliced bar. In this chapter, the seismic performance of bridge columns mechanically spliced with each of the nine coupler products is investigated through analytical studies. The displacement capacity and the displacement ductility capacity of mechanically spliced columns are the focus of this study.

First a modeling method is presented for mechanically spliced bridge columns, parameters of the analytical study are discussed, and then the results of the 243 pushover

analyses are discussed. Finally, summary and conclusions are presented at the end of the chapter.

5.2 Modeling Method for Mechancially Spliced Bridge Columns

Tazarv and Saiidi (2016) proposed a modeling method for mechanically spliced bridge columns (Fig. 5-1). This analytical model was adopted in the present study. Table 5-1 presents the key input of the model. A three-dimensional finite element model was constructed for spliced columns in Open Sees (2016) using three force-based elements and fiber sections. A pedestal (Element 1) was included in the model to monitor the stress-strain behavior of unspliced bars and to determine the column failure. For a column at the base, the height of pedestal, H_{sp}, is assumed to be 0.1 in. (2.5 mm). Element 2 is to include the exact length (L_{sp}) and location of the coupler.

Each column section was discretized into 30×10 segments for the core concrete and 10×10 segments for the cover concrete. "Concrete04" and "Concrete01" material models were used for concrete core and cover fibers, respectively. "Concrete04" exhibits an abrupt drop in stress when the concrete strain reaches the ultimate strain thus it is possible to determine the failure of a column when the core concrete fails (significant reduction in the lateral load carrying capacity of the column). Mander's model (Mander et al., 1988) was used to calculate the properties of the confined concrete. A uniaxial material model, "ReinforcingSteel", was used for steel fibers in both spliced (Element 2) and unspliced regions (Elements 1 and 3).

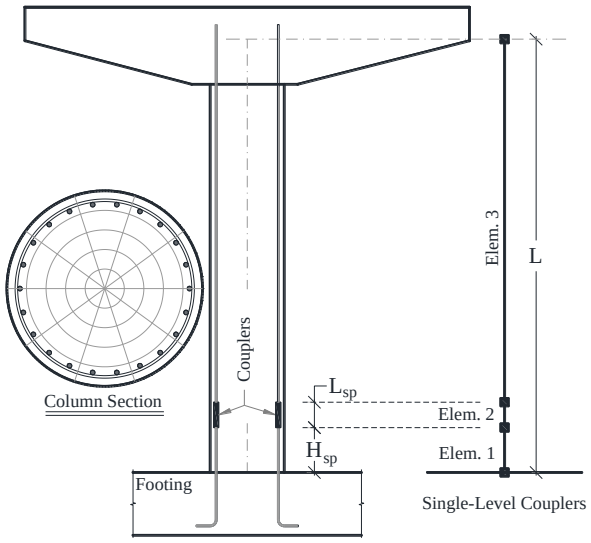

Figure 5-1. Analytical model details for columns with couplers at base

Table 5-1. Modeling method for mechanically spliced bridge columns

General Remarks	
Column Model: Three dimensions with 6 degrees of freedom per node Element Type: ForceBeamColumn with 5 integration points for both coupler regions and the reminder of the columns. $P-\Delta$ effects were included, no bond-slip effect was included	Sectional Properties (Fiber Section): Cover Concrete Discretization: 10 radials by 10 circumferential Core Concrete Discretization: 30 radials by 10 circumferential
Column Concrete Fibers	
Application: unconfined concrete Type: *Concrete01* f'_{cc} = -5000 *psi* (-34.47 *MPa*) ε_{cc} = -0.002 *in./in.* f'_{cu} = 0.0 *psi* (0.0 *MPa*) ε_{cu} = -0.005 *in./in.*	Application: confined concrete (based on Mander's model) Type: *Concrete04* f'_{cc}, ε_{cc}, f'_{cu}, ε_{cu} depends on cross-section, transverse bar size, type, and spacing, and clear cover according to Mander's model
Column Steel/Coupler Fibers	
Application: unspliced steel bars Type: *ReinforcingSteel* f_y = 68.0 *ksi* (468.8 *MPa*) f_{su} = 95.0 *ksi* (665.0 *MPa*) E_s = 29000 *ksi* (63252 *MPa*) $E_{sh} = 0.043E_s$ ε_{sh} = 0.005 *in./in.* ε_{su} = 0.09 *in./in.*	Application: spliced bars (Element 2) Type: *ReinforcingSteel* f_y = 68.0 *ksi* (468.8 *MPa*) f_{su} = 95.0 *ksi* (665.0 *MPa*) E_s, E_{sh}, ε_{sh} , ε_{su} depends on the type and size of coupler based on the model presented in Table 5-2.

5.2.1 Expected Mechanical Properties for Couplers

Only "seismic couplers" should be allowed in bridge columns. Due to a lack of test data and for compatibility with current seismic codes, all reinforcement of mechanically spliced bridge columns should conform to the requirements of ASTM A706 Grade 60. Table 5-2 represents the mechanical properties for couplers splicing ASTM A706 Grade 60 steel bars. Figure 5-2 shows the coupler material model parameters. This stress-strain material model, which is genetic and may be used for any "seismic coupler", was used in the present study. The rigid length factor (β) for each coupler product and size should be determined through testing. Refer to Ch. 4 or Sec. 5.3.2 for the recommended rigid length factor for the nine coupler products tested in the present study.

Table 5-2. Coupler mechanical properties splicing ASTM A706 Grade 60 reinforcing steel bars

Property	Notation	Bar Size	Value/Equation
Expected yield stress (ksi)	f_{ye}^{sp}	#3- #18	68
Expected tensile strength (ksi)	f_{ue}^{sp}	#3- #18	95
Expected yield strain (in./in.)	ε_{ye}^{sp}	#3- #18	$0.0023(L_{cr} - \beta L_{sp})/L_{cr}$
Modulus of elasticity (ksi)	E_s^{sp}	#3- #18	$f_{ye}^{sp}/\varepsilon_{ye}^{sp}$
Second Modulus of elasticity (ksi)	E_{sh}^{sp}	#3- #18	$0.041E_s^{sp}$
Onset of strain hardening (in./in.) *	ε_{sh}^{sp}	#3- #18	$0.005(L_{cr} - \beta L_{sp})/L_{cr}$
Reduced ultimate tensile strain (in./in.)	ε_{su}^{sp}	#4- #10	$0.09(L_{cr} - \beta L_{sp})/L_{cr}$
		#11- #18	$0.06(L_{cr} - \beta L_{sp})/L_{cr}$

Note: L_{sp}= coupler length; β= coupler rigid length ratio; Lcr= coupler region (L_{sp} + 2α.d_b); Alpha should not be more than 2.

*The strain at the onset of strain hardening is reduced compared to AASHTO SGS to improve convergence of analytical models. This change does not affect the seismic design of bridge columns.

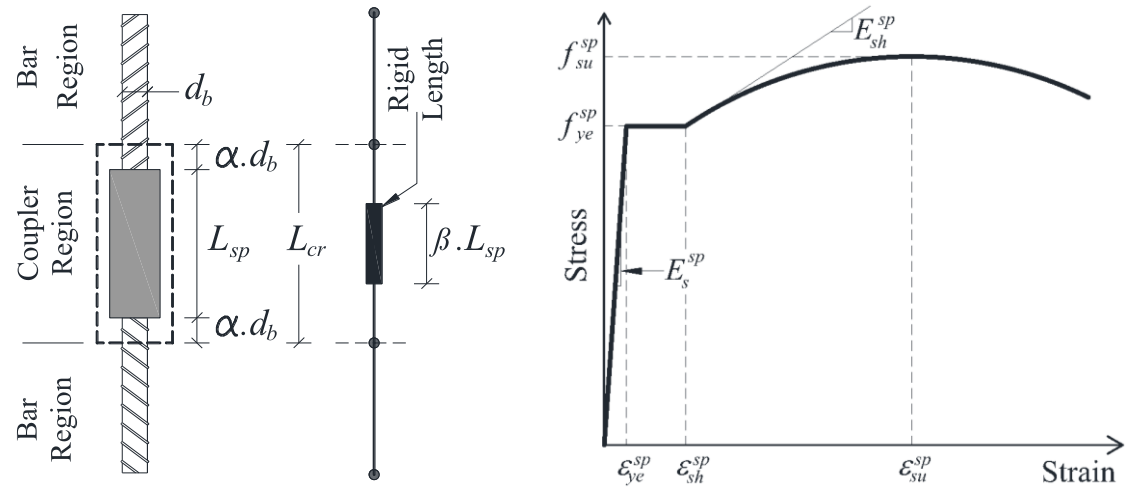

(a) Couplers Parameters (Tazarv & Saiidi, 2016) (b) Couplers Stress-Strain Model

Figure 5-2. Coupler model parameters splicing ASTM A706 Grade 60 reinforcing steel bars

5.3 Parametric Study

A parametric study was conducted to investigate the seismic performance of bridge columns spliced with different coupler products. First, 27 conventional reinforced concrete columns were designed to cover a practical range of bridge columns. Subsequently, the detailing of these RC columns was modified by incorporating bar couplers at the column base (mechanically spliced columns). Finally, a pushover analysis was performed for each spliced column and was compared to the results of its corresponding conventional column.

The column aspect ratio is the ratio of the column height to the column largest side dimension (or diameter). The axial load index is the ratio of the column axial load to the product of the column concrete compressive strength (f'_c) and the column cross-section area (A_g). The displacement capacity was determined at a point where the core concrete fails, the extreme steel bar fractures, or the column lateral load carrying capacity drops by 15% with respect to the peak lateral strength. The displacement ductility capacity was

calculated according to the AASHTO Guide Specifications for LRFD Seismic Bridge Design (2011). The drift ratio is defined as the ratio of the column displacement to the column height.

5.3.1 Reference Conventional Reinforced Concrete Columns (RC)

Tazarv and Saiidi (2016) designed 21 conventional RC columns, which covers a practical range of bridge columns. Six additional RC columns were designed in the present study for completeness. Three column aspect ratios of 4, 6 and 8, three axial load indices of 5, 10 and 15%, and three target displacement ductility's of 3, 5 and 7 were included in the design. Table 5-3 presents the general design parameters of the RC columns and Table 5-4 presents the details of the transverse reinforcement of the RC columns. All columns had 4-ft (1.22-m) diameter but the column height was varied based on the aspect ratio resulting in columns with a height of 16 ft (4.88-m), 24 ft (7.32-m) or 32 ft (9.75-m)

Table 5-3. RC column general design parameters

Parameter	**Value**
Column Diameter	4 ft (XX m)
Aspect Ratio (AR)	4, 6, 8
Column Length (*L*)	16 ft (4.88-m), 24 ft (7.32-m) or 32 ft (9.75-m)
Longitudinal Bar	No. 9 (29 mm)
Concrete Compressive Strength, f'_c	5.0 ksi (XX MPa)
Axial Load Index (ALI = P / f'_c. A_g)	5%, 10%, 15%
Displacement Ductility (D or μ)	$\mu = \frac{\Delta_u}{\Delta_{Yi}}$ where Δ_u : Ultimate Displacement Δ_{Yi} : Idealized Yield Displacement

Table 5-4. RC column transverse reinforcement, drift ratio, and displacement ductility capacity

Column ID	Transverse Reinforcement	Drift Ratio (%)	Ductility (μ)
RC-AR4-ALI5-D3	#3 hoops @10 in. (ρ_s = 0.08%)	1.60	3.01
RC-AR4-ALI5-D5	#4 hoops @4 in. (ρ_s = 0.45%)	2.86	4.94
RC-AR4-ALI5-D7	#6 hoops @4 in. (ρ_s = 1.02%)	4.13	7.05
RC-AR4-ALI10-D3	#4 hoops @8 in. (ρ_s = 0.22%)	1.48	2.92
RC-AR4-ALI10-D5	#5 hoops @4 in. (ρ_s = 0.71%)	2.63	4.98
RC-AR4-ALI10-D7	#7 hoops @3.5 in. (ρ_s = 1.59%)	3.88	6.92
RC-AR4-ALI15-D3	#5 hoops @7 in. (ρ_s = 0.40%)	1.45	3.00
RC-AR4-ALI15-D5	#7 hoops @5.5 in. (ρ_s = 1.01%)	2.61	5.04
RC-AR4-ALI15-D7	#8 hoops @3 in. (ρ_s = 2.43%)	3.55	7.11
RC-AR6-ALI5-D3	#3 hoops @10 in. (ρ_s = 0.10%)	2.40	3.16
RC-AR6-ALI5-D5	#4 hoops @4 in. (ρ_s = 0.45%)	4.24	5.12
RC-AR6-ALI5-D7	#5 hoops @3.5 in. (ρ_s = 0.81%)	5.45	7.33
RC-AR6-ALI10-D3	#4 hoops @10 in. (ρ_s = 0.18%)	2.13	3.39
RC-AR6-ALI10-D5	#3 hoops @4 in. (ρ_s = 0.71%)	3.74	5.05
RC-AR6-ALI10-D7	#7 hoops @5 in. (ρ_s = 1.11%)	4.90	6.73
RC-AR6-ALI15-D3	#4 hoops @8 in. (ρ_s = 0.22%)	2.15	2.92
RC-AR6-ALI15-D5	#7 hoops @5 in. (ρ_s = 1.11%)	3.72	4.92
RC-AR6-ALI15-D7	#9 hoops @3 in. (ρ_s = 2.43%)	4.98	6.55
RC-AR8-ALI5-D3	#3 hoops @3 in. (ρ_s = 0.08%)	2.34	3.03
RC-AR8-ALI5-D5	#4 hoops @4 in. (ρ_s = 0.4%)	4.50	5.11
RC-AR8-ALI5-D7	#6 hoops @4 in. (ρ_s = 1.02%)	6.07	7.12
RC-AR8-ALI10-D3	#4 hoops @8 in. (ρ_s = 0.23%)	2.78	3.11
RC-AR8-ALI10-D5	#5 hoops @4 in. (ρ_s = 0.7%)	2.85	5.15
RC-AR8-ALI10-D7	#7 hoops @3 in. (ρ_s = 1.86%)	5.25	7.02
RC-AR8-ALI15-D3	#5 hoops @7 in. (ρ_s = 0.40%)	1.60	3.13
RC-AR8-ALI15-D5	#7 hoops @3 in. (ρ_s = 1.85%)	3.79	5.01
RC-AR8-ALI15-D7	#8 hoops @3 in. (ρ_s = 2.43%)	3.91	6.04

Note: No. 3 bar is 10-mm diameter, No. 4 bar is 13-mm, No. 5 bar is 16-mm, No 6. bar is 19-mm, No. 7 bar is 22-mm, No. 8 bar is 25.4-mm

5.3.2 Parameters of Mechanically Spliced Columns

Nine coupler products were tested, and their mechanical properties were established in the previous chapter. Of nine, eight were selected as the parameter of the analytical study (Table 5-4) to investigate the seismic behavior of mechanically spliced bridge columns. Two threaded coupler products by Dextra were essentially the same and were not repeated herein. In addition to the conventional column variables (27 columns), the length and the rigid length factor for each coupler were varied in the parametric study resulting in a total of 243 pushover analyses. Note due to a lack of test data for No. 9 (29-mm) couplers, the rigid length factor and the coupler length for No. 10 bars (32 mm) were utilized in the analysis.

Table 5-4. RC column transverse reinforcement, drift ratio, and displacement ductility capacity

Coupler Type	Labeled as	Coupler Length, L_{sp}, in.(mm)	Rigid Length Factor (β)
Headed Reinforcement	HR	3.88 (98.5)	0.55
Threaded (Dextra)	TH	3.06 (77.7)	1.60
Threaded (Erico)	TH (Taper)	4.2 (106.7)	1.05
Swaged (Bar Splice)	SW	9.5 (241.3)	0.95
Grouted Sleeve (NMB)	GS NMB	18 (457)	0.85
Grouted Sleeve (Dayton)	GS Dayton	18 (457)	0.65
Hybrid (Dextra)	HY (Dextra)	10.63 (270)	0.85
Hybrid (Erico)	HY (Erico)	10.75 (273)	0.80

Note: These coupler lengths and rigid length factors are for No. 10 (32-mm) bars.

5.4 Parametric Analysis Results

To synthesize the effect of couplers on the seismic performance of bridge columns, the pushover analysis results were summarized under low-ductile (μ = 3), medium-ductile (μ = 5), and high-ductile columns (μ = 7). Two graphs were generated per analysis: one was a regular pushover curve (force-displacement or force-drift), and another was a moment-ductility curve to clearly show the effect of couplers on the displacement ductility capacity of columns.

5.4.1 Columns with Low Ductility

Columns with a target displacement ductility of three were considered as low ductile columns. Of 243 analysis, 81 was on low-ductile columns. Figures 5-3 to 5-11 show the force-drift and moment-ductility relationships for these columns. The results of a corresponding reference conventional RC column are included in each graph using dashed black lines for comparison. The drift capacity and the displacement ductility capacity of low-ductile columns were reduced when couplers were used at the base. For example, the displacement ductility capacity of AR6-ALI5-D3 was reduced between 8 to 22% compared to the reference RC columns. It is clear than couplers with higher rigid length factors and longer couplers have more adverse effects on the column displacement ductility. For example, columns with grouted and swaged couplers exhibited the lowest displacement ductility capacities (e.g. 25% lower than RC using grouted couplers).

Furthermore, it can be inferred that the force or moment capacity of mechanically spliced columns is higher than that in RC columns. For example, grouted coupler columns had 6.6% higher force capacity compared to their reference columns. The results also show that couplers did not affect the initial stiffness of the columns. This

maybe because the coupler length is insignificant compared to the column length thus minor versions in the splice modulus of elasticity (initial stiffness) do not affect the column overall stiffness.

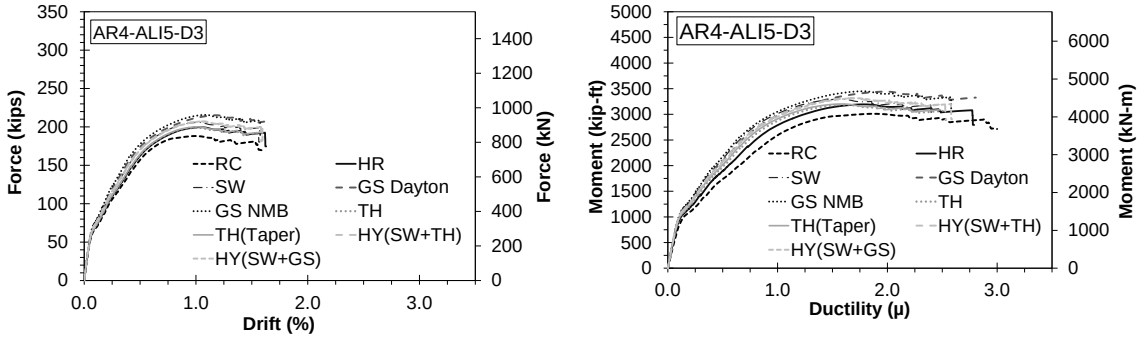

a. Force-drift relationship b. Moment-ductility relationship

Figure 5-3. Pushover analysis results for AR4-ALI5-D3

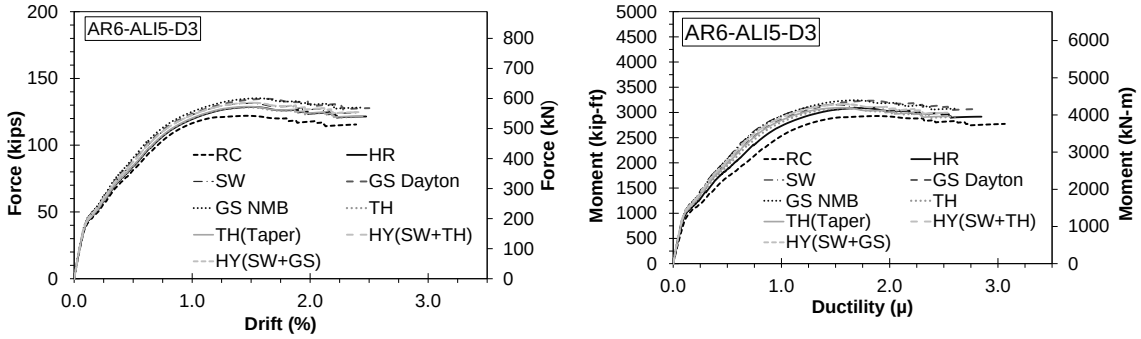

a. Force-drift relationship b. Moment-ductility relationship

Figure 5-4. Pushover analysis result for AR6-ALI5-D3

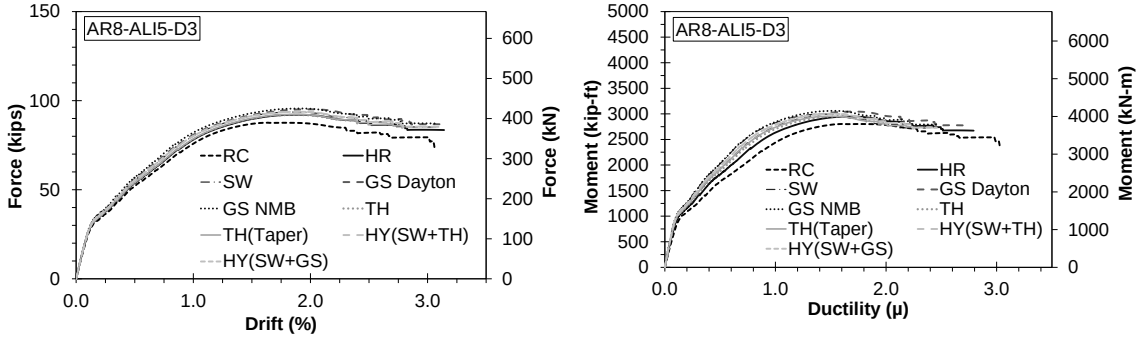

a. Force-drift relationship b. Moment-ductility relationship for

Figure 5-5. Pushover analysis result for AR8-ALI5-D3

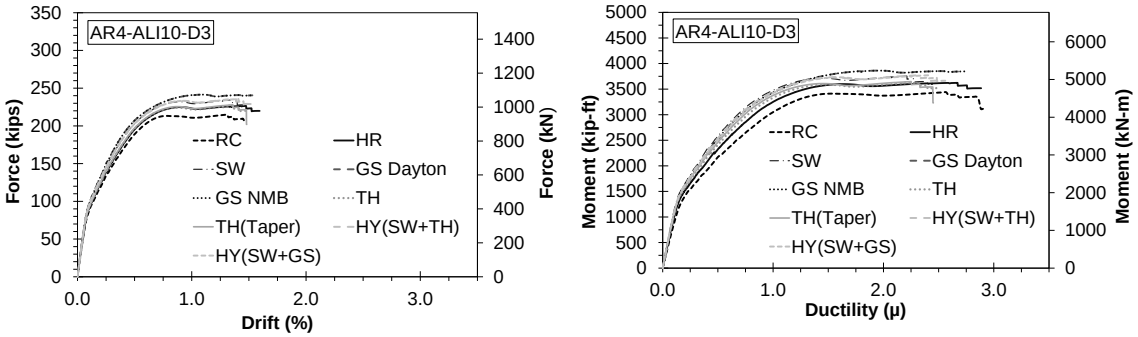

a. Force-drift relationship b. Moment-ductility relationship

Figure 5-6. Pushover analysis result for AR4-ALI10-D3

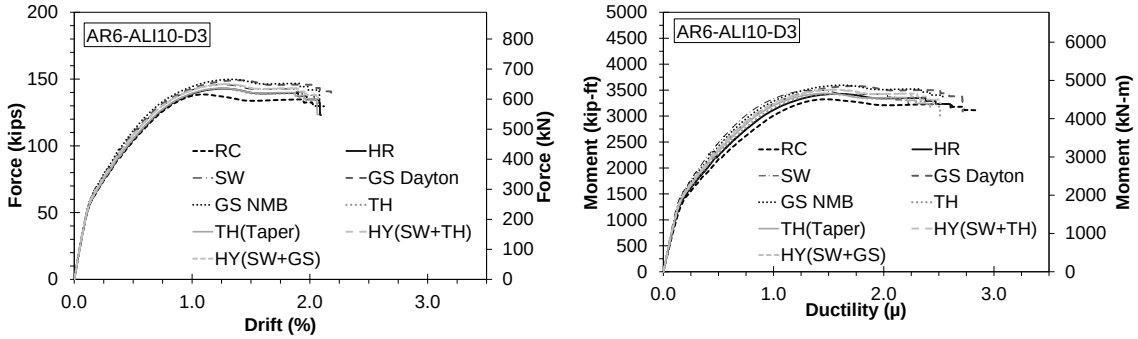

a. Force-drift relationship b. Moment-ductility relationship

Figure 5-7. Pushover analysis result for AR6-ALI10-D3

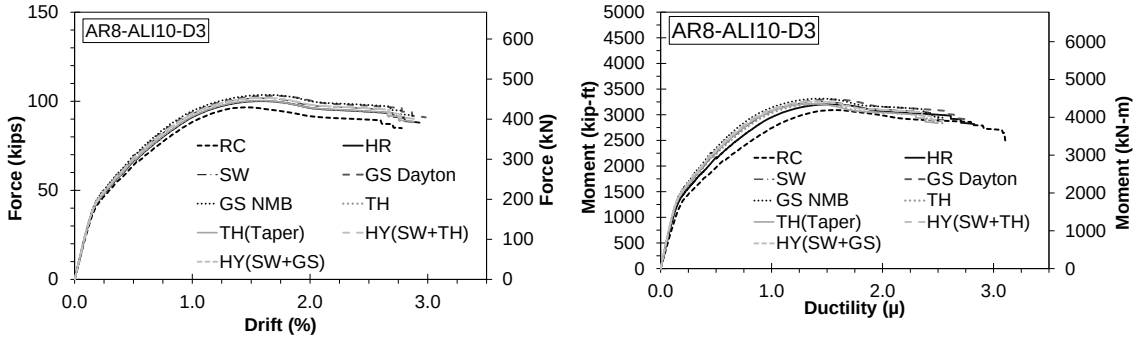

a. Force-drift relationship b. Moment-ductility relationship

Figure 5-8. Pushover analysis result for AR8-ALI10-D3

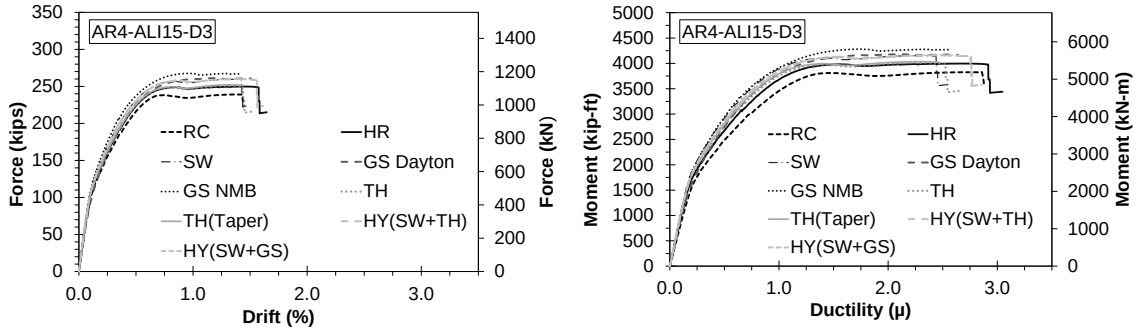

a. Force-drift relationship b. Moment-ductility relationship

Figure 5-9. Pushover analysis result for AR4-ALI15-D3

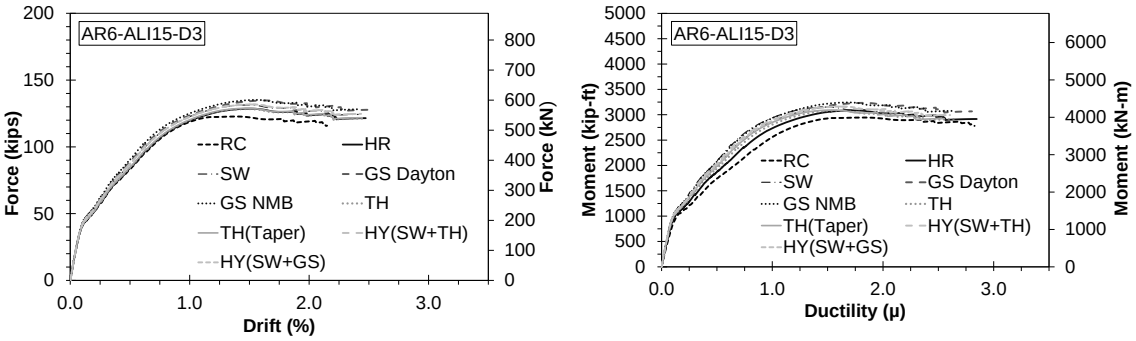

a. Force-drift relationship b. Moment-ductility relationship

Figure 5-10. Pushover analysis result for AR6-ALI15-D3

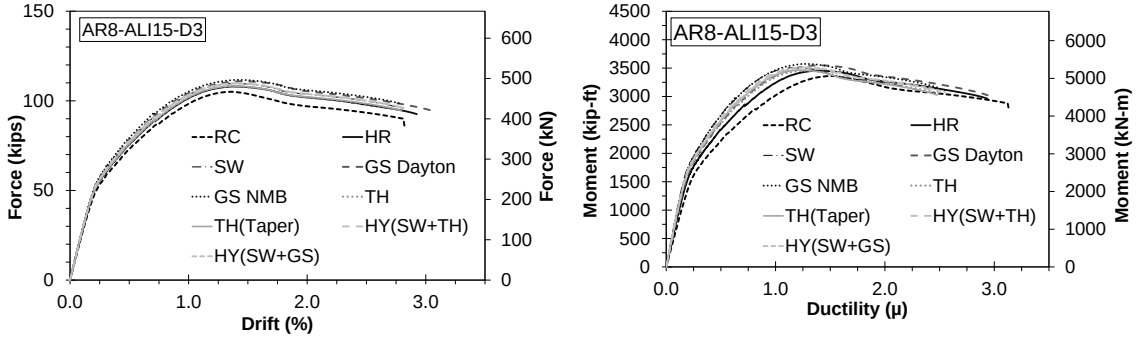

a. Force-drift relationship b. Moment-ductility relationship

Figure 5-11. Pushover analysis result for AR8-ALI15-D3

5.4.2 Columns with Medium Ductility

Columns with a target displacement ductility of five were considered as low ductile columns. Of 243 analysis, 81 was on low-ductile columns. Figures 5-12 to 5-20 show the force-drift and moment-ductility relationships for these columns. The results of a corresponding reference conventional RC column are included in each graph using dashed black lines for comparison. The drift capacity and the displacement ductility capacity of medium-ductile columns were reduced when couplers were used at the base. For example, the displacement ductility capacity of AR6-ALI5-D5 was reduced between 5 to 30% compared to the reference RC columns. It is clear than couplers with higher rigid length factors and longer couplers have more adverse effects on the column displacement ductility. For example, columns with grouted and swaged couplers exhibited the lowest displacement ductility capacities (e.g. 35.8% lower than RC using grouted couplers).

Furthermore, it can be inferred that the force or moment capacity of mechanically spliced columns is higher than that in RC columns. For example, grouted coupler columns had 9.1% higher force capacity compared to their reference columns. The results also show that couplers did not affect the initial stiffness of the columns. This maybe because the coupler length is insignificant compared to the column length thus minor versions in the splice modulus of elasticity (initial stiffness) do not affect the column overall stiffness.

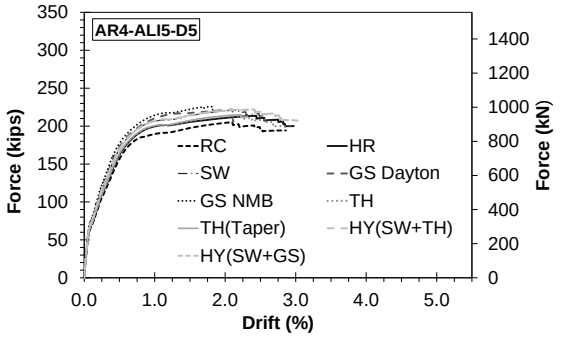

a. Force-drift relationship

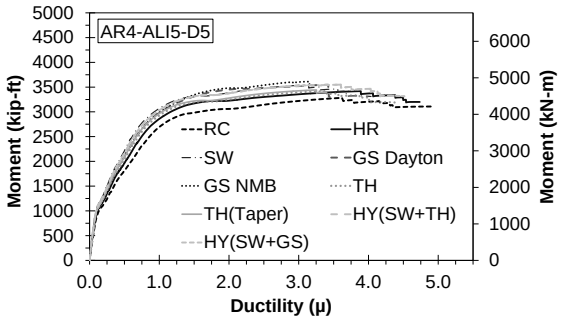

b. Moment-ductility relationship

Figure 5-12. Pushover analysis result for AR4-ALI5-D5

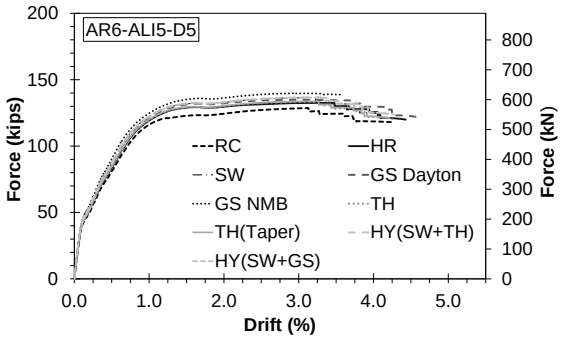

a. Force-drift relationship

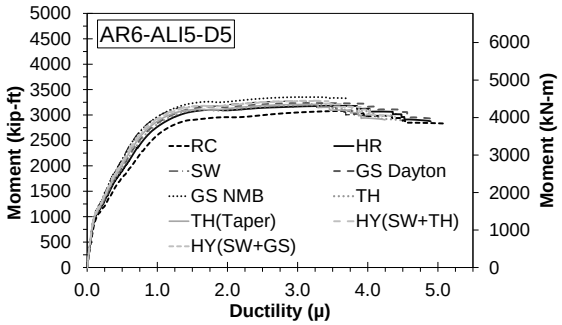

b. Moment-ductility relationship

Figure 5-13. Pushover analysis result for AR6-ALI5-D5

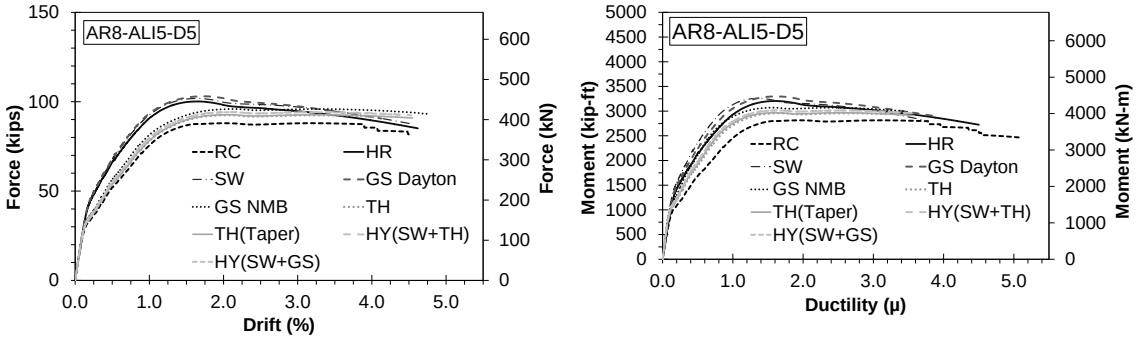

a. Force-drift relationship b. Moment-ductility relationship

Figure 5-14. Pushover analysis result for AR8-ALI5-D5

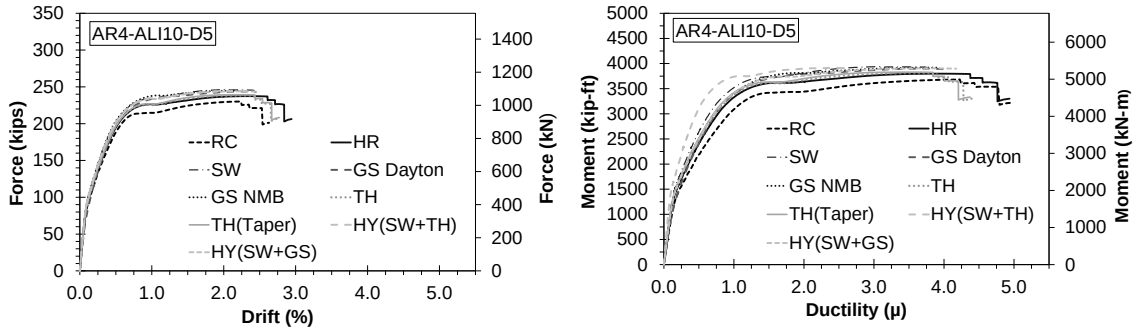

a. Force-drift relationship b. Moment-ductility relationship

Figure 5-15. Pushover analysis result for AR4-ALI10-D5

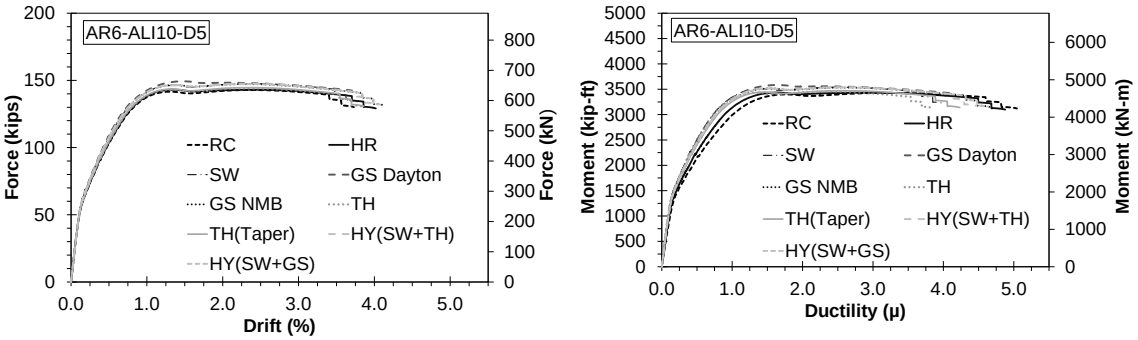

a. Force-drift relationship b. Moment-ductility relationship

Figure 5-16. Pushover analysis result for AR6-ALI10-D5

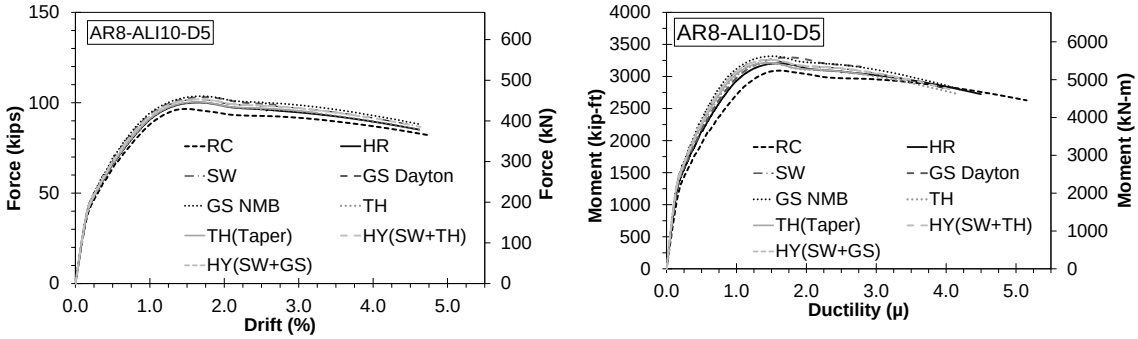

a. Force-drift relationship b. Moment-ductility relationship

Figure 5-17. Pushover analysis result for AR8-ALI10-D5

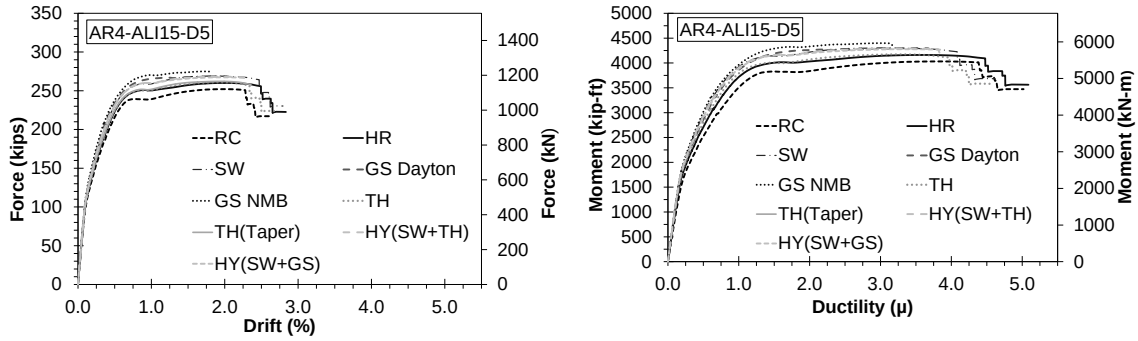

a. Force-drift relationship b. Moment-ductility relationship

Figure 5-18. Pushover analysis result for AR4-ALI15-D5

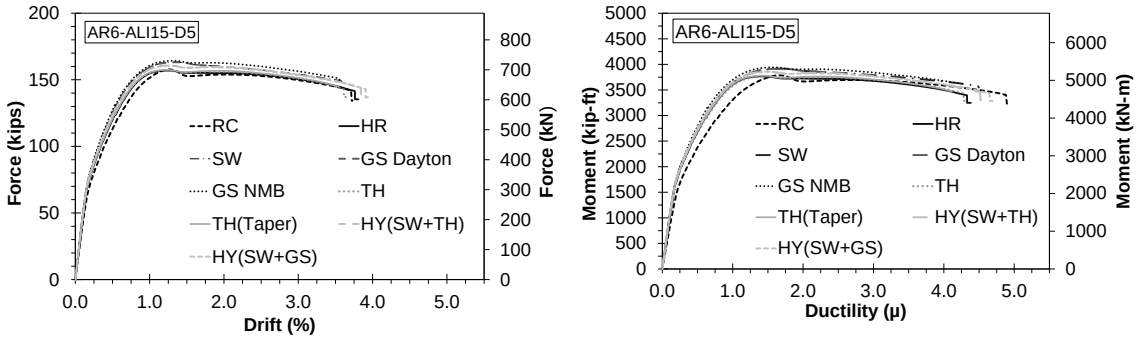

a. Force-drift relationship b. Moment-ductility relationship

Figure 5-19. Pushover analysis result for AR6-ALI15-D5

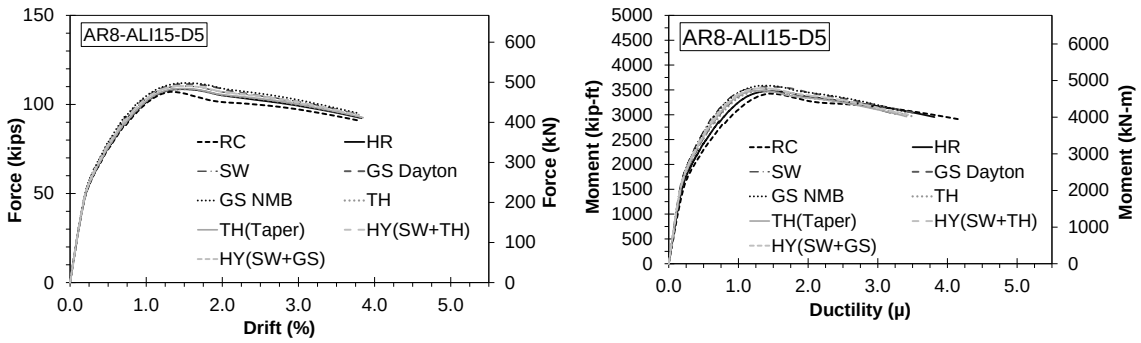

a. Force-drift relationship b. Moment-ductility relationship

Figure 5-20. Pushover analysis result for AR8-ALI15-D5

5.4.3 Columns with High Ductility

Columns with a target displacement ductility of seven were considered as high ductile columns. Of 243 analysis, 81 was on low-ductile columns. Figures 5-21 to 5-29 show the force-drift and moment-ductility relationships for these columns. The results of a corresponding reference conventional RC column are included in each graph using dashed black lines for comparison. The drift capacity and the displacement ductility capacity of high-ductile columns were reduced when couplers were used at the base. For example, the displacement ductility capacity of AR6-ALI5-D7 was reduced between 11 to 41% compared to the reference RC columns. It is clear than couplers with higher rigid length factors and longer couplers have more adverse effects on the column displacement ductility. For example, columns with grouted and swaged couplers exhibited the lowest displacement ductility capacities (e.g. 35.8% lower than RC using grouted couplers).

Furthermore, it can be inferred that the force or moment capacity of mechanically spliced columns is higher than that in RC columns. For example, grouted coupler columns had 6.8% higher force capacity compared to their reference columns. The results also show that couplers did not affect the initial stiffness of the columns. This

maybe because the coupler length is insignificant compared to the column length thus minor versions in the splice modulus of elasticity (initial stiffness) do not affect the column overall stiffness.

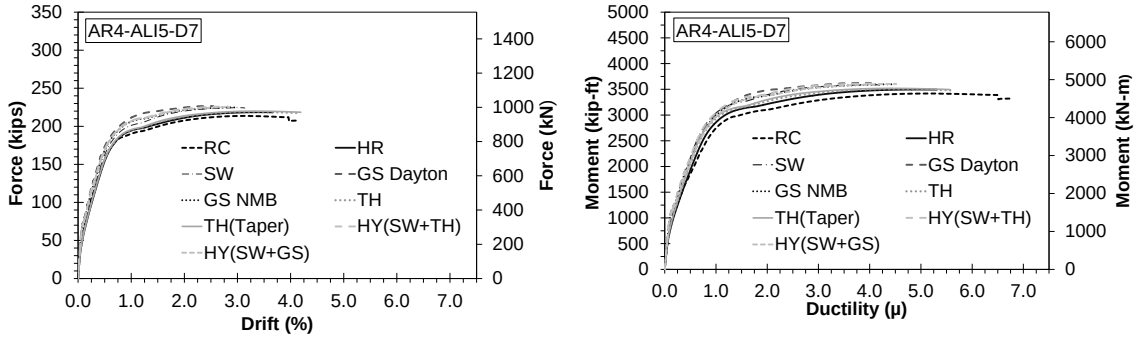

a. Force-drift relationship b. Moment-ductility relationship

Figure 5-21. Pushover analysis result for AR4-ALI5-D7

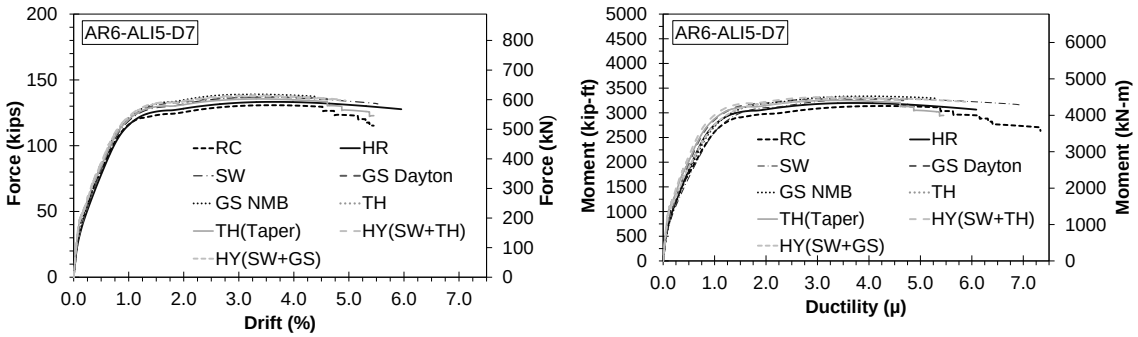

a. Force-drift relationship b. Moment-ductility relationship

Figure 5-22. Pushover analysis result for AR6-ALI5-D7

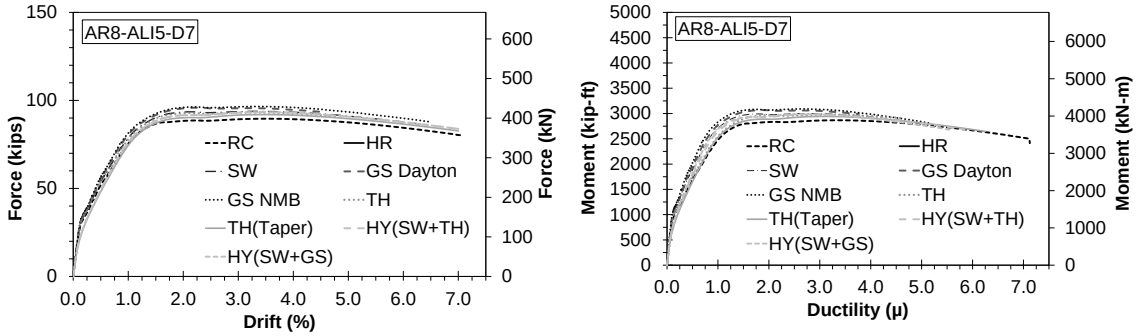

a. Force-drift relationship b. Moment-ductility relationship

Figure 5-23. Pushover analysis result for AR8-ALI5-D7

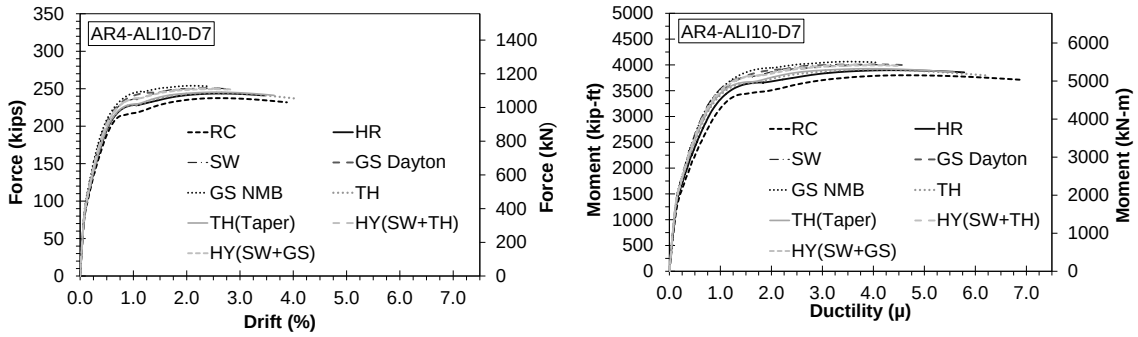

a. Force-drift relationship b. Moment-ductility relationship

Figure 5-24. Pushover analysis result for AR4-ALI10-D7

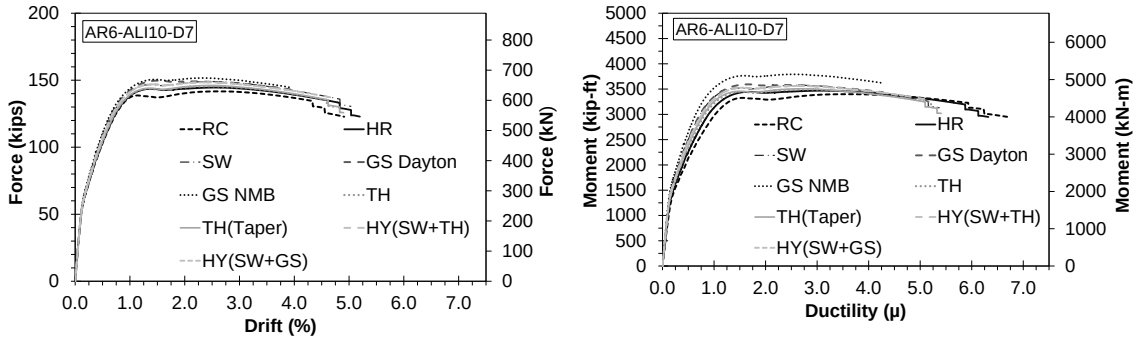

a. Force-drift relationship b. Moment-ductility relationship

Figure 5-25. Pushover analysis result for AR6-ALI10-D7

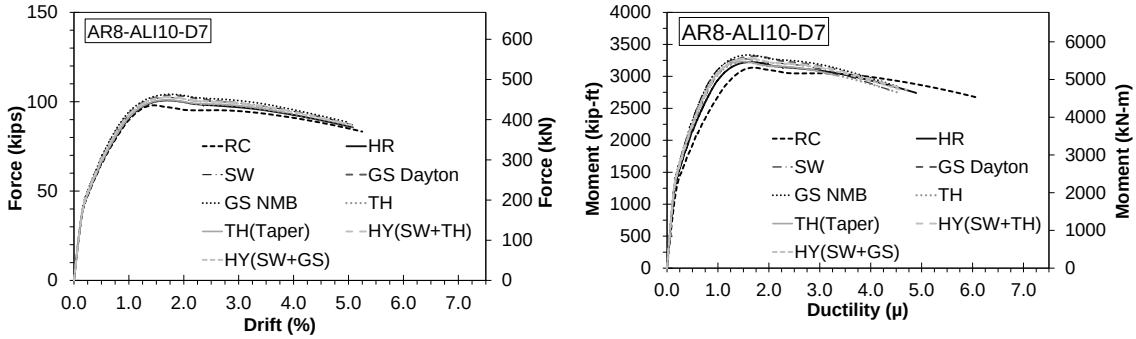

a. Force-drift relationship b. Moment-ductility relationship

Figure 5-26. Pushover analysis result for AR8-ALI10-D7

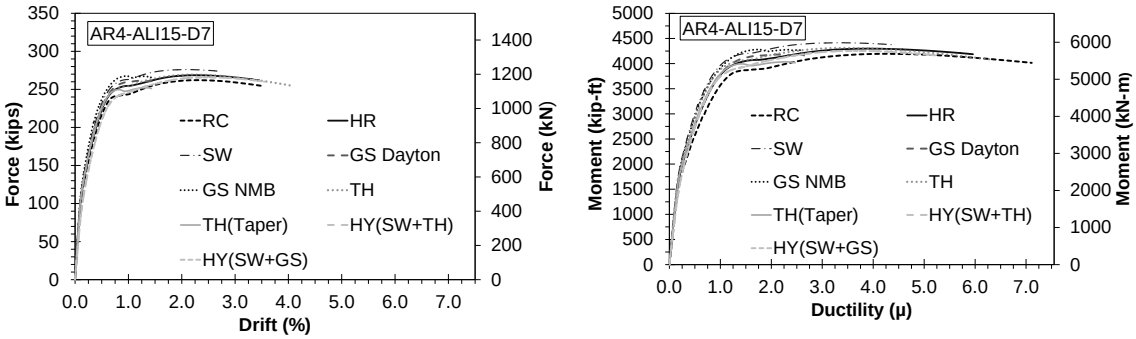

a. Force-drift relationship b. Moment-ductility relationship

Figure 5-27. Pushover analysis result for AR4-ALI15-D7

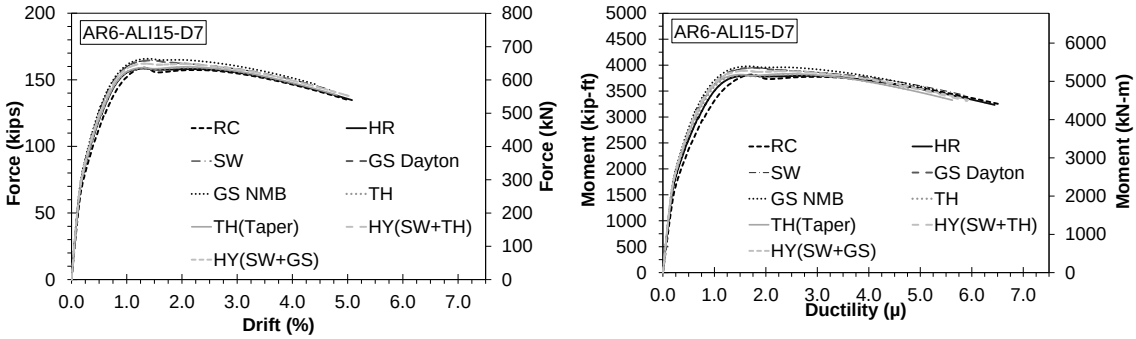

a. Force-drift relationship b. Moment-ductility relationship

Figure 5-28. Pushover analysis result for AR6-ALI15-D7

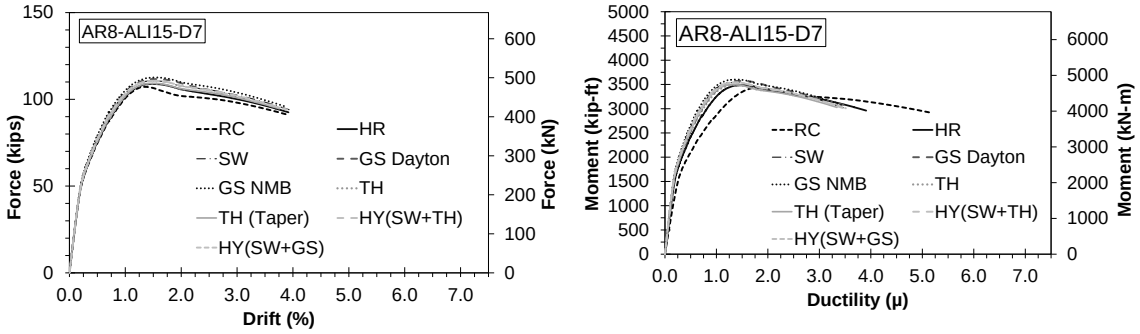

a. Force-drift relationship b. Moment-ductility relationship

Figure 5-29. Pushover analysis result for AR8-ALI15-D7

5.4.4 Summary of Parametric Study

Table 5-6 presents a summary of the parametric study in which the displacement ductility capacity and the reduction of the displacement ductility capacity of spliced to unspliced columns for all 243 analyses are included. Ductility presented under the second column of the table is for the reference conventional RC columns.

Even though there are significant versions in the results, the general trend is that mechanically spliced bridge columns with longer and more rigid couplers will exhibit lower displacement ductility capacities. Columns with higher ductility's are affected more when couplers are used in their plastic hinge regions. For example, the lowest displacement ductility capacity in all analyses was for AR8-ALI15-D7 spliced with grouted sleeve coupler (NMB). In this column, the displacement ductility capacity was 43% lower than that in its corresponding RC column. Furthermore, columns spliced with short couplers and low rigidity can show as large displacement capacity as RC columns. For example, AR5-ALI10-D5 spliced with headed reinforcement coupler (HRC).

Table 5-6. Summary of parametric study on mechanically spliced bridge columns

Column ID	Ductility (Ductility Reduction Compared to RC in %)								
	RC	HR L_{sp} = 3.88 in. β = 0.55	TH L_{sp} = 3.06 in. β = 1.65	TH-Taper L_{sp} = 4.20 in. β = 1.05	SW L_{sp} = 9.50 in. β = 0.95	GS-NMB L_{sp} = 18 in. β = 0.85	GS-Dayton L_{sp} = 18 in. β = 0.65	HY-Dextra L_{sp} = 10.63 in. β = 0.85	HY-Erico L_{sp} = 10.75 in. β = 0.80
AR4-ALI5-D3	3.0	2.8 (7.6)	2.6 (15.0)	2.5 (16.9)	2.4 (19.9)	2.6 (14.0)	2.6 (6.6)	2.5 (15.6)	2.6 (14.0)
AR4-ALI5-D5	4.9	4.9 (0.2)	4.4 (10.8)	4.2 (14.6)	4.0 (18.2)	3.2 (36.0)	3.4 (30.4)	4.5 (8.5)	4.5 (8.7)
RC-AR4-ALI5-D7	7.0	5.3 (24.8)	6.2 (12.2)	5.6 (21.1)	4.2 (40.7)	4.5 (36.4)	4.0 (42.8)	4.1 (41.4)	4.5 (35.7)
RC-AR4-ALI10-D3	2.9	2.9 (1.0)	2.5 (13.7)	2.5 (16.1)	2.3 (21.6)	2.7 (6.2)	2.7 (6.2)	2.5 (13.7)	2.6 (11.3)
RC-AR4-ALI10-D5	5.0	5.0 (0.0)	4.5 (10.7)	4.4 (12.3)	3.8 (24.7)	3.9 (20.9)	4.0 (20.1)	2.6 (47.6)	4.0 (19.9)
RC-AR4-ALI10-D7	6.9	5.8 (16.4)	6.3 (9.0)	5.6 (18.6)	4.3 (38.3)	4.1 (41.3)	4.6 (33.4)	4.4 (35.8)	4.6 (34.0)
RC-AR4-ALI15-D3	3.0	2.9 (4.0)	2.7 (11.7)	2.6 (13.3)	2.6 (15.0)	2.6 (14.3)	2.7 (11.7)	2.9 (4.7)	2.9 (4.3)
RC-AR4-ALI15-D5	5.0	4.9 (2.1)	4.6 (9.5)	4.5 (10.3)	4.6 (8.5)	3.2 (37.1)	3.7 (26.6)	3.9 (23.4)	3.9 (22.8)
RC-AR4-ALI15-D7	7.1	6.0 (16.3)	5.0 (29.8)	6.7 (5.5)	5.1 (28.1)	4.6 (34.9)	4.9 (30.9)	4.1 (42.1)	5.3 (25.5)
RC-AR6-ALI5-D3	3.1	2.9 (8.5)	2.6 (15.3)	2.6 (17.8)	2.4 (22.3)	2.6 (16.9)	2.8 (10.1)	2.6 (18.2)	2.6 (18.2)
RC-AR6-ALI5-D5	5.1	4.9 (4.5)	4.5 (11.9)	4.3 (17.0)	4.1 (19.9)	3.7 (28.1)	5.0 (3.3)	4.2 (17.2)	4.4 (14.3)
RC-AR6-ALI5-D7	7.3	6.5 (11.6)	4.8 (34.7)	6.2 (15.8)	5.0 (31.8)	4.3 (41.2)	4.8 (34.7)	4.7 (35.5)	5.1 (31.0)
RC-AR6-ALI10-D3	3.3	2.8 (14.0)	2.6 (21.9)	2.5 (24.0)	2.3 (29.2)	2.5 (22.8)	2.8 (16.4)	2.5 (24.3)	2.5 (22.8)
RC-AR6-ALI10-D5	5.1	4.9 (3.7)	4.3 (14.4)	4.2 (16.9)	4.0 (20.7)	4.7 (7.8)	4.5 (10.2)	4.5 (11.6)	4.7 (8.0)
RC-AR6-ALI10-D7	6.7	6.3 (6.1)	5.8 (14.3)	5.6 (16.8)	5.4 (20.2)	4.9 (26.9)	4.8 (28.1)	5.2 (23.0)	4.7 (29.6)
RC-AR6-ALI15-D3	2.9	2.8 (3.1)	2.6 (9.6)	2.6 (12.7)	2.4 (17.1)	2.6 (10.3)	2.9 (2.1)	2.6 (12.7)	2.6 (10.6)
RC-AR6-ALI15-D5	4.9	4.8 (2.2)	4.3 (11.8)	4.3 (13.4)	4.6 (6.3)	4.3 (13.4)	4.0 (17.7)	4.6 (7.1)	4.7 (4.5)
RC-AR6-ALI15-D7	6.6	6.4 (1.7)	6.0 (8.2)	5.9 (10.2)	5.9 (10.7)	5.4 (18.3)	4.3 (34.5)	6.0 (8.4)	6.0 (8.1)
RC-AR8-ALI5-D3	3.0	2.8 (7.9)	2.6 (14.5)	2.5 (17.5)	2.4 (22.4)	2.5 (19.1)	2.7 (10.9)	2.5 (18.2)	2.5 (18.2)
RC-AR8-ALI5-D5	5.1	4.5 (11.9)	5.3 (-2.7)	5.1 (0.8)	3.8 (26.0)	4.5 (11.7)	4.3 (16.4)	5.2 (-1.0)	3.5 (32.3)
RC-AR8-ALI5-D7	7.1	4.3 (40.2)	6.1 (14.5)	6.3 (12.2)	5.3 (26.1)	5.2 (27.4)	5.0 (30.2)	5.8 (18.0)	5.5 (22.2)
RC-AR8-ALI10-D3	3.1	2.8 (8.7)	2.6 (17.1)	2.5 (19.7)	2.6 (15.8)	2.6 (17.7)	2.8 (11.3)	2.5 (19.7)	2.5 (18.1)
RC-AR8-ALI10-D5	5.2	4.5 (12.8)	4.2 (19.0)	4.3 (17.3)	4.4 (15.3)	4.1 (19.6)	4.3 (17.1)	4.1 (19.6)	4.0 (22.1)
RC-AR8-ALI10-D7	7.0	4.8 (31.2)	4.6 (35.2)	4.4 (36.9)	4.5 (35.3)	4.6 (35.2)	4.5 (35.3)	4.7 (33.0)	4.6 (34.6)
RC-AR8-ALI15-D3	3.1	2.9 (6.2)	2.6 (18.3)	2.5 (20.8)	2.4 (25.0)	2.5 (20.2)	2.9 (6.2)	2.5 (20.5)	2.6 (18.6)
RC-AR8-ALI15-D5	5.1	3.8 (25.0)	3.5 (30.5)	3.4 (32.9)	3.3 (35.8)	3.4 (32.5)	3.5 (30.5)	3.4 (33.5)	3.4 (32.5)
RC-AR8-ALI15-D7	6.0	3.9 (35.4)	3.6 (40.1)	3.6 (40.7)	3.5 (42.4)	3.5 (42.7)	3.7 (38.9)	3.5 (42.7)	3.5 (41.9)

Note: 1 in. = 25.4 mm.

5.5. Summary and Conclusions

A parametric study was performed to investigate the seismic performance of bridge columns utilizing mechanical bar splices. A total 243 pushover analyses were performed on 27 columns spliced with eight different coupler products. The following conclusions can be drawn based on the pushover analysis.

- Columns incorporating mechanical bar splices will usually show lower displacement ductility capacities compared conventional RC columns.
- The parametric study showed that the coupler length and its rigidity length factor significantly affect the displacement ductility capacity of mechanically spliced columns. Coupler with higher rigid length factors and longer length will decrease the displacement ductility capacities
- The proposed modeling method for mechanically spliced RC members was simple and viable.

5.6 References

AASHTO. (2011). “AASHTO Guide Specifications for LRFD Seismic Bridge Design,” Washington, DC: American Association of State Highway and Transportation Officials.

ASTM A706/A706M-09b (2009). “Standard Specification for LowAlloy Steel Deformed and Plain Bars for Concrete Reinforcement,” ASTM International, West Conshohocken, PA.

Ameli, M.J and. Pantelides, Chris P (2016). “Seismic Analysis of Precast Concrete Bridge Columns Connected with Grouted Splice Sleeve Connectors.” American Society of Civil Engineers (ASCE), Vol 143

Mander, J.B, Priestly, M.J.N. and Park, R. (1988a). “Theoretical stress-strain model for confined concrete,” Journal of Structural Engineering, ASCE Vol 114, No. 8, pp. 1804 – 1826.

Haber, ZB, Saiidi, MS, and Sanders, DH (2013). “Precast Column Footing Connections for Accelerated Bridge Construction in Seismic Zones.” Rep. No. CCEER 13-08 Center for Civil Engineering Earthquake Research, Dept. of Civil and Environmental Engineering, Univ. of Nevada, Reno. NV.

OpenSees. (2016). “Open System for Earthquake Engineering Simulations,” Version 2.4.1, Berkeley, CA, Available online: http://opensees.berkeley.edu. 6.

Tazarv, M., and Saiidi, M.S. (2014). “Next Generation of Bridge Columns for Accelerated Bridge Construction in High Seismic Zones,” CCEER Report No. 14- 234 06, Center for Civil Engineering Earthquake Research, University of Nevada, Reno, NV.

Chapter 6. Summary and Conclusions

6.1 Summary

Mechanical bar splices can be used in bridges to connect precast columns to adjacent members. Nevertheless, current seismic codes prohibit the use of bar couplers in the plastic hinge region of columns in high seismic zones. This is because the behavior of couplers in largely unknown at the component level and when they are used in bridge columns. The main objective of present study was to establish the behavior of mechanical bars splices suited for bridge columns through experimental and analytical studies. Nine different coupler products were selected for testing, and more than 160 mechanical bar splices were tested to failure under monotonic and cyclic loading. Three bar sizes, No. 5 (16 mm), No. 8 (25 mm), and No. 10 (32 mm) were included in the test matrix. A coupler material model and acceptance criteria were selected from the literature and then the behavior of the nine type couplers was established through experiments. The first-of-its-kind database on the properties of bar couplers was developed and "seismic" and "non-seismic" couplers were identified. Furthermore, more than 240 pushover analyses were performed on bridge columns incorporating couplers in which their behavior was established in the experimental program of the study.

6.2 Conclusions

The following key conclusions can be drawn based on the experimental and analytical studies:

- The test data showed that the coupler length, size and type significantly affect the coupler performance. The general trend was that longer couplers showed lower strain capacities compared to shorter couplers. Couplers with higher rigid length factors showed the lowest strain capacities.
- The coupler acceptance criteria and the coupler stress-strain model proposed by Tazarv and Saiidi (2016) were found viable to identify couplers suited for bridge columns. These couplers were named as "seismic couplers".
- The test data showed that monotonic testing is sufficient to establish a coupler behavior using only one parameter, "coupler rigid length factor". No significant change was seen in the behavior of a coupler under monotonic and cyclic loading. Nevertheless, the cyclic loading is needed to verify the coupler performance under simulated seismic actions.
- Consistent results can be achieved using a standard testing method for couplers.
- The parametric study showed that the size, type and length of couplers can significantly affect the ductility of bridge columns. Longer couplers and couplers with higher "rigid length factors" may reduce a column displacement ductility capacity up to 40%.
- The analytical study showed that the lateral load carrying capacity of mechanically spliced bridge columns are slightly higher than conventional columns.

Appendix A: Caltrans Authorized List of Couplers

CALIFORNIA DEPARTMENT OF TRANSPORTATION

AUTHORIZED LIST OF COUPLERS FOR REINFORCING STEEL

Type of Splice	Splice Company	Coupler Model	Coupler List Unique Identification	Authorized Service Splice (Bar Sizes)	Authorized Ultimate Splice (Bar Sizes)	Expiration Date
Mechanical Couplers on ASTM A 706 (Grade 60) Reinforcing Steel – For Straight Bars						
Sleeve-Swaged (Deformation Dependent)	BarSplice http://www.barsplice.com	BPI-GRIP™ (BarGrip®)	SS-17-01	#3 through #18		06/2020
		BPI-GRIP™ (BarGrip®) XL	SS-17-02	#5 through #18	#5 through #18	06/2020
		Taper Threaded Grip-Twist®	SS-17-03	#3 through #18	#3 through #18	06/2020
		Taper Threaded Transition Grip-Twist®	SS-17-04	#11 to #18 transition; #11 to #14 transition; and #10 to #18 transition	#11 to #18 transition; #11 to #14 transition; and #10 to #18 transition	06/2020
		Grip Twist Position Coupler	SS-17-05	#5 through #18		06/2020
	Dextra America, Inc. www.dextragroup.com	Griptec®	SS-17-06	#4 through #18		06/2020
Sleeve-Forged	Dayton Superior (formerly Richmond Screw Anchor Co.) www.daytonsuperior.com	DB/DI	SF-17-01	#4 through #11	#4 through #11	06/2020
	Dextra America, Inc. www.dextragroup.com	Bartec Standard Splice (Type A)	SF-17-02	#4 through #18	#4 through #18	06/2020
		Bartec Position Splices (Type B)	SF-17-03	#4 through #18	#4 through #18	06/2020
		BartecPosition Splices Type C (with lock nut)	SF-17-04	#4 through #18	#4 through #18	06/2020
Sleeve-Lock Shear Bolts	Dayton Superior (formerly Bar-Lock) www.daytonsuperior.com	Bar-Lock S/CA Series - D250SCA (formerly S-series)	SL-17-01	#4 through #18		06/2020
	Dayton Superior (formerly Bar-Lock)	Bar-Lock Transitional Coupler S/CA Series – D220	SL-17-02	#5 to #6 transition		06/2020

Notes:

1. If there is a discrepancy between this list and the authorization letter issued by the California Department of Transportation ("Caltrans") to the splice company, the authorization letter and any conditions therein control.
2. The splice company shall inform Caltrans if any of the following occur: the design of the coupler changes, the material used in the coupler changes, changes to the manufacturing process including location changes of manufacturing plants. Caltrans may revoke the authorization of a mechanical coupler, and remove it from this list for any of these reasons or if the splice company engages in fraud or misrepresentation in order to comply with the quality control and quality assurance requirements in section 52 of the Standard Specifications.
3. Caltrans takes no position respecting the validity of any intellectual property rights asserted in connection with any coupler on this list. Users of this list are solely responsible for determining the validity of any such intellectual property rights.
4. All mechanical couplers are on plain black bar unless otherwise stated. Couplers on epoxy-coated bars require corrosion protection covering.
5. Service and ultimate splices are defined in section 52 of the Standard Specifications.
6. This table was prepared to provide a reference source for rebar splicing systems currently authorized for use by Caltrans. Caltrans assumes no liability or responsibility for the accuracy or validity of this information if used by other entities.
7. If you have any questions about this list, please contact the appropriate Structural Materials Representative at: http://www.dot.ca.gov/hq/esc/Translab/OSM/documents/smdocuments/StructuralMaterialsRepresentatives.pdf

UPDATED 06/23/2017

CALIFORNIA DEPARTMENT OF TRANSPORTATION

AUTHORIZED LIST OF COUPLERS FOR REINFORCING STEEL

Type of Splice	Splice Company	Coupler Model	Coupler List Unique Identification	Authorized Service Splice (Bar Sizes)	Authorized Ultimate Splice (Bar Sizes)	Expiration Date
Mechanical Couplers on ASTM A 706 (Grade 60) Reinforcing Steel – For Straight Bars						
Sleeve-Lock Shear Bolts	www.daytonsuperior.com	(formerly S-series)				
	BarSplice http://www.barsplice.com	ZAP Screwlok® Type 2 Series (Standard)	SL-17-03	#4 through #11		06/2020
		Double Row ZAP Screwlok® Type 2 Series (Standard)	SL-17-04	#14 & #18		06/2020
		ZAP Screwlok® Transition Coupler	SL-17-05	#7/#5		06/2020
	Dayton Superior (formerly Bar-Lock) www.daytonsuperior.com	Bar-Lock L Series – D250L	SL-17-06	#3 through #11		06/2020
		Bar-Lock L Series – D250L (20 bolts)	SL-17-07	#14		06/2020
	ERICO www.erico.com	LENTON®LOCK (B1 Series) Foreign Made	SL-17-08	#4 through #11	#4 through #11	06/2020
		LENTON®LOCK (S1 Series) Foreign Made	SL-17-09	#4 through #18		06/2020
Sleeve –Tapered Thread	ERICO www.erico.com	LENTON® Standard (A2)	ST-17-01	#3 through #18		06/2020
		LENTON® Transition (A2)	ST-17-02	#5/#4 through #18/#14		06/2020
		LENTON® Position (P8)	ST-17-03	#6 through #18		06/2020
		LENTON® Position (P9)	ST-17-04	#6 through #18		06/2020
		LENTON® FORM SAVER	ST-17-05	#3 through #11		06/2020
		LENTON® INTERLOK Rebar Splice System (grout filler)	ST-17-06	#8	#8	06/2020
		LENTON® PLUS Position Coupler	ST-17-07	#8 through #14	#8 through #14	06/2020

Notes:

1. If there is a discrepancy between this list and the authorization letter issued by the California Department of Transportation ("Caltrans") to the splice company, the authorization letter and any conditions therein control.
2. The splice company shall inform Caltrans if any of the following occur: the design of the coupler changes, the material used in the coupler changes, changes to the manufacturing process including location changes of manufacturing plants. Caltrans may revoke the authorization of a mechanical coupler, and remove it from this list for any of these reasons or if the splice company engages in fraud or misrepresentation in order to comply with the quality control and quality assurance requirements in section 52 of the Standard Specifications.
3. Caltrans takes no position respecting the validity of any intellectual property rights asserted in connection with any coupler on this list. Users of this list are solely responsible for determining the validity of any such intellectual property rights.
4. All mechanical couplers are on plain black bar unless otherwise stated. Couplers on epoxy-coated bars require corrosion protection covering.
5. Service and ultimate splices are defined in section 52 of the Standard Specifications.
6. This table was prepared to provide a reference source for rebar splicing systems currently authorized for use by Caltrans. Caltrans assumes no liability or responsibility for the accuracy or validity of this information if used by other entities.
7. If you have any questions about this list, please contact the appropriate Structural Materials Representative at: http://www.dot.ca.gov/hq/esc/Translab/OSM/documents/smdocuments/StructuralMaterialsRepresentatives.pdf

CALIFORNIA DEPARTMENT OF TRANSPORTATION

AUTHORIZED LIST OF COUPLERS FOR REINFORCING STEEL

Type of Splice	Splice Company	Coupler Model	Coupler List Unique Identification	Authorized Service Splice (Bar Sizes)	Authorized Ultimate Splice (Bar Sizes)	Expiration Date
Mechanical Couplers on ASTM A 706 (Grade 60) Reinforcing Steel – For Straight Bars						
Sleeve –Tapered Thread		(P14L) with cold worked taper threaded rebar				
		LENTON® PLUS Standard Coupler (A12) with cold worked taper threaded rebar	ST-17-08	#5 through #14	#5 through #14	06/2021
	Headed Reinforcement Corp. www.hrc-usa.com	HRC 410/420 Standard Coupler	ST-17-09	#8 through #18	#8 through #18	06/2021
		HRC 410/490 Position Coupler	ST-17-10	#8 through #18	#8 through #18	06/2021
	Dayton Superior www.daytonsuperior.com	Taper Lock D-310 Standard Coupler	ST-17-11	#6 through #14		06/2021
		Taper Lock D-330 Positional Coupler	ST-17-12	#6 through #14		06/2021
		Taper Lock D-340 Flange Coupler	ST-17-13	#6 through #14		06/2021
	HY-TEN Reinforcement www.hy-ten.co.uk	HT.P Positional Coupler (3-Part Friction Welded)	ST-17-14	#5 through #14	#5 through #14	06/2021
		HT.S Standard Coupler (Friction Welded)	ST-17-15	#4 through #14	#4 through #14	06/2021
		HT.LT Positional Coupler (4-Part Friction Welded)	ST-17-16	#6 through #14	#6 through #14	06/2021
Sleeve-Filler Metal	ERICO www.erico.com	CADWELD®	SM-17-01	#18		06/2021
Sleeve-Filler Grout	Splice Sleeve North	NMB	SG-17-01	#4 through #18		06/2021

Notes:

1. If there is a discrepancy between this list and the authorization letter issued by the California Department of Transportation ("Caltrans") to the splice company, the authorization letter and any conditions therein control.
2. The splice company shall inform Caltrans if any of the following occur: the design of the coupler changes, the material used in the coupler changes, changes to the manufacturing process including location changes of manufacturing plants. Caltrans may revoke the authorization of a mechanical coupler, and remove it from this list for any of these reasons or if the splice company engages in fraud or misrepresentation in order to comply with the quality control and quality assurance requirements in section 52 of the Standard Specifications.
3. Caltrans takes no position respecting the validity of any intellectual property rights asserted in connection with any coupler on this list. Users of this list are solely responsible for determining the validity of any such intellectual property rights.
4. All mechanical couplers are on plain black bar unless otherwise stated. Couplers on epoxy-coated bars require corrosion protection covering.
5. Service and ultimate splices are defined in section 52 of the Standard Specifications.
6. This table was prepared to provide a reference source for rebar splicing systems currently authorized for use by Caltrans. Caltrans assumes no liability or responsibility for the accuracy or validity of this information if used by other entities.
7. If you have any questions about this list, please contact the appropriate Structural Materials Representative at: http://www.dot.ca.gov/hq/esc/Translab/OSM/documents/smdocuments/StructuralMaterialsRepresentatives.pdf

CALIFORNIA DEPARTMENT OF TRANSPORTATION

AUTHORIZED LIST OF COUPLERS FOR REINFORCING STEEL

Type of Splice	Splice Company	Coupler Model	Coupler List Unique Identification	Authorized Service Splice (Bar Sizes)	Authorized Ultimate Splice (Bar Sizes)	Expiration Date
Mechanical Couplers on ASTM A 706 (Grade 60) Reinforcing Steel – For Straight Bars						
Coupler	America www.splicesleeve.com					
	ERICO www.erico.com	LENTON® INTERLOK Rebar Splice System (taper threaded)	SG-17-02	#8	#8	06/2022
Upset Bar Ends-Dowel Bars Included	Dayton Superior www.daytonsuperior.com	US/MC Forged	UB-17-01	#6 through #11	#7 through #11	06/2022
Two Piece Sleeve/Forged Ends	Headed Reinforcement Corp. www.hrc-usa.com	Xtender® 500 XL/510 XL Coupler (formerly 507/571)	TP-17-01	#7	#7	06/2022
		Xtender® 500 XL/510 XL Position Coupler (formerly 507/571)	TP-17-02	#11	#11	06/2022
		Xtender® 500/510 Standard Coupler	TP-17-03	#4 through #14	#4 through #14	06/2022
		Xtender® XT 500/510 Transition Nut Coupler	TP-17-04	#5 through #11	#5 through #11	06/2022
		Xtender® XT 500/510 Transition Nut Coupler	TP-17-05	#11 to #14	#11 to #14	06/2022
		Xtender® 500/520 Form Protector	TP-17-06	#4 through #14	#4 through #14	06/2022
Wedge-Thru Sleeve (Mechanical Lap Splice)	OCM, Inc. (formerly Splice Sleeve North America) www.ocm-inc.com	O-S Splice Clip (one clip per splice)	WT-17-01	#4 through #6		06/2022

Notes:

1. If there is a discrepancy between this list and the authorization letter issued by the California Department of Transportation ("Caltrans") to the splice company, the authorization letter and any conditions therein control.
2. The splice company shall inform Caltrans if any of the following occur: the design of the coupler changes, the material used in the coupler changes, changes to the manufacturing process including location changes of manufacturing plants. Caltrans may revoke the authorization of a mechanical coupler, and remove it from this list for any of these reasons or if the splice company engages in fraud or misrepresentation in order to comply with the quality control and quality assurance requirements in section 52 of the Standard Specifications.
3. Caltrans takes no position respecting the validity of any intellectual property rights asserted in connection with any coupler on this list. Users of this list are solely responsible for determining the validity of any such intellectual property rights.
4. All mechanical couplers are on plain black bar unless otherwise stated. Couplers on epoxy-coated bars require corrosion protection covering.
5. Service and ultimate splices are defined in section 52 of the Standard Specifications.
6. This table was prepared to provide a reference source for rebar splicing systems currently authorized for use by Caltrans. Caltrans assumes no liability or responsibility for the accuracy or validity of this information if used by other entities.
7. If you have any questions about this list, please contact the appropriate Structural Materials Representative at: http://www.dot.ca.gov/hq/esc/Translab/OSM/documents/smdocuments/StructuralMaterialsRepresentatives.pdf

CALIFORNIA DEPARTMENT OF TRANSPORTATION

AUTHORIZED LIST OF COUPLERS FOR REINFORCING STEEL

Type of Splice	Splice Company	Coupler Model	Coupler List Unique Identification	Authorized Service Splice (Bar Sizes)	Authorized Ultimate Splice (Bar Sizes)	Expiration Date
Mechanical Couplers on ASTM A 706 (Grade 60) Reinforcing Steel – For Straight Bars						
Side-by-Side (Mechanical Lap Splice)	ERICO www.erico.com	LENTON® QUICK WEDGE Mechanical Lap Coupling Device (Two Clips per splice)	WT-17-02	#4 through #6		06/2022
	BarSplice http://www.barsplice.com	Double Barrel ZAP Screwlok® Transition Coupler	SB-17-01	#4/#3 through #6/#5, #6/#7 and #7/#8		06/2022
		Double Barrel ZAP Screwlok® Standard Coupler	SB-17-02	#4 through #8		06/2022

Type of Splice	Splice Company	Coupler Model	Coupler List Unique Identification	Authorized Service Splice (Bar Sizes)	Authorized Ultimate Splice (Bar Sizes)	Expiration Date
Mechanical Couplers on ASTM A 706 (Grade 60) Reinforcing Steel - For Hoops						
Sleeve-Swaged	BarSplice http://www.barsplice.com	BPI-GRIP™ (BarGrip®)	SW-17-01	#5 through #8, and #14		06/2022
Two Piece Sleeve/ Forged Ends	Headed Reinforcement Corp. www.hrc-usa.com	Xtender® 500/510	TF-17-01	#5 through #11	#7, #8, #9 and #11	06/2022
		Xtender® 500/515 adjustable tension hoop coupler	TF-17-02	#8		06/2022
		Xtender® 500 XL/510 XL Position Coupler (formerly 507/571)	TF-17-03	#8	#7 and #8	06/2022

Notes:

1. If there is a discrepancy between this list and the authorization letter issued by the California Department of Transportation ("Caltrans") to the splice company, the authorization letter and any conditions therein control.
2. The splice company shall inform Caltrans if any of the following occur: the design of the coupler changes, the material used in the coupler changes, changes to the manufacturing process including location changes of manufacturing plants. Caltrans may revoke the authorization of a mechanical coupler, and remove it from this list for any of these reasons or if the splice company engages in fraud or misrepresentation in order to comply with the quality control and quality assurance requirements in section 52 of the Standard Specifications.
3. Caltrans takes no position respecting the validity of any intellectual property rights asserted in connection with any coupler on this list. Users of this list are solely responsible for determining the validity of any such intellectual property rights.
4. All mechanical couplers are on plain black bar unless otherwise stated. Couplers on epoxy-coated bars require corrosion protection covering.
5. Service and ultimate splices are defined in section 52 of the Standard Specifications.
6. This table was prepared to provide a reference source for rebar splicing systems currently authorized for use by Caltrans. Caltrans assumes no liability or responsibility for the accuracy or validity of this information if used by other entities.
7. If you have any questions about this list, please contact the appropriate Structural Materials Representative at: http://www.dot.ca.gov/hq/esc/Translab/OSM/documents/smdocuments/StructuralMaterialsRepresentatives.pdf

CALIFORNIA DEPARTMENT OF TRANSPORTATION

AUTHORIZED LIST OF COUPLERS FOR REINFORCING STEEL

Type of Splice	Splice Company	Coupler Model	Coupler List Unique Identification	Authorized Service Splice (Bar Sizes)	Authorized Ultimate Splice (Bar Sizes)	Expiration Date
Mechanical Couplers on ASTM A 615, Grade 75 – For Threaded Bar						
Sleeve-Threaded Bar	Dywidag Systems International www.dsiamerica.com	A 615, grade 75 reinforcement bar splice	SE-17-01	#11, #18 and #20	-	06/2022
	Williams Form Engineering www.williamsform.com	A615, grade 75 reinforcement bar splice	SE-17-02	#14 and #18	-	06/2022
Threaded Bar	Skyline Steel www.skylinesteel.com	A615, grade 75 reinforcement bar splice	TB-17-03	#8 through #14	-	06/2022

Notes:

1. If there is a discrepancy between this list and the authorization letter issued by the California Department of Transportation ("Caltrans") to the splice company, the authorization letter and any conditions therein control.
2. The splice company shall inform Caltrans if any of the following occur: the design of the coupler changes, the material used in the coupler changes, changes to the manufacturing process including location changes of manufacturing plants. Caltrans may revoke the authorization of a mechanical coupler, and remove it from this list for any of these reasons or if the splice company engages in fraud or misrepresentation in order to comply with the quality control and quality assurance requirements in section 52 of the Standard Specifications.
3. Caltrans takes no position respecting the validity of any intellectual property rights asserted in connection with any coupler on this list. Users of this list are solely responsible for determining the validity of any such intellectual property rights.
4. All mechanical couplers are on plain black bar unless otherwise stated. Couplers on epoxy-coated bars require corrosion protection covering.
5. Service and ultimate splices are defined in section 52 of the Standard Specifications.
6. This table was prepared to provide a reference source for rebar splicing systems currently authorized for use by Caltrans. Caltrans assumes no liability or responsibility for the accuracy or validity of this information if used by other entities.
7. If you have any questions about this list, please contact the appropriate Structural Materials Representative at: http://www.dot.ca.gov/hq/esc/Translab/OSM/documents/smdocuments/StructuralMaterialsRepresentatives.pdf